

Rationality for Engineers: Part III: Content and Context of Heuristics
Sirous Yasseri

Temperature and Salinity Effects in Sensitive Area of Qeshm Island: Mangrove Forests
Sahar Ghanbarzad Dashti; Mehrnaz Farzingerhar; Alireza Souri

The Effect of Silica Nanoparticles' Coating on the Ion Resolution of Anionic Membrane in SGP System
Abdol reza Sabetahd Jahromi; Hesameddin Mehrfar

Caspian rapid Sea level fluctuation and intensity of displacement of the shorelines in the Gorgan Bay and Miankaleh coast
Homayoun khoshnavan

Pile Length Optimization in Fixed Template Offshore Platform Using Risk Reduction Approach
zahra omrani; Rouhollah Amirabadi; Mahdi Sharifi

Wavelet based detection of vortex shedding around a cylinder oscillating in still water
Seyede Masoome Sadaghi; Seyed Taghi Omid Naeeni; Hasan Yousefi Ghalejoogh



Since 2015

International Journal of
Coastal, Offshore
& Environmental
Engineering

ISSN: 2980-8731 (online)








Message from the Editor-in-Chief

The IJCOE journal office was established in 2015, and its first issue was published in 2016. The IJCOE covers a wide range of research in the fields of oceanography & ocean technology, as well as marine industries & marine engineering. The editorial board of IJCOE consists of nearly 130 of the greatest scientists and researchers from over 30 countries worldwide, and the journal's review board comprises 1,000 members from all five continents. The membership and application process for joining the editorial and review boards of this journal is ongoing. IJCOE is a research-academic quarterly journal that has publication and distribution permissions from the Press Organization and permission to publish scientific-research articles from the Ministry of Science, Research, and Technology (MSRT) with an "A" rating. It also holds a "Q1" rating from the ISC institute with an impact factor (IF) of approximately 0.43 and is considered a "core journal" (prestigious and outstanding journal). IJCOE is an open-access journal and allows the download and receipt of accepted articles in full text for free. It respects and adheres to copyright and COPE regulations. The journal's office operates 24/7, providing services to researchers. In addition to publishing a regular quarterly journal, IJCOE has 16 special issues on specific topics in preparation. It also provides conditions for publishing specialized books, references, and handbooks. Moreover, it is ready to cooperate with the secretariats of reputable international conferences to publish their selected and outstanding articles. IJCOE evaluates, appraises, and publishes books, articles, and the scientific achievements and findings of esteemed researchers and scientists worldwide who are innovating and conducting in-depth research in the "important and strategic field of the maritime technology & Ocean engineering." It welcomes any form of joint cooperation with universities, research institutes, and related research centers at the national, regional, and international levels, and extends a hand for collaboration.

Classification of Editorial Board in IJCOE

[Editor-in-Chief](#)
[Director-in-Chief](#)
[Deputy Editor](#)
[Executive Managers](#)
[English Text Editor](#)
[Technical Editor](#)
[International Editorial Board](#)
[National Editorial Board](#)
[Editorial Board Associate](#)
[Editorial Board Assistant](#)
[Guest Editorial Board](#)
[Advisory Board](#)
[Administrative Coordinator](#)
[Honorary Board Member](#)
[Methodology Advisor](#)

Author Benefits

-  Open Access
-  Rapid Publication
-  Thorough Peer-Review
-  No Copyright Constraints
-  Coverage by Leading Indexing Services
-  Discounts On Article Processing Charges (APC)
-  No Space Constraints, No restriction on the maximum length of the papers, number of figures or colors

Aims of IJCOE

Hydrodynamics
Marine equipment
Structural mechanics
Ocean environmental predictions
Stochastic calculations Experimental
Automatic Control of Marine Systems

Scope of IJCOE

Marine Hazards
Ocean Acoustics
Naval Architecture
Ocean Engineering
Coastal Engineering
Marine Meteorology
Marine Earth Sciences
Underwater Technology
Marine Renewable Energy
Polar & Arctic Engineering
Marine Renewable Energy
Marine Geography & Geodesy
Marine Environmental Engineering
Automatic Control of Marine Systems
Hydro Physics & Physical Oceanography

Type of papers

- Case Studies
- Book Reviews
- Review Article
- Letters to the Editor
- Methodology Papers
- Editorials and Commentaries
- Response or Rejoinder Papers
- Perspective or Opinion Papers
- Conceptual or Theoretical Papers
- Meta-Analysis and Systematic Reviews
- Short Communications or Brief Reports
- Research Articles (Original Research Papers)

Scientific Research Journal

Ministry of Science, Research And Technology (MSRT)

[Jurnal Ranking 2023: A](#)

Ministry Of Science, Research And Technology (ISC)

[Citation Impact 2022: 0.429](#)

[Quartile 2022 : Q1](#)

Core Collection

IJCOE is a Member of



Contact Us

Office 1 | Research Institute of Meteorology and Atmospheric Science

Address | Tehran, Shahid Kharrazi Highway, Pajoohesh Blvd, Research Institute of Meteorology and Atmospheric Science, Sand and Dust Storm International Research Center (SDS-IRC), No. 13, 1st floor.

Phone | +982144787652

Postal code | 13611-14977

website | www.rimac.ac.ir

Office 2 | Iranian National Institute for Oceanography and Atmospheric Science

Address | Tehran, Dr. Fatemi Gharbi St., Shahid Etemadzade St., No. 3, third floor.

Phone | +982166944873

Postal code | 13389 – 14118

website | www.inio.ac.ir

Email | Info@ijcoe.org

Website | www.ijcoe.org

Follow Us



Volume & Issue:

Volume 6, Issue 4, November 2021

Number of Articles: 6

Content

Rationality for Engineers: Part III: Content and Context of Heuristics Sirous Yasseri	1
Temperature and Salinity Effects in Sensitive Area of Qeshm Island: Mangrove Forests Sahar Ghanbarzad Dashti; Mehrnaz Farzingohar; Alireza Souri	13
The Effect of Silica Nanoparticles' Coating on the Ion Resolution of Anionic Membrane in SGP System Abdol reza Sabetahd jahromi; Hesameddin Mehrfar	19
Caspian rapid Sea level fluctuation and intensity of displacement of the shorelines in the Gorgan Bay and Miankaleh coast Homayoun khoshravan	24
Pile Length Optimization in Fixed Template Offshore Platform Using Risk Reduction Approach zahra omrani; Rouhollah Amirabadi; Mahdi Sharifi	33
Wavelet based detection of vortex shedding around a cylinder oscillating in still water Seyede Masoome Sadaghi; Seyed Taghi Omid Naeeni; Hasan Yousefi Ghalejoogh	44

Rationality for Engineers: Part III: Content and Context of Heuristics

Sirous F. Yasseri

Brunel University London; Sirous.Yasseri@Brunel.ac.uk

ARTICLE INFO

Article History:

Received: 02 Jun. 2021

Accepted: 05 Nov. 2021

Keywords:

Judgment errors

Heuristics

Biases

Engineering judgment

Intuition & Perception

Situation appreciation

Content & Context

ABSTRACT

The focus of heuristics is on the content of decisions; however, the contexts are equally important; that is, where and how heuristics are used will often have a great influence on the outcome. Engineers need a lot of specialized skills, hard as well as soft, to successfully apply heuristics, i.e., to identify the heuristic that best fits the environment. Heuristics can help to lessen (not eliminate) the cognitive burden. This part of the four-part paper discusses how heuristics are created, improved, and refuted, and describes what judgment errors they might cause. In using heuristics, engineers must be aware of biases, which is examined in this part. The context of decision-making is also considered, and finally, the paper shows how heuristics should be used.

In engineering, heuristics are experience-based methods used to reduce the need for calculations such as equipment size, performance, or operating conditions. Heuristics are fallible and do not guarantee an optimal solution. It is important to understand their limitations when applying them to a different context. Heuristics work well in a stable environment, but if the environment is complex and changing, heuristics may lose their relevance and require updating. Though the applicability of heuristics is conditional, they can be of value when used expertly.

1. Introduction

Imagine heuristics as tools in a toolbox. You need to choose the correct tool for the job. There might be several tools that could be used, and each may have some advantages and disadvantages. One may be too big for the tight space, another too short to provide enough leverage. Yet the third one is difficult to use. You can establish the connection and suitability of each tool to the task, but the task determines which tool is preferable. Tools wear out and become obsolete, and there is a need for a renewal or replacement process. Tools can be borrowed, rented, or bought, but nothing can compete with the ones that you own and have deep insight into their workings. Even poor heuristics used with great insight can be formidable tools.

Tools are the content, and the task is the context. Content is the material/matter/methods that are available to the engineer, and the context is where the engineer applies it, i.e., the environment. Context is created by the positioning of the content, storyline, or purpose that provides value. As Bate [2] said, "Context is everything."

The context, in heuristic literature, is also referred to as the environment or domain of application. A heuristic developed for one context may not work in a different environment; the portability of heuristics is uncertain.

Heuristics are just working hypotheses until proven wrong. They should not be considered as universally true or as relevant now as they were 20 years ago; due to the dynamic nature of the engineering profession. As time passes some heuristics may become less relevant as technologies evolve, thus there is a need for practitioners to invest in continuous professional development. The ability to learn is a characteristic of humans. Learning is faster when it is supervised by a skilled guide. Take a foreign language, how much you can learn from a teach-yourself book compared to learning with a tutor, or even better, to be surrounded by native speakers. This shows the importance of learning on the job. Learning never stops, it comes as a series of lessons, with the last one being the most important. What an engineer learns after formal education is mostly heuristics and how to apply them. In this context mistake is a very effective teacher. Another skill that Engineers need, is

employing mental mapping to design from the perspectives of the users of their creation, how users would interact with their creation.

Engineering at its core is a marriage of art and science. which requires both judgment and skill in execution. Skill is obtained in stable and regular environments, with the opportunity to learn from ordinary events through prolonged practice (exposure), while also perfecting judgment at the same time. Heuristics blend theory and pragmatism in equal measures. Excessive reliance on theory can lead to blind faith in manufactured numbers; too much emphasis on pragmatism may prevent engineers from moving forward with technology. Successful design requires both; but when in doubt, this author suggests that more emphasis on pragmatism will increase the odds of success.

The Hegelian model “Thesis, antithesis, synthesis” for the progression of ideas is also known as a dialectic. Hegel believed that A better understanding can be achieved by creating two diametrically opposed views or explanations of a situation (i.e., a thesis and antithesis). By clashing thesis and antithesis, something better would emerge. The result is a more complete, enhanced knowledge--what Hegel called a synthesis. Such a philosophy suggests that problems are solved not through conformity but through confrontation. Greater understanding is created by pitting present views against their most compelling counterarguments. Such controlled conflict has both positive and negative consequences. Among the advantages are: better ideas were produced; a new way of looking at a problem; hidden problems would surface; assumptions were clarified. Analytical ability and experience would help engineers to decided which heuristic to use. The heuristic of “chop & change, integrate, simplify” is an example of a heuristic used for a conceptual design. For a development design concept, engineers break down a system nto several manageable modules, ommensurate with constructability, skill set, transportation, access roads, ability to analyse, etc. It seems likely that explicit training in developing the effective use of heuristics would enhance the creation of the idea generation skills for engineers, which are generally left to be learned on the job. Engineers are emigrants to the land of engineering. They can perfect their accent by associating with those who have a few more years over them. Every engineer speaks engineering with an accent, but gradually the rough edges of the accent get smoother, and they understand each other more easily without straining their wits.

People look for evidence to support their beliefs and objectives, not to refute them. They often do not use reasoning to correct their beliefs, but to advance them, and to defend them against others— I’m the best; I deserve the last sweet. Similarly, people use reasoning to tear apart other people’s arguments.

When it dawns on them that they are defending the undefendable, they shift their focus from winning at all costs to wresting the most value.

A primary tool of engineers is their imagination. This is as true now as it was in ancient times. The particular set of assumptions about the world that Engineers adopt guides their actions and directs them towards success or failure. The three primary characteristics of engineers are:

- concern about the future states of the world and the need to protect them.
- seeking to secure a preferred future state to achieve certain ends.
- Believing there is more than one choice of different qualities.

2. Some Common Heuristics

Following are a few examples of heuristics that may help people decide or solve a problem:

- "Consistency heuristic" is a heuristic that requires a person to respond to situations in a way that allows them to remain consistent.
- "Educated guess" is a heuristic that allows one to decide without exhaustive research. The educated guess is based on past observations and applies to a situation where a more definite solution has not been found.
- "Absurdity heuristic" is applied when a claim or a belief seems silly or defies common sense, i.e., an absurd or very atypical and unlikely situation.
- "Contagion heuristic" causes an individual to avoid something that is thought to be associated with contagion. In an epidemic, someone might apply this simple heuristic and decide to avoid social interaction altogether to avoid being infected.
- " Thinking forward and reasoning backward". Supposing to know the solution and working backward to see how such a solution can be obtained.
- "Familiarity heuristic” Assuming a familiar situation is like the situation under consideration, and thus taking the same decision as before. A military man only sees a military solution.
- "Scarcity heuristic" is used when a particular object becomes rare, which means if something is scarce, then it is more desirable.
- “Going with your gut” is when you make a snap judgment based on a quick impression. This heuristic looks at a situation quickly and decides without further check. It is worth remembering that instinct and emotion are the basis of all decisions, actions, values, and worldview.

- "Authority heuristic" refers to believing the opinion of a person of authority just because that person is in a position of authority. Engineers apply this heuristic all the time by referring authorities to authoritative texts or quoting. A variation of this heuristic is known as the "Halo effect", which states; if somebody is seen as infallible (such as a politician or a religious leader), then she/he cannot do wrong.
- "Less is more". Truth is lost when too many messy details are included.
- Not seeing the wood because of the trees.
- Everything happens for a reason; It is in God's hand.

By reviewing these heuristic examples one can get a general idea of techniques of decision-making and how to use them.

Individuals are constrained by limited resources, which applies to all engineers while making decisions, or formulating a question. Heuristics may be answering the wrong question, namely, the actual question is unknowingly replaced with a familiar question.

A love story is just one story, but whoever tells it you feel as if you have not heard it before. The word love evokes a different emotion, and each person has a different connotation and context. Some likened the word 'risk' to the word 'love'. It means different things to different people; you need to know the context to make sense of it.

Some common heuristics used by engineers are explained below.

#1: Considering more parameters will make a problem better defined but including too many parameters will make it intractable.

The idea is to select parameters that:

- have the best explanatory power, and
- are logically the most appropriate and have a high impact.

#2: Break the problem into smaller size problems. The engineer should decide on the right amount of granularity. Engineering education for problem-solving liberally uses the idea of deconstructing a problem, analysing it, and assembling the result. An important balance must be struck, i.e., the level of detail provided by the solution. Availability of data, analytical method, and time are all constraints when considering a problem that has too many details. Equally important is the need for enough detail, as the heuristic explains "problems must be simplified as much as possible but no more than that".

#3: Let available data drive the boundaries of the solution space.

#4: Do not lift a large stone that could fall on your feet; or do not bite more than you can chew.

#5: Be mindful of parameters and data you did not use or decided not to collect. Data collected by others

may be irrelevant (not valid for the problem at hand) hence all data must be looked at with suspicion. Collecting more data may not be fruitful if one is entrenched in biases.

#6: Do not do more analysis than the data or the problem warrant. Torturing yourself will not yield better results. Do not labour at a problem, because it can be done; if it can be done, it does not mean that it should be done.

#7: Mental models are used to come up with a solution; A model is not reality, since it is an abstraction of what the participants think (and hope) the system and its environment will look like. The real world is messy, and reliance on a model that will solve all problems is risky.

#8: All models are wrong, but some of them are useful. This heuristic is due to George Box [18] entitled Robustness in the Strategy of Scientific Model Building. The message models have many limitations but at the same time provide useful information. Starting with the sceptical view that all models (heuristics) are wrong may sound negative but helps to be cautious.

#9: Begin with the end in mind. Think about what you would like to see when the dust has settled.

#10: Requirements are supreme. What you trying to achieve is the requirement; subject to verification; provided you know what you need.

#11: Not all requirements are equally important. Requirements have different levels of complexity and importance, and various level of difficulty associated with their implementation.

#12: Free is a special price that you or somebody must pay. Some solutions sound free but are accompanied by external costs to somebody else down the line. Routing of a railway through a floodwater runoff may look cheap/free, but when floods occur, somebody must pay for the flood damage.

#13: Remember that personnel capability or the budget is not infinite, when you are dealing with a large project or disaster, you must live within your means. When contemplating a large project that is being designed or constructed, it is reasonable to limit your expectation to your budget and skillset and other available resources. Thinking that you will cross the next bridge when you get there, could cause you to lose sight of what is achievable.

#14: If you are thinking to sin, be sure to sin consistently. This is the principle of consistent crudeness. The capability of engineering in an organization is determined by the skill set and its resources. If you are including or excluding something or someone, be consistent, although it may be difficult to be consistent. Consistency may not solve all your problems, but it will stop enough people from trying to find a hole in your argument and actions. Where there is a want of inconsistency, then there must be some error in reasoning.

#15: Whatever you do evaluate early, often, and correctly. The focus must be to catch problems early and arrest the drift from the original goals. This also provides an opportunity to revisit the original assumptions.

#16: Experts will disagree forever. If there is a situation where many experts are involved, they will usually disagree on the relative influence of certain parameters. Limit the expertise by defining the boundaries.

The above set of heuristics which are not mutually exclusive are a baseline that every engineer can build from by applying, validating, or refuting, based on their empirical work. They may be applied to individual tasks, large projects, or even organizations. Engineers must gather knowledge from all things in life. Where data and analytical capability are abundant and experience is reliable, then the use of heuristics should simply serve as sanity checks.

17: Similarity heuristic. This heuristic operates when we seek patterns and look for similar situations. We may notice in some way a situation is like another one and infer that what happened before will therefore be more likely to happen now. This heuristic works much like analogies and metaphors. When the similarity is relevant, it would make the inference more pertinent. For example, the boss fired your colleague for sleeping on the job, and you draw the reasonable conclusion that if you sleep on the job, you will be dismissed too. On the other hand, a similarity might be superficial or not connected with the outcome at all, which would make the inference incorrect. For example, you see a TV commercial showing a slim young person sporting an outfit and infer that it would look as good on you, even if you can shed 30 kg.

18: Doing the same thing again and again while expecting a different outcome is pointless. A once failed decision may be a mistake, a second failure you may call experience, but a third failure must be considered insanity.

19: Jumping to a conclusion, or think before you jump, is a heuristic warning against the hasty decision. Act in haste repents in leisure. It seems jumping to the conclusion was Einstein's favourite sport as the following quote attributed to him signifies "*If I had only one hour to save the world, I would spend fifty-five minutes defining the problem, and only five minutes finding the solution.*".

20: The indicator heuristics (used for methods, novel concepts, etc.). Novelty is categorized into five classes (1) new or unusual and never used; (2) used by others in a different region of the world or different industry; (3) used by others in our industry; (4) used by us in a different project; (5) it is commonly used by us. This use heuristic is useful for ranking risky situations or risk mitigation measures, when new material, a new concept, or a new approach.

#21 Credible bounds heuristics. How big or small something can be.

#22 "Think outside the box "(if dead, you have to think inside the box)". This a heuristic suggested for creative thinking [22].

3. Using, Improving, and Refuting Heuristics

A heuristic about heuristic:

"Do not assume that the original statement of the problem is necessarily the best or even the right one." [15]

Understanding that the problem requires a solution is the first step. In doing so one needs to ask questions. The effort to understand "what is the question" leads to pondering "what is the right question to ask". This is a trial-and-error process with many blind alleys.

The wrong question will divert you from the right path, but who knows what the right question is? Asking questions with different slants could help to find the right path. Colleagues can also help if you are in learning mode, not the convincing mode. Curious and enquiring minds feed upon themselves.

The following heuristics suggest the need to make sure that the right question is asked. Generally, engineers are faced with two primary questions.

- Am I solving the right problem? i.e., is the right problem being posed?
- Am I solving it correctly?

This is important when we know what we need (and want) and the solution is not out of reach, i.e., when some leap of imagination may bring the need closer to the solution, to make it attainable. In such a situation the desire for a solution may influence the question we ask, which consciously or not, we try to shape the problem so that we can solve it.

- There must be agreement among experts that the heuristic which is used is useful and correct.
- The applicability of the heuristic must be obvious.
- The heuristic must be resilient across different types of scenarios and environments, but not necessarily in different domains.

What Can We Do?

- Think Bayesian: Don't suspend your common sense because you are caught up in numbers.
- Think broadly and deeply: Look at any important problem from multiple perspectives. Do not bet on a particular model.
- Think critically: Question everything.
- Maintain a sense of proportion.
- Remember ABC: Assume nothing; Believe nothing and Check everything.
- The devil may be in the detail, but the sting is in the tail.

Emphasising 'assumes nothing' is all well and good, but we need assumptions to make a start; their validity is at stake. We cannot function without them,

especially assumptions which help to suppress other assumptions. We also use assumptions (perhaps fallacies) to prove cherished pet theories or reject others. Creating a heuristic starts with conjecture. Most people will try to find reasons to validate their assumptions. You can always find reasons to believe something is true. Popper [14] believes we must find a reason to refute the conjecture. He said, two people, reading the same newspaper article can find reasons for and against a theory.

We are generally eager to build an explanatory narrative when the observed data is the effect of chance. There is a need for a backup plan (plan B) and a triggering mechanism to change course.

The world is too chaotic to understand without a coherent story (some may call it a theory). We create a narrative of our lives to make sense of it. We tend to dismiss new information that does not fit with our narrative of how the world works. This is known as "Confirmation Bias," which reinforces our belief. Unexpected events sometimes surprise us, to make sense of them in our world, we make more stories. Thus, we believe in correlation and causation from insignificant observed samples when there is none. Another effect is an inability to consider the "regression" effect whereby, in any series of observations, any extreme value is likely to be followed by another which is closer to the mean of the ensemble. For example, the variation of the learning performance of a person is a "noise" around a slow learning curve, where each outstanding performance would naturally be followed by a poorer one. Lack of understanding of regression has led to widespread beliefs in the value of punishment towards improving people's performance [5].

We observe that certain heuristics applied in a specific situation may cause side effects. We conjecture that the use of heuristics may make it more likely to lead to that side effect. This conjecture is legitimate, but to become a respectable theory it would need either a causal explanation, or an analysis of a sample of many similar cases where different approaches are pursued, and the side effects of that heuristic were not observed but a significant correlation was detected. New evidence would cause a heuristic to be reinforced, modified, or refuted. Heuristics are based on past data, i.e., what you know. Using old heuristics and dusting them down has a certain appeal, but the change is to look for new data to assure they are still usable.

Emergencies demand a different mental framework. Responders need to think on their feet. An emergency is not a lab environment in which you can devise experiments, produce, and analyse data and then decide. In an emergency, data, come slowly (one at a time) and there may not be time to update your prior belief. On such occasions, the subjective probability is all you must act on. Humans are better to discover

connections between bits of information. Whatever comes to your senses (attention) influences your decision. The quality of the decision is not equal to the quality of the decision. In the short run, chance elements may not be favourable, thus do not confuse luck with skill. In an uncertain environment, it is better to focus on improving the process of decision-making rather than the outcome alone without accounting for the element of luck. In an emergency, data comes in simultaneously from different sources, creating an incomplete picture of an evolving situation. You need to use each piece of information to update your prior belief as to what is going on. It is not a laboratory condition where you can undertake 10,000 experiments to update and reduce uncertainties.

4. Situation Appreciation

Real-life situations are not like a museum where every exhibition is fake, or a carefully constructed fiction, because the context is not really replicated. Or like an advert that leaves out reality or dismisses causal relationships and falls into the abyss of irrationality. Engineers cannot ignore the environment and how it influences the likely solutions. Engineers need the practice to see the relationship of the problem and its environment and how any problem interaction would affect solutions can be employed. Moreover, the environment changes as time goes on. This requires constant practice; One cannot leave the profession and come back later expecting everything to be preserved in a time capsule.

You need to understand how we perceive your environment and interpret information within it. Perception is defined as the way we gather information from our environment and interpret what it means. Thus, *Perception* is the multiple ways in which we receive information from our surroundings, help us to understand our environment and what is going on. On the other hand, cognition i.e., *the way we comprehend our environment*, is through immediate sensory experience coupled with memories and experiences from the past. Psychological studies of perception and cognition look at how we organise, identify and interpret information through our senses. Acquired knowledge and experience are situated at the interface between us and the environment. Specific places and moments shape understandings and lead us to recognize things or respond in particular ways. To some *extent*, *Seeing is believing* is true, as eyes allow us to see our environment, but what we perceive in any given moment is not only determined by sensory input, but also by our physical abilities, feelings, our memory, and experience, and more. Things that seem true and universal are often just our own unique experiences of the world. This is useful to know—we understand

what irrelevant factors manipulate what we see and think, we can perhaps find ways to overcome these influences and make better sense of information to make better decisions.

Understanding how engineers perceive and make decisions enhances their ability to be better decision-makers. Appreciation of the situation and planning to resolve the problem (posed by a situation in an environment) is one of the engineer's key functions. A five-step planning process is suggested for engineers to approach a situation to determine tasks that must be carried out for achieving the desired outcome. The objectives are to understand the problem, find a solution and ways and means of implementing the chosen solution as well as to allocate resources to achieve the set objectives. This planning process has the following five steps [4].

1. Characterise the situation and identify goals to be achieved (the desirable end state).
2. Decide on what must be achieved to obtain the desired end-state;
3. Order the sequence of actions that lead to the achievement of goals;
4. Allocate resources and develop the concept of operation;
5. Identify how to monitor and continually improve- what data must be collected and how to judge if the goals are obtained; suggest modification is deemed necessary.

In a similar vein, Australian Military has developed the concept of **situation Appreciation** to help commanders to gain an understanding of the situation. According to the Australian Army Manual [1] "*An appreciation is a logical process of reasoning, the object of which is to determine, from facts known or assumed, the best or better course of action to take in any given circumstance.*" This describes a logical process to identify a course of action which fits the circumstance. This is, in essence, a process of clear thinking and logical reasoning. Arthur Conan Doyle said through Sherlock Holmes, "*Appreciation is problems solving by logical assessment of all known facts.*"

Australian Army appreciation process consists of six distinct steps, the first two steps are to understand what must be done and the rest for deciding how it should be done. The parts or steps to be taken are as follows:

1. what are we confronted with? - the situation.
2. What goals to be achieved
3. What course of action to take?
4. Consider all **factors** but select the most relevant ones and make a **deduction**.
5. What are the options? Possible ways to attain the goals.
6. Decide on the best **course of action** – what to be done

Each step includes several sub-steps that break down the overall process into manageable chunks for more granularity.

The problem with this model is that it does not consider the cognitive and emotive effects that influence decision-making. However, the foundation on which the Australian army situation appreciation has been designed is the assumption that decision-makers are rational in neu classical economic sense. The above Discussion sketched the situation appreciation. Another important awareness issue especially for those who are on the scene responder is situational awareness.

Awareness of what is happening around you is required for making a decision to fit the situation. Understanding the environment, judging the consequence of one's actions and the potential risks are necessary components for sound decision-making. The method of understanding a situation is known as Situation Awareness (SA) SA is covered in some detail in [23] with some details.

5. Context and Content of a Decision

Klein [10,11] suggests that the chances of getting intuitive decisions right are much improved by good situational awareness, which in turn depends at least in part on effective pattern recognition; it is the way we organize, make sense of and use our experience. So, memory and recall are fundamental to recognition primed analysis. Situational awareness differentiates between luck and skill. The brain looks for information from experience. Pattern recognition is emotional tagging Emotional tags help us to act fast. Most of the time pattern recognition works well, especially when past patterns are appropriate for the current situation. Pattern recognition in driving, when negotiating a sharp bend, may turn out wrong. The brain fills in data by pattern recognition. Deep-seated desires look for a pattern when there is none.

In our decision making, it is necessary to obtain an understanding of what are we trying to achieve (goals), how to achieve it (plans), the impact on others or their impact on us, and where we think we will end up in the system's domain once the dust has settled. This requires forward projection (imagining the future state) and backward reasoning; looking from the outside in and vice versa; seeing things from the eyes of the system's element and their demands and constraints. As Kierkegaard suggests "life must be understood backward but lived forward".

Engineers' first task in any situation is to comprehend what the problem is and understand the lay of the land (the context of the problem). There is always more than what you can see. Nothing stands in isolation; the problem must be understood in its environment (context) [2]. There are many elements in that environment, and everything is connected to

everything else, making a system of things with varying degrees of relationship. We are all part of the system in which we function, and we each influence those systems, even though we are also influenced by them. Controlling nature is not easy but understanding how it works enhances the effectiveness of the knowledge we have for decision-making. We are part of a system; hence we must learn to work with it. Generally, content is less important than context.

Seeing everything as a system means that one can deconstruct (breaking down a larger system into its modules) and reconstruct (putting it back together). The gains are:

- The ability to see relationships (dependencies)
- Accounting for constraints
- Understanding Trade-offs

The word 'system' is used to describe something that comprises more than one element. In other words, a system is a collection of individual elements that together produce results not achievable by a single element alone; hence the adage "a system is larger than the sum of its elements (parts?)". However, assembling elements does not necessarily create a system. Elements must be arranged and related to each other in a particular way to achieve the system's goals. The elements may represent people, facilities, software, hardware, procedures, policies, and infrastructures. The relationship between the elements and how they are interconnected creates value. Within a system, there are likely to be multiple agents. An agent is defined by its role within the system and may be an individual, an organization, or a collective entity that gets value from the system in some way (i.e., the public). For example, a country's transportation system consists of road, air, railway, and underground systems, which must be connected in a meaningful way to be effective. Moreover, the transportation system must be connected to the energy system to function, since in a system everything is connected to everything else, and dysfunction of one part could bring down a larger part of a system. The same fact is true for implementing a change to a system that could propagate through the system and result in unforeseen consequences. Engineers need coordinated strategies that consider the consequence of treating a single issue in isolation and remember key causal relationships, leverage points, and gaining foresight across a system by whatever means, including using data-driven methods. The world is dynamic, not static, there is always a second step, and many more steps after that. Thus, engineers should think in terms of the system when trying to influence an element of it. Senge [16] in his book "The Fifth Discipline" states that: "*Systems Thinking is a framework for seeing interrelationships rather than separate things, for*

seeing patterns rather than static snapshots. It is a set of general principles, spanning fields as diverse as physical and social sciences, engineering, and management."

Systems Thinking is a conceptual framework for understanding how and why systems behave as they do. A complete understanding of a complex open system may elude us, because of the number of entities within them, and the infinite interconnections and relationships between infinite parts, leading to nonlinear and unpredictable behaviour. Engineering systems are not often open, except the ones that include social systems. However, it may require stripping out weak relationships to reduce their complexity for simplification. People tend to focus on the short-term consequences and believe that long-term behaviour is inconsequential. We tend to see one part of a system and ignore the rest and are surprised when we have unintended consequences. The challenge is to identify all elements and their relationships and to consider the problem overall, not just a selection of fragmented parts.

Framing complex engineering problems with many agents using a Systems Thinking framework allows us to gain valuable insights. What may seem haphazard behaviour to others, maybe rational and perhaps predictable, to a decision-maker who thinks in terms of systems. As we become familiar with Systems Thinking, we realize that our systems are not erratic but behaving exactly as they should give the capabilities and the relationships of its parts, the goals of its agents, the effects of various policies and rules, and the complex interactions that produce reactions and future actions.

Systems Thinking can also be defined as a process of looking at a problem in its entirety and focusing on the relationship between its parts, rather than considering the parts individually. For example, one can study each part of a car independently, or one can study cars, and see where each distinct element plays a relationship role in the function of the system. Reductionism only allows the study of individual parts, while Systems Thinking enables the study of the whole car. We need both; by reducing a problem to its constituent elements we may be able to solve it but ignoring the position of each element in the system might result in unpredictable behaviours. The current approach, as taught in dominant engineering schools, calls for a combination of both. Some people like to think of the systems approach as "seeing the world through the eyes of others and how your decision affects them". Not seeing a problem, is not a sign of everything is all right, but you might not see the problem.

To acquire System Thinking [3], engineers must understand their system by studying the underlying cause and effect interactions that produce the observable behaviours. Whether the system is a

hospital with its access roads, safety system, or ecosystem, there exists a small set of common principles that help us to understand its dynamics and behaviours, and why often things do not go the way we assumed. The message is changing one element of a system may have unforeseen consequences; “walk before you run”.

Also, you need a plan and be ready to revise it considering new information. You cannot say where a boat is going until you know the ocean, it is like setting sail without a map. In the language of Yogi Berra “if you don't know where you are going you won't get there.”

6. Engineering and risk

Heuristics are not a recipe that turns engineering into a cookbook. A brain is needed to sit between heuristics and the real world. Engineering judgment is needed to turn ideas into reality. It also does not require engineers to be all-knowing, but optimistically cautious in their ability to deliver. For these engineers need practice to enhance their skills and be more effective. It is a container that can lose its usefulness. If foods frequently go bad in your fridge, do you suspect the food or the fridge?

Heuristics are likened to a *hammer*. It can help a blacksmith shape a piece of metal, but it does not guarantee the solution. A hammer may be critical to a skilled blacksmith while being of little use to an unskilled person who does not know what to pound, how hard to pound, or when to stop pounding. Heuristics do not replace skill, but they can make skilled people more productive. Heuristics can be considered as the best practice, but they need a skilled engineer to apply them. Skills that are needed are both social and mathematical.

Learning where a heuristic will work, how to apply it, how it can go wrong, when to stop, and finally when to use an alternative heuristic to change tack.

Hammurabi, the sixth king of Babylon, ruled from 1792 BC to 1750 BC. The Code of Hammurabi contains 282 laws which were inscribed on twelve stone tablets and placed on public view. “*The code also includes the earliest known construction laws that are designed to align the incentives of builder and occupant to ensure that builders created safe homes:*

229. *If a builder builds a house for a man and does not make its construction firm, and the house which he has built collapses and causes the death of the owner of the house, that builder shall be put to death.*

230. *If it causes the death of the son of the owner of the house, they shall put to death a son of that builder.*

231. *If it causes the death of a slave of the owner of the house, he shall give to the owner of the house a slave of equal value.*

232. *If it destroys property, he shall restore whatever it destroyed, and because he did not make the house which he builds firm and it collapsed, he shall rebuild the house which collapsed at his own expense.*

233. *If a builder builds a house for a man and does not make its construction meet the requirements and a wall falls in, that builder shall strengthen the wall at his own expense.”*

The suggested reparations are harsh, and there is no suggestion of any compensation, and it appears that any financial loss would be borne alone by the homeowner. Hammurabi thought life mattered not property. Perhaps he was not wrong since if a seed does not perish it can grow again. Hammurabi's memory is still haunting researchers as they feel there is a need to add a disclaimer at the end of the technical paper to warn against its use.

This rule makes several assumptions including perfect knowledge, materials last forever, and no budgetary constraints. Hammurabi's tablets have lasted a long time and are kept in the Louvre Museum. You know that there is a risk that any house you build might collapse due to a variety of reasons. So, what do you do? You allow for the widest possible margin of safety. You plan for any possible risk you can imagine. You try to detect any flaw that could lead to a disaster. Cutting corners is not worth the risk. You want to walk away unhurt yourself.

Every engineering decision is an economic decision. You can tie up a substantial part of a nation's wealth in one edifice, or you can provide shelter for many, albeit with some risk of injury or loss of property. Who decides what level of risk is tolerable? In Europe, the state decides what is tolerable, explicitly, or implicitly, through codes. In the US, the tolerable risk is indirectly decided by the Codes of Practice.

Hammurabi's approach to establishing the probability of guilt was practiced until 800 years ago when the jury system was introduced in Britain, ‘Trial by ordeal’ was used to establish guilt or innocence of the accused. Fire and water were the two main forms of the ordeal, with God being used as the jurors to establish guilt or innocence as revealed by the result. The accused would then be bounded and thrown into the water. Like trial by combat, trial by ordeal was based on the belief that God would intervene on behalf of the innocent by performing a miracle. A betting person should have a good idea of guilt or innocence before betting.

Engineering involves risk, albeit calculated ones. It is impossible to construct a project or an operation without accounting for the inherent uncertainty. However, the risk is difficult to comprehend. Countless behavioural and neurobiological studies show that human beings tend to avoid risk whenever possible and misconstrue it otherwise [7]. The trouble is further exacerbated by imprecise data. A

natural reaction to this is to add more parameters or constraints or decimal places, hoping these would enhance the accuracy. Specified probabilities are approximate and it is dangerous to pretend otherwise. We hedge our bets towards the middle of our uncertainties; thus, we may not be as biased as we think.

In modern engineering, it is recognized that it is not possible, or practical, to eliminate risk but it can be reduced to a tolerable level. In the UK, the practice is to reduce risk as to the “As Low as Reasonably Practicable” (ALARP) principle [30].

7. How Heuristics Ought to be Used

Trial and Error is the most basic heuristic that can be utilized for everything, from matching nuts and bolts to solving numerical problems. By examining initial results, one may decide to go through another trial to close the gap even further. Engineers use the same concept to improve their decision-making process with each project they execute. This is achieved through “Lessons Learnt” by understanding the root cause of mistakes and exploring the ways and means for improvement. The ubiquitous design errors and their cumulative decremental effect upon the structural integrity of infrastructure are costly. Such costs are significantly higher in the event of an engineering failure leading to loss of life [13]. Most of these failures can be avoided by not forgetting the simple heuristic of “Lessons Learnt”. It is illuminating sometimes to ask ourselves; how did we get into this mess?

However, we do not always get a second chance to learn and improve i.e., no time for rehearsal. Thus, every decision you make should be considered as your last chance and as if your life depends on it. Builders in Hammurabi time were faced with the same dilemma, of course, they can do better next time, but there might not be the next time, as their previous works could be a dead weight around their necks, causing them to sink for good. Natural phenomena can unleash their destructive powers in ever-increasing ferocity. Though the required knowledge in Hammurabi time was non-existence, buildings were not spectacular and those who desired a prestigious monument had the money to pay for their oversizing.

It has been recognized that in complex situations decision-makers often deviate from the normative prescriptions of logic and probability theory, and resort to simple, non-optimal strategies that have been variously termed as intuitive, muddling through, heuristic, fuzzy, boundedly rational, or recognition-primed. Klein et al [8,9] examined how decisions are made by military personnel under extreme time pressure, and in environments where the consequences of the decisions are high. They concluded that recognition primed, rather than

calculation or analysis, is used for rapid decision making.

Rationality for engineers is generally the avoidance of disasters. When dealing with natural phenomena, there is a need for conscious decisions as to how much money you can lock into one building, just to avoid the rarer events. According to Hammurabi law, if an engineer gives an opinion, and someone takes it, the engineer is morally obligated to be exposed to its consequences, which is not very different now. The client does not want to know what you “think,” but does want to be assured that you are taking potential risks into account. This is about rational (and ethical) behaviour and that the design will stand the test of time, not just a one-year limited warranty. Rational behaviour in the real world is something vastly deeper and evidence-based and is linked to the engineer’s survival; liars and outliers are the exceptions to this rule. Real-life situations are not science fiction, adverse situations could happen at any given time. This puts a lot of emphasis on using correct methods and materials.

Engineering ethics require the mitigation of suffering and risk, as well as safeguarding society's well-being. Engineers do not share possible harms with victims, only their reputations are at stake. An old engineer who is enjoying fame is a sign that she has considered all possible harms with her client.

Consider a situation where engineers are engaged to design for extreme events that are by any measure ill-defined problems. They generally use two well-known heuristic strategies:

- (i) A Common Event Heuristic - design for a more frequent event with no damage.
- (ii) A Worst-Case Heuristic - design for a less frequent event and try to avoid loss of life, not property.

The consequences of an event happening are more important than its probability. Some events may break your back and you cannot stand up and dust yourself down. Thus, one should consider all events and see which has the worst consequence and which is difficult to recover from. Consider living to see another day.

The Common Event Heuristic aligns well with classical Bayesian probability [12]. The assumption that guides a decision considers what is the most likely event based on prior probabilities (i.e., something experienced before) and current requirements (i.e., what is adequate given the situation and regional history i.e., if there are codes of practice or regulations in place; good practice; engineering judgment, etc.). This heuristic directs engineers toward a ‘Confirmatory’ looking for something like their beliefs, the beliefs of their peers, and what might be accepted by the engineering community. Then the engineer would seek evidence confirming the most likely event.

The worst-case heuristic shifts the focus from mitigation against likely future events to mitigation against potential consequences from extreme events. For example, the design for the defence of a nuclear facility is based on a plausible scenario of intrusion. Of course, the plausibility of a theory is not proof of its validity. The system is designed to guard against total loss, or at least to keep the disaster within the facility's boundaries. If you let your imagination loose, there is no upper bound on possible events. As technology improves, the ability of intruders will improve with it. There may emerge a serious likelihood of missing or overlooking some condition that might ultimately lead to serious harm (i.e., unpredicted, or unpredictable Worst Cases). The Worst-Case heuristic directs engineers toward a disconfirming search to rule out possible Worst Cases, often when simultaneously contemplating the more likely event. Each heuristic on its own may reflect bounded rationality but combining them forms the basis for a type of rationality that differentiates between Worst Cases and Common Events.

To address the question of a satisfactory criterion for discriminating between Common Events and Worst Cases, it is necessary to consider the domain-specific values associated with the potential consequences of an error, or something which has been discounted. Thus, the decision is not simply a function of logic and discerning the 'truth', rather, it is a value-driven trade-off that could involve ethical issues. What costs are associated with the protection measures that would be required to conclusively rule out all Worst Cases? How severe would the accident consequences be of ignoring/missing a potential Worst-Case be? Governments around the world have taken this decision to some extent out of engineer's hands via codes of practice, rules, and regulations. However, those dealing with high-risk installations still face this dilemma in their work.

"Technological solutions to the problem of coping with hazards have typically been justified by a computation of benefits and costs that assume the people involved will behave in what the policymaker considers to be an economically rational way. However, it has slowly become evident that technological solutions, by themselves, are inadequate without knowledge of how they will affect decision making" [17]. The debate of engineering rationality and the way an engineer decides how to formulate rules for reflecting on the social and ethical issues in engineering requires consideration. Ethics and rules of moral behaviour are needed for large-scale engineering projects such as dams.

In normal situations, engineers engage in planning and mitigation efforts to reduce the damage caused by disasters. They are supposed to identify all hazards threatening a community including fires, floods, and industrial accidents, and then develop a plan to

address those hazards. In the case of floods, engineers develop plans to mitigate the effects of heavy rainfall and overflow before they happen. Biases and heuristics may shape these decisions. For example, engineers might follow the lead of neighbouring provinces without taking the time to consider all relevant facts. They also might allocate more resources when an action to prevent damage is framed as potentially preventing a loss, rather than when it is framed as potentially securing a benefit. Both options would be consistent with Kahneman & Tversky [6], and Tversky & Kahneman [19], research. There is nothing wrong with being extra cautious, but engineers in emergencies are charged with using collective resources prudently and fairly. We pay more attention when a clear threat exists.

Resilience is a heuristic used in design against natural disasters. Resilience in the context of the natural disaster means systems can maintain their integrity and remain stable when subject to a disturbance; that is, the system's ability to make a smooth transition to a new stable state in response to the disturbance, say, from an earthquake. There is no clear definition for resilience and as such, it is a design heuristic. It implies your best efforts to mitigate the effect of a disaster without throwing money at it. What is acceptable resilience depending on the acceptable risk, which means that engineers are dealing with two fuzzy concepts. Despite this fuzziness, this heuristic works very well by encouraging engineers to look for ways and means of mitigation without extra cost. These heuristics do not tell you what to do but require you to search if you can improve it for multi-hazard. The level of limitation gives you a clue if a system is resilient enough within your constraints. Resilience is the product of many decisions among competing options and actions.

In system design, another concept frequently referred to is robustness. Robustness is the property of a system and is defined as "the ability of a system to resist change without losing its initial stable configuration".

8. Conclusions

If heuristics did not exist, we would need to invent them. This part of the four-part series is about how heuristics are constructed and used. There is no guarantee that heuristics will not lead to errors, but mistakes are 'fast and unforgiving teachers.'

According to an adage: 'the brain is like a parachute, and it works better if it is open'. Having an open mind is a prerequisite of being a good decision-maker, but you must be alert and keep a guard at the gate. A dose of scepticism will act as a guard against being tripped up by baseless beliefs. You need facts when your gut talks to you.

A heuristic may not become obsolete, but it may become worn out. With each use, its relevance can be

perfected. The job is not only to determine which heuristic is the best fit but also how to implement it. There are mental traps, or biases, in using heuristics and there is evidence that indicates it is not possible to get rid of biases.

What makes a person an engineer? Is it a lot of common sense combined with an open mind and a pinch of scepticism. As Theodor von Karmann said, “if science aims at revealing what is, engineering aims at introducing into the world what never was, for the sake of acting on the world in new ways.” Engineering is overwhelmingly a matter of projecting imagined possibilities onto a world that lacks them and then making those possibilities actual. Thus, engineers are required to act when there is no clarity or certainty. Heuristics are tools that help in such situations. Engineers shape their environment, which in turn shapes us. What engineers know may be important, but things that they do not know are even more important. We need System 1 Thinking to free some mental space for other activities. Suppressing System 1 is not possible nor desirable. However, we can train System 2 to kick in faster.

engineers may choose whichever approach seems to promise the desired results, often blending different heuristics. the art of engineering is the ability to blend many things to achieve the best possible solution.

Acknowledgments

The authors would like to thank Chris Millyard, Sassan Rezaei, Mehrdad Rahbari, Kabir Sadeghi, and Michael Vigne, Mohsen Mirza, Giles Thompson for their counsel and feedback, who have assisted to improve the quality and integrity of these papers. I am very much indebted to Mehrdad Rahbari for his patience and help with improving successive revisions.

This research did not receive any specific grant from funding agencies in the public, commercial, or not-for-profit sectors.

9. References

- [1] Australian Defense Force Procedures (ADFP) 5.0.1—Joint Military Appreciation Process, edition 2 is issued for use by the Australian Defense Force and is effective forthwith. This publication supersedes ADFP 5.0.1 Edition 2 AL3. 15 August 2019
- [2] Bate, P., (2018). *Perspectives on context-Context is everything*, The health foundation perspective on context.
- [3] Meadows, D.H.(2008), *Thinking in Systems: International Bestseller Illustrated Edition*, Kindle Edition Chelsea Green Publishing; Illustrated edition.
- [4] Jackson, A.P.,(2017), *The Evolution of the Australian Defense Force’s Joint Operational Art* Author(s): Vol. 13, No. 1, Getting the Balance Right (2017), pp. 59-80 Published by: Institute for Regional Security.
- [5] Kahneman, D., and Tversky. A. (1982). “Intuitive Prediction: Biases and corrective procedures,” in *Judgment under uncertainty: heuristics and biases*, ed. D. Kahnemann, P. Slovic and A. Tversky, pp. 414-421, Cambridge University Press.
- [6] Kahneman, D., & Tversky, A. (1979). *Prospect theory: An analysis of decision under risk*. *Econometrica: Journal of the Econometric Society*, 47, 263-291.
- [7] Kahneman, D. 2011. *Thinking, fast and slow*. New York: Macmillan.
- [8] Klein, G. A., Calderwood, R., & Clinton-Cirocco, A. (1986). *Rapid decision-making on the fire ground*. *Proceedings of the Human Factors and Ergonomics Society Annual Meeting*, 30,576–580.
- [9] Klein, G., Calderwood, R., & Clinton-Cirocco, A. (2010). *Rapid decision making on the fire ground: The original study plus a postscript*. *Journal of Cognitive Engineering and Decision Making*, 4, 186–209.
- [10] Klein, G (1993) *A Recognition-Primed Decision Model of Rapid Decision-Making in G.A Klein et al Decision-Making in Action: Models and Methods* pp 138-147, Ablex Publishing: Norwood, NJ
- [11] Klein, G (1998) *Sources of Power: How People Make Decisions*. Cambridge MA: MIT Press.
- [12] Lambert, B. (2018). *A Student’s Guide to Bayesian Statistics* SAGE Publications Ltd, 520 pages.
- [13] Love, P. E., R. Lopez, D. J. Edwards, and Y. M. Goh. 2012. “Error begat error: Design error analysis and prevention in social infrastructure projects.” *Accid. Anal. Prev.* 48 (Sep): 100–110.
- [14] Popper, K., (2002). *Conjectures and Refutations: The Growth of Scientific Knowledge*, Routledge Classics, 2nd edition.
- [15] Reichtin, E., (1991), *Systems Architecting: Creating & Building Complex Systems*. Upper Saddle River, NJ: Prentice-Hall.
- [16] Senge, P. M. (1990). *The Fifth Discipline: The Art and Practice of the Learning Organization*. New York: Doubleday/Currency, 1990.
- [17] Slovic P, Kunreuther H, White G: (2000). *Decision Processes, Rationality, and Adjustment to Natural Hazards*. In: *The Perception of Risk* Edited by Slovic, P. Sterling: Earthscan Publications Ltd; 2000:1-31.
- [18] Smith, A. F. M. (2015). "George Edward Pelham Box. 10 October 1919 – 28 March 2013". *Biographical Memoirs of Fellows of the Royal Society*. 61: 23-37.
- [19] Tversky, A., & Kahneman, D. (1992). *Advances in prospect theory: Cumulative representation of*

uncertainty. *Journal of Risk and Uncertainty*, 5, 297-323.

- [20] Yasseri,S,(2013), The ALARP Argument.
- [21] Yasseri, S., (2015), Evidence-based practice in subsea engineering *Underwater Technology*, The International Journal of the Society for Underwater 32(4).
- [22] Yasseri, S., (2017), Thinking Like an Engineer.
- [23] Yasseri, S. and Bahai, H, (2018) Safety in Marine Operations *IJCOE Vol.2/No. 3/Autumn 2018* (29-40).
- [24] Yasseri, S., (2021), Rationality for engineers, Part II, *IJCOE Vol.4/No. 2/Summer 2020* (1-13)
- [25] Yasseri, S., (2021), Rationality for engineers, Part II, *IJCOE Vol.4/No. 2/Summer 2020* (1-13)
- [26] Yasseri, S., (2021), Rationality for engineers, Part IV, *IJCOE Vol.4/No. 2/Summer 2020* (1-13)

Temperature and Salinity Effects in Sensitive Area of Qeshm Island: Mangrove Forests

Sahar Ghanbarzad Dashti¹, Mehrnaz Farzingohar^{1*}, Alireza Souri²

¹ Department of Non-living Marine and Atmospheric Science, Faculty of Marine Science and Technology, University of Hormozgan, Iran; Corresponding Email address: mfgohar@yahoo.com

² Department of Functional and Evolutionary Ecology, University of Vienna, Vienna, Austria

ARTICLE INFO

Article History:

Received: 11 Sep. 2021

Accepted: 12 Nov. 2021

Keywords:

Temperature
Salinity
Mangrove Forest
Khor-e-khoran
Anomaly

ABSTRACT

Mangrove forests of Qeshm Island could be considered as one of the most important and sensitive ecosystems of the Persian Gulf. The Growth and evolution of mangrove forests are affected by various factors such as pollution, light penetration, depth, water flow, and water quality. Consequently, it is vital to monitor the environmental changes of these mangrove forests. Hence, this study was aimed to evaluate the effects of sea surface temperature and salinity changes on vegetation level in the Khor-e-khoran protected area in two distinct time periods (1986-1999 & 2001-2015). In order to achieve the desired accuracy and details, various data sources were applied including recorded data in the department of environment of Iran, satellite imagery, drawing profiles and charts by standard models of ECMWF and Giovanni. The results of the present study clarified that Sea Surface Temperature and Salinity increased by about 0.2°C and 0.5 ppt respectively. Comparing the total areas of studied mangrove forests indicated that the total area of Khor-e-khoran protected area was decreased from about 6800 hectares in 2003 to 6350 hectares in 2015 which was more than 1.5%. It was suggested sewages and wastewaters delivered from shrimp farming pools as well as fuel and crude oil leakage caused salinity and pollution anomalies in this region.

1. Introduction

Qeshm Island located on the eastern side of the Strait of Hormuz which is one of the most important and sensitive areas of the Persian Gulf, due to its unique geographical, economical, geopolitical, environmental, and ecological conditions. In order to achieve sustainable land use, it is vital to consider the conservation and restoration of regional ecosystems, which should be the priority of the regional environmental programs [1]. Therefore this area was classified as an international sensitive area based on the Ramsar Convention which was designated in 1971 [2]. In the 1992 IUCN's agenda, governments have been urging to identify and protect sensitive areas with the priority of coral reef ecosystems, tropical wetlands, mangroves, sea buckthorns, aquaculture spawn, and regeneration areas. Therefore, the presence of mangrove forests in the list of sensitive and protected national and international areas is one of the most important factors in the coastal areas of Qeshm Island [3]. Determining the coastal protected areas, especially the national parks in the northern coasts of the Persian Gulf is not only an issue but also politically important and gaining global credibility for the country, due to

the presence of major biodiversity focal areas such as coral rocks, mangroves, birds and aquatic species [4]. Sea surface temperature can affect the metabolism and biological activities rate of aquatic organisms [5] and thus affect the habitats [6]. Some of these species, especially aquatic plants, flourish at higher temperatures, while others prefer lower temperatures [6]. The mangrove plant does not expand when the annual average temperature is less than 19 °C and the ecosystem is out of balance [7]. The photosynthesis rate of most mangrove species decreases sharply when the temperature is more than 35 °C. Temperature seems to be important regulators for the survival or destruction of mangrove habitats. Some adaptations of mangrove ecosystems to prevent excessive dehydration are sweating, thick leaves, small hairs on leaves, adjustment of respiratory pores, and water conservation in leaves [8].

There are various water-soluble salts which improve salinity balance. Major ions in seawater (with a practical salinity of 35 ppt) are chlorine, sodium, magnesium, sulfate, calcium, potassium, bicarbonate, and bromine [6]. Salinity anomalies could be considered

as one of the major disturbances of aquatic plants. Generally, salinity anomaly leads to physiological drought, nutritional imbalance, or a combination of all of these factors. Due to the lack of oxygen in the manure habitats, the vertical roots are efficient for gas exchange and respiration in the sludge. The concentration of salt in the stem of different mangroves species is recorded from 0.5 ppt to 8 ppt, usually higher values might be observed in *Avicennia marina* specie. This relatively consistent value is much lower than the salinity of the seawater [9].

According to the carried out studies, physicochemical factors such as water temperature, salinity, penetration, local flow, and contamination that play a decisive role in identifying coastal-marine protected areas are highly effective parameters in the reproduction and survival of mangrove ecosystems species [10]. By comparing and interpreting the aerial photos of two separate periods in 1985 and 1993, it was identified that the area of Mangrove forests observed in the Qeshm region (including Mangrove forests in the north and southeast) was decreased from an approximate area of 8026 hectares to 8016 hectares [11].

Manson et al. (2003) applied two methods of spatial-temporal analysis and variation detection to estimate and report the variations in the distribution and expansion of mangrove habitats in the Moreton Gulf and southwest areas of Queensland over the past 25 years. Results indicated that about 3800 hectares have been destroyed by natural losses and clearing mangroves because of urban development, aquaculture, industrial and agricultural development and only about 15,000 hectares of mangrove habitats remained in this bay currently [12].

Coastal-marine protected areas, despite being more sensitive, fragile, and rich are not old enough, and their conservation and management have many failures due to this negligence, today [3]. Therefore, the importance of further investigation in the area of Khor-e-khoran and filling of the existing gap highlights the necessity for this research. Also, the scientific background shows that the area of Mangrove forests in Khor-e-khoran has been decreased over the last decades.

Since the physical factors such as sea surface temperature and sea surface salinity are affected directly or indirectly the resilience and rehabilitation of Mangrove habitats of this region [13], this study was aimed to investigate the changes of temperature and salinity in two distinct periods and its relationship with reducing the area of mangrove forests. Mangrove forests in Iran are mainly composed of the *Avicennia marina* species, moreover, the marshlands of *Rhizophora mucronata* were observed around the Qeshm Island, and the Khamir port. The mangrove tree of *Rhizophora mucronata*, a dominant biotic species of Qeshm Island, is a fundamental ecologic specie that grows in tropical and subtropical waters and absorbs large quantities of carbon dioxide, and its existence is

a factor for the regulation of salinity in the area, also it is considered as the habitat of many birds and rare species [14]. The economic value of natural products and ecosystem services generated by mangrove ecosystems is significant. Mangrove forest provide various economic and ecological services such as protection against floods and shoreline recession as well as maintenance of biodiversity [15].

2. Materials and Methods

2.1. Study area

The present investigation was accomplished in a mangrove protected area which is located between the north of Qeshm Island and Bandar Khamir (Khor-e-khoran International Lagoon). The mangrove habitats of this area could be considered as the most conserved mangrove ecosystem of the Persian Gulf in terms of quality. According to reports of the department of environment of Iran, the area of Mangrove forests has declined over recent decades [14]. The Mangrove forests of Qeshm Island are located between the delta of Mehran and Gavazrin rivers in the northern section of the Qeshm Island ($45^{\circ} 26'$ to 27° N and $20^{\circ} 55'$ to $51^{\circ} 55'$ E) (Figure 1).

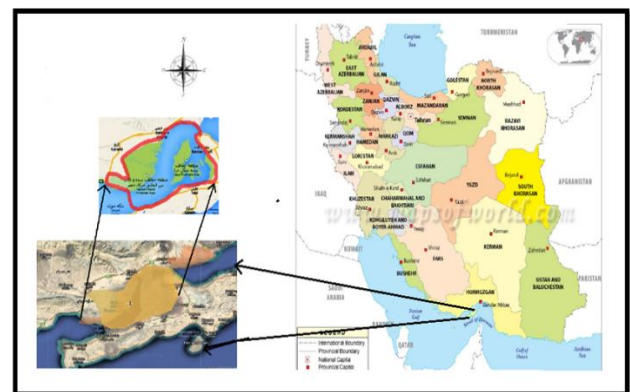


Figure1: Geographical location of Khor-e-khoran international lagoon

2.2. Temperature Data

The ECMWF model was used to measure sea surface temperature data. This model provides weather forecasts for an average period of time. The main task of this model is to generate numerical predictions as well as, conduct scientific and technical researches to improve the accuracy of forecasting and maintaining the meteorology data archives. The sea surface temperature data for over 30 years in two distinct periods were applied for the present study (1968-1985 and 2001-2015). Totally, 24 data collection points were considered and parameters were recorded in two interval times periods per day (12:00 am and 12:00 pm). The data files were downloaded in netCDF format and retrieved using Panoply software, and then the average monthly sea surface temperature was calculated using Excel software.

2.3. Salinity Data

Regarding the collection of sea surface salinity data for the statistical period, only there were continuous data for 7 years available (2007 to 2014). Seasonal variations were plotted for 3 years by the Giovanni model, and the data used for the years 2007 to 2011, was found in the reports of the Iran Fisheries Research Institute and documentation available at the Library of the Persian Gulf and The Oman Sea Ecological Institute [16].

2.4. Variable Vegetation Changes Data

Changes in vegetation over the past 30 years investigated by Landsat 4 and 5 satellite images (TM sensors) from 1985 to 1986 and 1999 to 2000, Landsat 7 (ETM + sensor) from 2000 to 2014, and Landsat 8 (OLI Sensor) was been used for 2015. Khor-e-khoran is located at the 160-41 scene of Landsat data [17]. Detection of variations and determining the most appropriate indicator in a region depends on the applied remote sensing technique to specify the spatial, and temporal characteristics of the sensor system. Satellite data from the OLI, ETM +, TM, and MSS sensors from Landsat satellite was used to a large extent for monitoring vegetation changes [18]. In this study, OLI, ETM +, and TM images from the Landsat satellite were used. The satellite images which were used for 2015, 2001, 1999, and 1986. In order to achieve the highest possible efficiency in terms of identifying the changes in vegetation over time, the input pictures were in the same tidal conditions. Additionally, Khor-e-khoran mangrove vegetation was also at the peak of physiological potential. Some studies suggested that in order to characterize land cover changes in tidal areas with a desirable accuracy, the best time is winter season and around March. Therefore, winter tide images were prepared from the study area [17].

In this research, the normalized difference vegetation index (NDVI) was applied. The NDVI vegetation index

is a two-variable index that has been developed to describe vegetation and can be used to differentiate between near-infrared (which is strongly reflected by plants) and red light (which is absorbed by plants), that provides vegetation points. This index is widely used based on spectral values in identifying vegetation [19, 20]. In order to reveal vegetation changes, two methods of differentiation and comparison after classification were used with a threshold of twice the mean deviation. In the variation method, the depicted image of a date decreased from the image shown on another date (the second date from the first date). If the result of this difference was not significant, it was indicated that changes were neglectable. Negative values mean a decrease and positive values mean an increase [21]. In the comparison method after classification, a map of the Khor-e-khoran mangrove forest area was required at two-time intervals. After categorizing, images were compared independently. For categorization, they were first selected on each colored image in the forest class and non-malleable. Then, the degree of separation between classes and the appropriate selection of samples with divergence criteria were examined. Classification is performed using the maximum probability algorithm [22].

3. Results

3.1. Sea Surface Temperature

The sea surface temperature data in the study area was collected throughout 30 years-1985 to 2015-by the ECMWF model. The results are presented in Table 1 and Table 2. Furthermore, changes in the sea surface temperature are plotted in Figure 2. Results exhibited an average increase in the sea surface temperature in two studied periods (1986-1999 and 2001-2015) in Khor-e-khoran, which was about 0.2 °C. These variations had a short-term fluctuation and also in recent years, there has been an increase in sea surface temperature average.

Table 1: Mean sea surface temperature changes (°C) in Khor-e-khoran over the 1986-1999 period

Year / Month	JLY	AGU	SEP	NOV	OCT	DEC	Annual Average
1985	32.77	33.09	31.61	30.18	28.26	24.86	28.25
1986	32.86	32.2	31.61	30.67	28.08	25.83	28.15
1987	32.66	32.94	31.64	30.71	27.95	24.48	27.95
1988	32.08	31.9	31.3	30.41	27.81	24.27	27.6
1989	31.99	32.04	30.85	29.89	28.02	25.26	27.68
1990	32	32.95	32.19	30.58	28.05	25.58	27.73
1991	32.17	32.12	31.48	30.56	27.98	24.19	27.75
1992	32.07	32.61	31.82	29.88	27.61	25.25	27.57
1993	31.9	32.1	31.3	30.41	27.42	24.46	27.46
1994	31.81	31.92	31.92	30.09	27.28	24.54	27.27
1995	31.93	32.22	31.54	30.61	27.84	25.3	27.82
1996	31.77	32.07	31.81	30.22	27.49	24.58	27.5
1997	31.78	31.87	31.7	30.11	27.64	24.82	27.19
1998	31.63	31.58	31.13	30.18	27.14	24.67	27.21
1999	32.22	32.07	31.82	30.21	26.73	24.44	27.31

Table 2: Mean sea surface temperature changes (°C) in Khor-e-khoran over the 2001-2015 period

Year / Month	JLY	AGU	SEP	NOV	OCT	DEC	Annual Average
2001	32.01	32.68	31.02	29.95	27.48	24.49	27.68
2002	31.39	32.73	33.03	30.86	27.55	28.46	28.05
2003	33.33	33.67	32.23	30.75	28.15	25	28.14
2004	31.81	32.84	31.61	30.16	28.51	25.56	27.78
2005	32.13	32.66	31.76	30.52	25.35	25.42	27.38
2006	32.85	27.36	31.84	30.43	28.27	25.78	27.48
2007	31.53	31.45	30.87	29.52	27.46	24.93	27.2
2008	31.46	32.34	32.06	29.88	28.05	25.03	27.24
2009	32.43	33.07	32.38	30.21	28.07	25.2	27.69
2010	31.61	32.34	31.86	30.02	28.17	24.91	27.84
2011	31.81	32.32	32.1	30.67	27.53	24.44	27.55
2012	32.71	32.57	31.68	29.57	27.23	24.56	27.72
2013	32.16	32.06	32.3	30.99	28.07	25.33	27.6
2014	32.38	33.2	32.16	30.56	28.62	26.43	28.24
2015	32.57	33	31.56	30.56	28.65	25.92	28.73

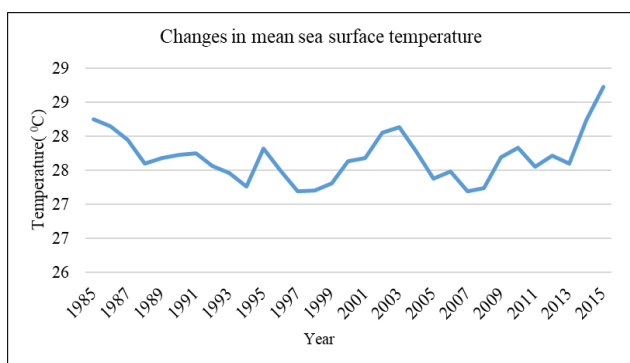


Figure 2: Mean sea surface temperature changes (°C) in Khor-e-khoran for the last 30 years, ECMWF model.

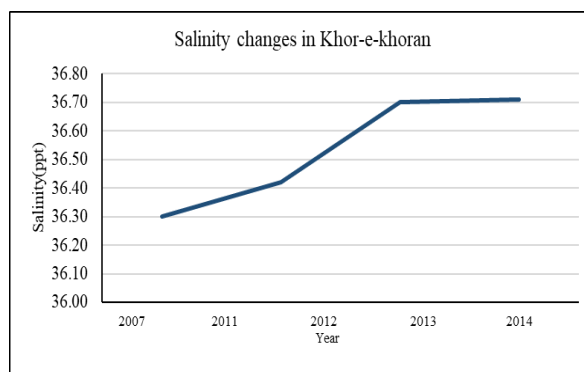


Figure 4: sea surface salinity changes (ppt) in Khor-e-khoran during 2007-2014.

3.2. Sea Surface Salinity

The seasonal variations in sea surface salinity between 2012 and 2015 were indicated by Giovanni model and plotted in figure 3. This chart indicated the average sea surface salinity values in Khor-e-khoran were increased in winter, spring, and summer-during 3 years while only there was a decrease in the mean salinity in fall. The trend of Figure 3 and library documentation indicated that the mean sea surface salinity increased during the studied periods (Figure 4). Since our goal was to investigate the effect of salinity changes on the mangrove trees growth at a low depth. The study of the trend of salinity changes in deep areas was not in line with our objective and could be ignored.

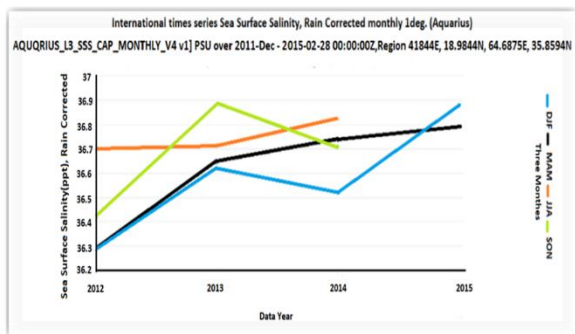


Figure 3: Seasonal variations of sea surface salinity (ppt) in Khor-e-khoran, the Giovanni model, during 2012-2015.

3.3. Vegetation cover

Various methods applied to determine the variation of vegetation cover of mangroves included (i) reduction percentage of mangrove forest by comparison after classification, (ii) reduction percentage of mangrove forest by the variation, (iii) secondary area by comparison after classification, (iv) secondary area by the variation, (v) reduction rate by comparison after classification, and (vi) reduction rate by the variation. The average salinity, average temperature and initial area of mangrove forest per hectares in mangrove habitats of the Khor-e-Khoran area tabulated in table 3. The results of the reduction percentage of mangrove forests by comparison after classification and variation indicated that the area of studied mangrove habitat declined about 2.85 and 2.3%, respectively. Additionally, based on the secondary area by comparison after classification and variation results, it was clarified that the area of studied mangrove habitat is decreased about 2000m2. Moreover, the rates of reduction were recorded about 194 and 151 hectares by comparison after classification and rate of reduction by variation, respectively. As well as, a relative increase was recorded in average sea surface temperature (about 0.2 °C) whereas the initial area of mangrove forest decreased about 1700 hectares during the studied period. Accordingly, all studied methods shown similar results. Results implied a significant decrease in the

area of mangrove habitats in the Khor-e-khoran during the last decades.

4. Discussion and Conclusions

This study was aimed to investigate the sea surface temperature and sea surface salinity changes and its impact on the area of mangrove forests in the Khor-e-khoran region in the last 30 years. The results of satellite and field data showed that the temperature and salinity levels have increased during the studied period, while the area of the mangrove forests has been decreased. In other words, the highest rates of area changes were recorded between 2001 to 2015 which was coincided with the highest variations in sea surface salinity and temperature. So it is suggested that salinity and temperature growth affected the resistance and resilience of mangrove ecosystems of the Khor-e-khoran region against harsh environmental conditions which led to a significant decrease in the area of the studied mangrove habitats.

The observed changes in the mean sea surface temperature in two distinct periods during the last 30 years (1989-1999 and 2001- 2015) indicated that the mean temperature increased 0.2 °C and the average salinity was increased by 0.5 ppt in the second statistical period (2001-2015), compared to the first period (1986-1999). Also in the second period, the decreasing trend of mangrove forests was observed on a larger scale. Therefore, it could be suggested that temperature and salinity anomalies adversely affected the growth of this biological species. As well as, other regional anthropogenic sources of contamination and hypersaline sewages such as wastewaters delivered from industrial areas, petroleum and refinery centers, shrimp farming pools, and fuel and crude oil leakage could ultimately lead to out of balance changes in the natural composition of seawater. The mentioned increase in the sea surface salinity in the Khor-e-khoran area, coincided with a growth in sea surface temperature, indirectly.

Since the temperature and salinity changes are in full interaction, it could not be determined which one has a greater effect on the growth of mangrove forests. Based on the findings of Sabzagbhai et al. (2015) and Tovisekani and Najafipour. (2016), comparing Landsat satellite images in 2002 and 2014, and monitoring the classification, mangrove forests have decreased by 11%. Which is consistent with the result of this research [23, 24]. Also, Noor et al. (2015), in a paper titled "Effects of siltation, temperature and salinity on mangrove plants", mentioned that fluctuations in temperature and salt stress are two important factors in the creation of different anatomical and physiological characteristics in the mangrove trees of the region, which indicates that the area of this ecosystem was reduced [25]. Mangrove species in this region are similar to those in the Qeshm Island. Therefore, it can be concluded that salinity rise or change in its

composition in the region's water has a negative effect on the reproduction and life cycle of mangrove forests and may slow down their growth. Due to the similarity of mangroves in the mentioned studies, this result is also generalized to the mangrove forests of the Khor-e-khoran area.

Additionally, the increase in unemployment and the increase in poverty in the region and the local population's economic dependence on these regions, the difference in the price of fuel in Iran with neighboring countries and its global price has led to an increase in new economic activities for earning money, such as smuggling of fuel. Discharging fuel in water, sometimes in the vicinity of mangrove forests, can damage the roots of mangrove and dehydrate them [22]. The most important regional threats to these forests in the studied area are the wastewater of shrimp farming pools established in the vicinity of the mangrove forests. These hypersaline flows could affect the sea surface salinity of coastal ecosystems. Additionally, the evacuation of fuel and oil in water affected the quality of seawater in shallow ecosystems. Subsequently, unsustainable anthropogenic coastal activities causing biologic changes in the region and ultimately the destruction of its environment [26]. A similar study accomplished by Karimi et al. (2019) reported that untreated wastewaters released from shrimp farms of Say-e-khosh in Bandar-e-Lengeh, located in the western part of the studied area, could be considered as a dominant factor in the degradation of mangrove forests in southern coasts of the Persian Gulf [22]. Besides, harvesting mangrove leaves for livestock, especially camels, during the dry seasons is also a threat to mangrove forests [26].

It is suggested that in order to enrich the region database; more attention will be required to implementing point-to-point water monitoring projects so more sustained programs in line with this issue can be done. Since the rehabilitation of shrimp pools has altered the salinity of the region and has a negative impact on the biology of the area, it is recommended that a proper solution must be adopted in relation to the withdrawal or treatment of wastewaters delivered from shrimp pools in this area. In order to prevent increasing the sea surface temperature and sea surface salinity and to improve the growth of mangrove forests in the target area, managing and monitoring human activities in the region, such as fuel smuggling, is a small, but effective step which can be done.

8. References

- [1] C. C. Jakovac et al., "Costs and carbon benefits of mangrove conservation and restoration: a global analysis," *Ecological Economics*, vol. 176, p. 106758, 2020.
- [2] S. T. Hosseini and V. Chegini, "Seasonal Variation of Physicochemical Parameters in the Coastal Water around the Bushehr Peninsula," (in eng), *Journal of*

- Oceanography, Research* vol. 5. Available in: <http://joc.inio.ac.ir/article-1-528-en.html>, no. 17, pp. 125-143, 2014. [Online]. Available: <http://joc.inio.ac.ir/article-1-528-en.html>.
- [3] R. Mirza, M. Moeinaddini, S. Pourebrahim, and M. A. Zahed, "Contamination, ecological risk and source identification of metals by multivariate analysis in surface sediments of the khouran Straits, the Persian Gulf," *Marine pollution bulletin*, vol. 145, pp. 526-535, 2019.
- [4] B. S. Kuchaksaraei, A. Danehkar, S. M. R. Fatemi, S. A. Jozi, and E. Ramezani-Fard, "An investigation on the human impact intensity on the selected ecoregions of coastal areas of Hormozgan Province, Persian Gulf, Strait of Hormuz, South of Iran," *Environment, Development Sustainability*, pp. 1-17, 2020.
- [5] R. G. Wetzel, *Limnology: lake and river ecosystems*. gulf professional publishing, 2001.
- [6] EPA, "Water Quality Standards Handbook, Chapter 3: Water Quality Criteria," *United States Environmental Protection Agency (EPA)*.
- [7] D. M. Alongi, "Mangrove forests: resilience, protection from tsunamis, and responses to global climate change," *Estuarine, Coastal Shelf Science*, vol. 76, no. 1, pp. 1-13, 2008.
- [8] C. Orwa, A. Mutua, R. Kindt, A. Simons, and R. H. Jamnadass, "Agroforestry database: a tree species reference and selection guide version 4.0," *World Agroforestry (ICRAF)*.
- [9] P. Drennan and N. Pammenter, "Physiology of salt excretion in the mangrove *Avicennia marina* (Forsk.) Vierh," *New Phytologist*, vol. 91, no. 4, pp. 597-606, 1982.
- [10] N. B. Toosi, A. R. Soffianian, S. Fakheran, S. Pourmanafi, C. Ginzler, and L. T. Waser, "Comparing different classification algorithms for monitoring mangrove cover changes in southern Iran," *Global Ecology Conservation*, vol. 19, p. e00662, 2019.
- [11] A. Salehipour Milani and M. Jafar Beglu, "Satellite based assessment of the area and changes in the Mangrove ecosystem of the QESHM island, Iran," *Journal of Environmental Research And Development*, vol. 7, pp. 1052-1060, 2012.
- [12] F. Manson, N. Loneragan, and S. Phinn, "Spatial and temporal variation in distribution of mangroves in Moreton Bay, subtropical Australia: a comparison of pattern metrics and change detection analyses based on aerial photographs," *Estuarine, Coastal Shelf Science*, vol. 57, no. 4, pp. 653-666, 2003.
- [13] R. Zarezadeh, P. Rezaee, R. Lak, M. Masoodi, and M. Ghorbani, "Distribution and accumulation of heavy metals in sediments of the northern part of mangrove in Hara Biosphere Reserve, Qeshm Island (Persian Gulf)," *Soil and Water Research*, vol. 12, no. 2, pp. 86-95, 2017.
- [14] M. A. Zahed, F. Rouhani, S. Mohajeri, F. Bateni, and L. Mohajeri, "An overview of Iranian mangrove ecosystems, northern part of the Persian Gulf and Oman Sea," *Acta Ecologica Sinica*, vol. 30, no. 4, pp. 240-244, 2010.
- [15] B. A. Polidoro et al., "The loss of species: mangrove extinction risk and geographic areas of global concern," *PloS one*, vol. 5, no. 4, p. e10095, 2010.
- [16] G. Akbarzadeh, "Evaluation of physicochemical properties and their relationship with chlorophyll in coastal waters of Hormozgan province," *National Institute of Fisheries Research*, 2016.
- [17] A. Kouros Niya, J. Huang, H. Karimi, H. Keshtkar, and B. Naimi, "Use of Intensity Analysis to Characterize Land Use/Cover Change in the Biggest Island of Persian Gulf, Qeshm Island, Iran," *Sustainability*, vol. 11, no. 16, p. 4396, 2019.
- [18] T. D. Pham and K. Yoshino, "Mangrove mapping and change detection using multi-temporal Landsat imagery in Hai Phong city, Vietnam," *International symposium on cartography in internet and ubiquitous environments*, 2015, pp. 17-19.
- [19] B. Govaerts and N. Verhulst, "The normalized difference vegetation index (NDVI) Greenseeker (TM) handheld sensor: toward the integrated evaluation of crop management part A: concepts and case studies," ed: *CIMMYT*, 2010.
- [20] N. Pettorelli et al., "The Normalized Difference Vegetation Index (NDVI): unforeseen successes in animal ecology," *Climate research*, vol. 46, no. 1, pp. 15-27, 2011.
- [21] S. Shekhar and H. Xiong, *Encyclopedia of GIS*. Springer Science & Business Media, 2007.
- [22] M. Karimi and F. Darabinia, "The Effects of Wastewater from Shrimp Farm in South Qeshm," 2019.
- [23] G. R. Sabzghabaei, S. S. Dashti, M. B. Baleshti, and K. Jafarzadeh, "Change Detection of Khor_e_khooran Harra Protected Area Using Remote Sensing and GIS," *Journal of Marine Biology* vol. I. A. U. Ahvaz – Summer 2015 –VOL.26.
- [24] H. Tovisekani and S. Najafipour, "Change Detection of Khor_e_khooran Harra Protected Area Using Remote Sensing and GIS," *Journal of Marine Biology*, vol. 7, no. 4, pp. 1-12, 2016.
- [25] T. Noor, N. Batool, R. Mazhar, and N. Ilyas, "Effects of siltation, temperature and salinity on mangrove plants," *European Academic Research*, vol. 2, no. 11, pp. 14172-14179, 2015.
- [26] A. S. Milani, "Mangrove forests of the Persian Gulf and the Gulf of Oman," *Threats to Mangrove Forests*: Springer, 2018, pp. 53-7.

The Effect of Silica Nanoparticles' Coating on the Ion Resolution of Anionic Membrane in SGP System

Abdoreza SabetAhd Jahromi^{1*}, Hesameddin Mehrfar²

^{1*} Collage of Basic Science, Jahrom Branch, Islamic Azad University, Jahrom, Iran; ar.sabetahd@yahoo.com

² Faculty of Marine and Oceanic Sciences, University of Mazandaran, Mazandaran, Iran; hmehrfar@gmail.com

ARTICLE INFO

Article History:

Received: 24 Aug. 2021

Accepted: 12 Nov. 2021

Keywords:

renewable energy
salinity gradient
reverse electro dialysis membranes
nano silica particles

ABSTRACT

One of the new sources of renewable energy, is salinity gradient power (SGP) being described as; the entropy energy of mixing the two solutions with different salt concentrations. The extraction of this energy is possible through SGP; the function of this system is based on membrane processes. A system of reverse electro dialysis (RED) was used in this study. Power density (W/m^2) and energy efficiency of the system were evaluated due to the impact of nanotechnology on the use of membranes. The analyses showed that when the concentration of silica nanoparticles in the matrix membrane used in the system is 20 percent and when ion concentration in the solution is 0.055mol/lit , the selectivity of the membrane for ions will be Na^+ , 98.4 percent. However, the selectivity of matrix membrane without the presence of nanoparticles is 82 percent. Also compared to non-nanoscale membranes, the efficiency is increased about 11 percent due to the use of the particles on the anionic membrane as well as their appropriate structure design.

1. Introduction

One of the newest renewable energy issues that have been raised in recent years in the world, is the extraction of energy from salinity gradient in the seas and the ocean. This salinity difference can be found in the residual water of desalination plants, Halocline and estuaries. Reverse electro dialysis (RED) is a promising technology for extracting energy from salinity gradients [1]. The concept of energy production through mixing salt and fresh water was introduced by Patel in 1954 [2]. The way to evaluate the extraction and production of salinity gradient energy and electro dialysis methods were studied in IRENA institute in 2014 [3]. May et al. (2018) investigated energy extraction by reverse electro dialysis and found the use of nano membranes effective in increasing energy and flow [4]. Ju et al. conducted a study comparing RED and PRO processes using different solutions with low and high salinity water in terms of power density and deposition potential [5]. SGP system is a system for energy extraction and based on spontaneous processes and membrane techniques. Spontaneous Process refers to a reaction that is performed without receiving energy from an external source. To realize this kind of process, three thermodynamic quantity of entropy, enthalpy and temperatures are examined. Entropy (S) is a thermodynamic state function that shows the distribution of energy and matter in a system.

Spontaneity of a process is concerned with the total entropy's changes or in other words; the system's and the environment's total entropy [6].

$$\Delta S_{Total} = \Delta S_{system} + \Delta S_{environment} \quad (1)$$

However, it is impossible to calculate the entropy changes of the environment. To avoid this problem, we limit ourselves to the processes that occur at fixed temperature and pressure. In practice, this limitation does not cause serious problems. Another important point is that neither entropy nor enthalpy can indicate the spontaneity of a reaction. For this purpose, a new thermodynamic function is introduced. The function is called Gibbs free energy (G)[6].

$$G = H - TS \quad (2)$$

Equation (2) is a thermodynamic equation of state for each transformation from Mode 1 to Mode 2 at fixed temperature and pressure and it is written as follows:

$$G_2 - G_1 = (H_2 - H_1) - T(S_2 - S_1) \quad (3)$$

Equation (3) can be written as follows;

$$\Delta G_{system} = \Delta H_{system} - T\Delta S_{system} \quad (4)$$

This equation is called Gibbs – Helmholtz. Spontaneous condition can now be defined exactly for

the system that is under constant pressure and temperature. According to the second law of thermodynamics, for a spontaneous process we will have $\Delta S_{Total} > 0$ in this case, $-T\Delta S_{Total} < 0$ and thus we will have $\Delta G_{system} < 0$. In other words, when a spontaneous process occurs in a system being under constant pressure and temperature, the total entropy is increased and Gibbs' free energy is decreased.

Table 1. Gibbs free energy and the type of transformation
the type of transformation ΔG_{system} In constant T and P

Spontaneous	$\Delta G_{system} < 0$
Balance	$\Delta G_{system} = 0$
Non-Spontaneous	$\Delta G_{system} > 0$

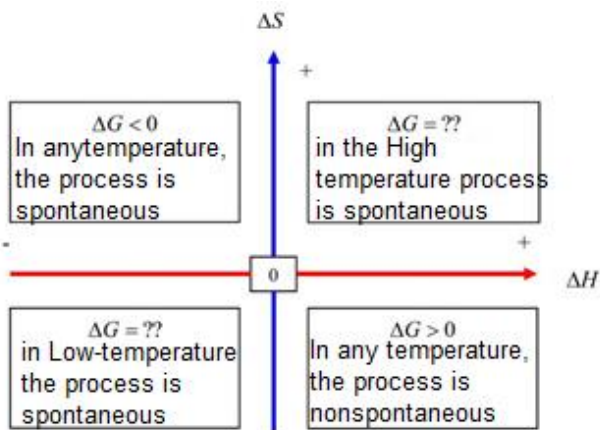


Figure 1. Gibbs free energy and the process

Membrane techniques used in this study, is the Reverse Electro Dialysis (RED) in which the anionic and cationic membranes are used. Electrodialysis techniques (ED) was invented by Maigrot and Sabates(1982). One application of this technique is its use in seawater desalination systems [7].

reuse of consumed electrical energy is possible by the reverse membrane process (Fig 2).

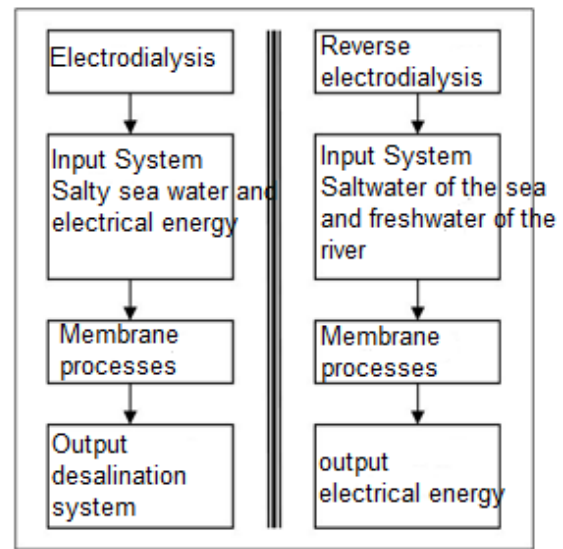


Fig. 2. Different stages of electro dialysis and reverse electro dialysis

In contrast to the electro dialysis method, in reverse electro dialysis, the concentration difference between consecutive cells is used instead of the power supply to excite the ions to cross the anionic and cationic membranes. The ions are then separated by membranes, and entered electrodes chamber on both sides, through where redox reactions, an ionic current is turned into an electron current. This phenomenon creates a potential difference between the electrodes, resulting in a battery charging. Figure (3) shows the performance of anionic and cationic membranes in the separation of sodium and chloride ions [9].

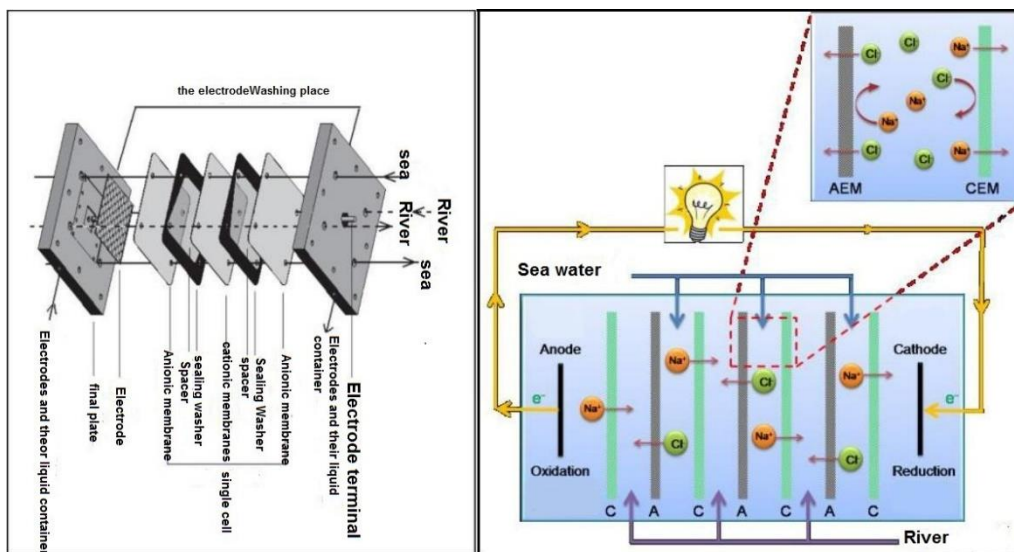


Figure 3. a view of the SGP system based on reverse electro dialysis membrane process RED

Manecke(1852) proposed to save energy by using reverse electro dialysis process[8]. He proved that the

In the figure (3) AEM represents the anion exchanger membrane and CEM represents the cation exchange

membrane. The use of this process in the physical model design is an important part of this research.

2. Calculation of entropy energy of mixing the two solutions with different concentrations

As shown in Figure 3, containers of reverse electro dialysis system are filled with a volume of seawater (V_S) and river (V_R) with different salt concentrations of C_S and C_R . In this system, an ionic current is produced and turned into electron current by redox reactions in the electrodes. This process continues until the concentration of the solution is the same on both sides of each chamber. The concentration is shown by C_M and calculated as follows [10,11].

$$C_M = \frac{C_S V_S + C_R V_R}{V_S + V_R} \quad (5)$$

To calculate the recoverable energy from mixing the two solutions of different concentrations, we need to calculate the entropy of mixing between the two solutions. To calculate this quantity we can use the following equation;

$$\Delta S = \int \frac{dQ}{T} \quad (6)$$

The first law of thermodynamics states that any thermodynamic system in equilibrium has a variable called internal energy (U) whose changes is obtained through the equation (7);

$$dU = dQ - dW \quad (7)$$

In the above equation, dQ and dW are a small fraction of the heat exchanged and the amount of work performed by system. For processes that occur at fixed temperature and pressure, internal energy change of the system is zero ($dU = 0$) and consequently $dQ = dW$. However, it can be noted that in reverse electro dialysis system with the movement of ions, concentration of solutions has changed and then the system will be faced with volume changes, though slightly. In this case, the amount of work done can be calculated from equation (8);

$$W = \int dQ = \int \Pi dV \quad (8)$$

In relation (8), Π osmotic pressure is based on p_a that can be calculated through (9) classical state equation.

$$\Pi V = nRT \quad (9)$$

In this regard, volume (v) is calculated based on m^3 and n represents the number of moles which is defined as $n = 2CV$. Factor 2 is Van 't Hoff factor that is caused by the decomposition of a one-mole $NaCl$, to two-mole ions and C is the concentration of the solution. Given the approximate isothermal process, Gibbs free energy is obtained through (10) relationship.

$$\Delta G = -T\Delta S_{total} = -\left[\int \Pi_S dV + \int \Pi_R dV\right] = \left[-n_S RT \int_{C_S}^{C_M} \frac{dC}{C} - n_R RT \int_{C_R}^{C_M} \frac{dC}{C}\right] \quad (10)$$

Equation (3) can be written as follows;

$$\Delta G = -2RT \left[C_S V_S \ln \frac{C_S}{C_M} + C_R V_R \ln \frac{C_R}{C_M} \right] \quad (11)$$

3. SGP System

SGP system used in this study is based on the performance of reverse electro dialysis membrane; it is an electrochemical cell being based on the concentration gradient. The system is a single-cell system that uses two anionic membrane and a cationic membrane. In addition, the membranes are another important part of this system includes spacer, electrode compartment electrode, electrolyte and sealing washers. Figure 4 video system shows the SGP made in this project [12]. In addition to the membranes, the system has other important: spacer, electrodes, electrode compartment, electrolyte and sealing washers. Figure 4 shows a picture of the SGP made in this project.



Figure 4. SGP system with nano-structured membranes used in this study

4. Cationic and anionic heterogeneous membranes coated with nano

As it was stated the construction of the battery involves heterogeneous membrane ion exchanger (Figure 5)



Figure 5. Heterogeneous anionic and cationic membranes of nanostructures on preservatives frames

Table 2, represents physical and chemical characteristics of the membranes before the placement of nano particles on them.

Table 2. Physical and chemical properties of heterogeneous ion exchanger membranes

Items tested	Unit	Membrane type	
		cationic membranes (CEM)	Anionic membranes (AEM)
Exchange capacity \geq	<i>mol/kg</i>	2.0	1.8
Resistance of membranes	$\Omega.cm^2$	2	2
The degree of dimensional change \leq	%	3	3
Bearable pressure due to membrane's strength against tearing \geq	<i>MPa</i>	0.6	0.6
Chemical stability	<i>PH</i>	1 ~10	1 ~10
Selectivity of the membrane \geq	%	90	89
Penetrability and water permeability \leq	<i>ML/h.cm²</i>	0.1	0.1
Thermal or heat stability \leq	$^{\circ}C$	40	40
Dimensional properties of membranes			
Thickness	Error thickness in the dry state		
0.42 mm	$\pm 0.04mm$		

In the desalination systems of seawater whose activity is based on electro dialysis, heterogeneous membranes have shown a unique technical performance. These membranes are widely used in other industries such as the semiconductor industries, input water heaters, boilers, machinery, electronics, pharmaceutical industries, biological experiments and researches related to water use. The use of these nano-structured membranes for reverse electro dialysis systems paves the way for the arrival of the product to renewable energy industries.

In this project the performance of the uncoated membranes with nanoparticles, were studied in their structure. The function of the membranes in reverse electro dialysis battery was studied and compared with the results of research conducted by Veerman [13,14]. It was found that in all studies, membranes' performances were faced with considerable problems:

- High deposition rate on the surface of the membrane and disruption in reverse electro dialysis process.
- Low speed and volume of ion transfer in membrane, followed by the reduction of energy extraction process

Nanotechnology was used to overcome the problems. In this regard, the idea of using nanoparticles in the membrane structure of the ion exchanger was formed. The investigation showed that the nanoparticles enhance thermal and mechanical stability due to their unique properties of the membranes. Also according to

the type of nanoparticles, we can increase the selectivity of the membrane. Therefore, desirable properties of the membrane can be improved by adding suitable nanoparticles to the matrix of a polymer membrane. For this purpose, after careful study of the performance of nano-particles on the membrane ion exchanger, we decided to use silica nanoparticles in the structure of cation exchanger heterogeneous membrane. Silica or silica dioxide is the most abundant material on earth's crust. The compound with the chemical formula of SiO₂ has a structure similar to diamond being a white crystalline substance. It has a relatively high melting and boiling temperature and exists in the nature as crystal and amorphous. Nanoparticles of silicon dioxide are spherical with a diameter of less than 100nm. These particles are in the form of dry powder or solution. In this study, the coating of silica nanoparticles is used with an average diameter of 40nm. After the coating of membrane with silica nanoparticles, its features were evaluated through the produced images by a scanning electron microscope (SEM) (Figure 6).

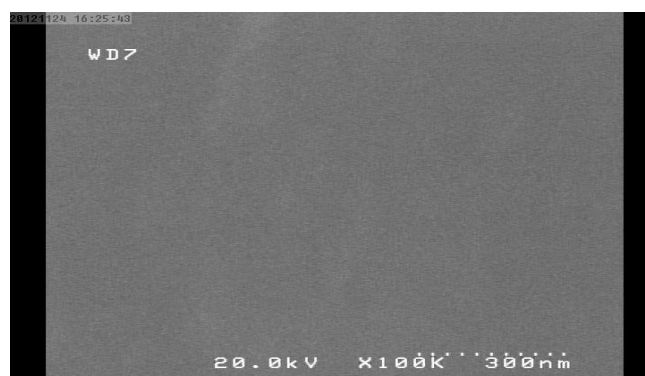


Fig. 6 Obtained images of the cation exchanger membrane coated with nanoparticles produced by SEM

The analyses showed that when the concentration of silica nanoparticles in the matrix membrane used in the system is 20 percent and when ion concentration in the solution is 0.055 *mol/lit*; the selectivity of the membrane for ions will be Na⁺, 98.4 percent. However, the selectivity of matrix membrane without the presence of nanoparticles is 90 percent. If the concentration of silica nanoparticles in the matrix membrane is 0.28 percent, ion diffusion coefficient of Na⁺ will be obtained through $11.16 \times 10^{-12} m^2/s$. While the diffusion coefficient for the ion in the cation exchanger membrane and without the presence of silica nanoparticles is $3.71 \times 10^{-12} m^2/s$. Comparing these two features shows the importance of the presence of silica nanoparticles in the membrane structure. The cationic membranes with nano-coating have other features that some of them are mentioned below.

- Silica nanoparticles reduce water's alkalinity through chemical reactions with calcium hydroxide (Ca (OH)₂) and prevent its deposition on the membrane. So the particles increase the membrane

antifouling properties and cause long persistence of ions' flux (to overcome the first problem)

- Silica nanoparticles lead to high thermal and mechanical stability of the membrane.
- Silica nanoparticles do not have any environmental emission
- For membranes containing silica nanoparticles, surface morphology of the membrane, the water capacity, selectivity (ions selection) (water absorption) hydrophilicity and capacity of ion exchange of membranes were measured and evaluated. For example, the selectivity of the membrane with silica nanoparticles (SiO_2) increases but its increase is related to the concentration of the nanoparticles in the membrane matrix.

5. Discussion and Conclusion

So far, a few research centers and businesses have manufactured reverse electro dialysis batteries. Some of these centers work on membranes with high efficiency and low cost activities and others on the design of the battery its cells. Table 3, indicates several types of batteries that are designed from 1854 up until now; they are compared with each other in terms of output power density. As you can see with the passage of time and improvements in the designing membrane batteries' structure, their output power density has increased significantly.

Table 3. Membrane's thickness and power density $P(W/m^2)$ inRED System

Power density W/m^2	Membrane thickness	year	Researcher	No
0.05	0.7	1955	Pattel	1
0.17	1	1976	Weinstein and Litz	2
0.40	3	1983	Adynus	3
0.41	0.55	1986	GroZynsky et al.	4
0.46	0.19	2007	Turkish	5
0.26	1	2007	Sevda	6
0.95	0.2	2008	Veerman et al	7
1.18	0.2	2009	Veerman et al	9
0.52	Non nano-coating			
	0.42	2014	SabetAhd et al	8
0.58	nano-coating			

Another feature of the RED system is the application of silica nanoparticles on the membrane surface. This led to the 11 percent increase of the extraction of membrane surface unit provided in the physical model. Therefore, the coating of silica nanoparticles' membrane has had an effective role in improving system performance. Of course, this laboratory process was limited due to high costs and lack of financial resources. Therefore, more research is needed to assess the exact impact of nano-coatings.

8. References

- [1] Tian, H., Wang, Y., Pei, Y. and Crittenden, J. C., (2020), *Unique applications and improvements of reverse electro dialysis*, A review and outlook, Applied Energy, Vol.262, p.114482.
- [2] Pattle, R. E., (1954), *Production of electric power by mixing fresh and salt water in the hydroelectric pile*, Nature, Vol.174(4431), p.660-660.
- [3] IRENA Ocean Energy Technology Brief 2, salinity gradient energy technology brief, June 2014
- [4] Mei, Y. and Tang, C. Y., (2018), *Recent developments and future perspectives of reverse electro dialysis technology*, A review, Desalination, 425, p.156-174.
- [5] Ju, J., Choi, Y., Lee, S. and Jeong, N., (2021), *Comparison of fouling characteristics between reverse electro dialysis (RED) and pressure retarded osmosis (PRO)*, Desalination, Vol.497, p.114648.
- [6] Zemansky, M. W. and Dittman, R., (1981), *Heat and Thermodynamics*, sixth edition, Mc Graw-Hill, p.233-267.
- [7] Maigrot, E. and Sabates, J., (1890), *Apparat zur Läuterung von Zuckersäften mittels Elektrizität*, Germ. Patent, (50443).
- [8] Manecke, G., (1952), *Membranakkumulator*, Zeitschrift für Physikalische Chemie, Vol 201(1), p.1-15.
- [9] Veerman, J., Saakes, M., Metz, S. J. and Harmsen, G. J., (2009), *Reverse electro dialysis: Performance of a stack with 50 cells on the mixing of sea and river water*, Journal of Membrane Science, Vol 327(1-2), p.136-144.
- [10] Post, J. W., (2009), *Blue Energy: electricity production from salinity gradients by reverse electro dialysis*, Wageningen University and Research.
- [11] Post, J. W., Veerman, J., Hamelers, H. V., Euverink, G. J., Metz, S. J., Nymeijer, K. and Buisman, C. J., (2007), *Salinity-gradient power: Evaluation of pressure-retarded osmosis and reverse electro dialysis*. Journal of membrane science, Vol 288(1-2), p.218-230.
- [12] Sabetahd, A. R. et al., (2011), Study of extracting energy systems from salinity gradient and selection of suitable system for southern coasts of Iran, 26th International Power System Conference (PSC), Tehran, Iran.
- [13] Veerman, J., De Jong, R. M., Saakes, M., Metz, S. J. and Harmsen, G. J., (2009), *Reverse electro dialysis: Comparison of six commercial membrane pairs on the thermodynamic efficiency and power density*. Journal of Membrane Science, Vol 343(1-2), p.7-15.
- [14] Veerman, J., (2010), *Reverse electro dialysis: design and optimization by modeling and experimentation*. University of Groningen.
- [15] Pattle, R. E., (1955), *Electricity from fresh and salt water-without fuel*. Chem. Proc. Eng., Vol 35, p.351-354.

Caspian rapid Sea level fluctuation and intensity of displacement of the shorelines in the Gorgan Bay and Miankaleh coast

Homayoun Khoshnavan

Associated professor of the water research institute, Caspian Sea national research & study center, Tehran, Iran,
H_khoshnavan@yahoo.com

ARTICLE INFO

Article History:

Received: 26 Jun. 2021

Accepted: 20 Oct. 2021

Keywords:

**Caspian Sea
Fluctuations
Gorgan Bay
shoreline relocation**

ABSTRACT

Displacement of coastlines under the influence of hydrodynamic factors and rising sea levels cause serious damage to economic, social and environmental infrastructure, and rapid fluctuations in the Caspian Sea water level since the twentieth century have created adverse conditions for the coastal environment. The main objective is to assess the severity of changes in the shores of Gorgan Bay and Miankaleh coast as protected environmental areas of wildlife sanctuaries and biosphere reserves during a period coinciding with the decrease of the Caspian Sea water level during the years 1995-2019. The morphological conditions of the coastlines of Gorgan Bay and Miankaleh coast were investigated by field observations and analysis of satellite images. A total of 10 study axes were selected around Gorgan Bay and Miankaleh and the intensity of shoreline movement by processing multi-time satellite images belonging to the years (1995-2019) in the GIS environment and with the help of digital software for coastal line analysis (DSAS), was calculated. Based on the shoreline movement, the study area was classified into three groups with shoreline changes (high, medium and low). The results show that the northeastern extremities of Miankaleh and the western extremity of Gorgan Bay have the highest coastline displacement and the central areas south of Gorgan Bay and the north-central part to the western part of Miankaleh coast have very little displacement. For comprehensive management of coastlines in the study area, focus on areas with high physical vulnerability is necessary and continuous control of quantitative and qualitative changes in coastal habitats affected by fluctuations in the water level of the Caspian Sea can reduce the existing challenges.

1. Introduction

Global warming and rising ocean water level during the Anthropocene have created the right conditions to increase the physical vulnerability of coastal areas, and large areas of the Earth's coast have been flooded and eroded [10]. The relocation of coastlines has a direct impact on various economic infrastructures such as commercial ports, fishing docks, thermal power plants and coastal tourism facilities [11, 34]. The Caspian Sea coast is no exception to this rule and has undergone serious changes and extensive environmental challenges due to fluctuations in sea level, which is sometimes more than a hundred times faster and sometimes in the opposite direction of the oceans [19, 25, 16]. Fluctuations in the water level of the Caspian Sea since the twentieth century have caused the deformation of coastal processes and the joint impact of the fluctuating phases of the Caspian Sea and human factors, conditions of sedimentation regime change,

shoreline displacement and the development of erosion phenomena on the coast [17, 25, 6]. The economic consequences of a 250 cm increase in the Caspian Sea water level during the period 1978-1995 are estimated at more than \$ 17 billion [24]. The rapid decline of the Caspian Sea water level during the periods 1930-1978 and 1995-2019 has led to major deformation of natural habitats, extinction of coastal wetlands and the impact of centralized economic capacity in coastal areas [21, 27]. Qara Baghaz Bay, as the largest reservoir on the eastern shore of the Caspian Sea and with very high environmental value, during the eighties of the twentieth century, due to the increasing decline in the water level of the Caspian Sea completely dried up and lost its wetland ecosystem services. The effect was to inflict great economic and social damage on the former Soviet government [24]. At present, about 30% of the area of Gorgan Bay and a large part of Miankaleh wetland has dried up due to the decrease of water level

in the Caspian Sea and its important coastal habitats have been destroyed [24]. Calculating the intensity of variability of coastlines in different regions of Gorgan Bay and Miankaleh coast from the decrease of Caspian Sea water level is the main question in this study. The average rate of decline of the Caspian Sea water level during 1995-2019 was about 6 cm per year and during the last 24 years, the Caspian Sea water level has decreased by 150 cm [24]. The quantitative and qualitative impact of wetland and sand environments around Gorgan Bay during the mentioned time is very different and with the process of wetland drying, terrestrial ecosystems have quickly replaced aquatic ecosystems [24]. Behavioral response of coastlines to sea level fluctuations depend to important natural criteria, such as: average shore slope, embankment width, type and texture of coastal sediments, rate of change in sea level, coastal landforms, intensity of tidal currents and the energy of the waves [23]. The rate of shoreline displacement in Gorgan Bay is also a function of the topography of the wetland bed and the dry coastal part and the highest intensity of shoreline shifts occurred in the western and northeastern regions of Gorgan Bay [24, 34]. Gorgan Bay is a suitable dynamic system for analyzing the impact of Caspian Sea water level fluctuations on the coastal environment [24]. A large part of the western part of Gorgan Bay dried up during the 1930s-1978 with the decrease of the Caspian Sea water level and today, again, similar hydromorphological conditions have occurred for Gorgan Bay [24, 34]. Gorgan Bay, under the Caspian Sea declining scenario, will move towards complete drought by 1402 due to the closure of its connection [34]. The high rate of sedimentation in the area of the communication channel between Gorgan Bay and the Caspian Sea has provided the conditions for changing the topography of the bed and the drying process [12, 7]. Fluctuations in the Caspian Sea level and its common hydrodynamic phenomena such as: riparian currents, wind turbines, density and fluvial flows of river waters have a very important role in the morphodynamic deformation of Gorgan Bay [30]. The growth of the Miankaleh sandy spit at the edge of the submerged depression parallel to the Great Mazandaran fault during the late Holocene period has created suitable conditions for the creation of Gorgan Bay [24]. Gorgan Bay has progressed to complete drought many times during the geological period, but the increasing oscillating phases of the Caspian Sea water level have created conditions for its regeneration and reconstruction [13]. Today, the use of digital shoreline analysis system (DSAS) software to calculate and statistically analyze the shoreline movement of the Earth's seas, in the GIS environment is widely used [11, 12, 36]. It is also possible to study the changes of the coastline of Sefidrud delta using satellite images [5] and to evaluate the changes of the coastline in the Caspian delta basin using the digital shoreline analysis

system (DSAS) deltas: Haraz, Babolrood and Talar [34] pointed out in Iran. The results of studies on the displacement of the Sefidrud delta coastline have shown that coastal landforms have undergone significant changes over time due to fluctuations in the water level of the Caspian Sea [2, 4, 35, 20]. A study of shoreline changes in Gujarat and Arisa, India has shown that rising Indian Ocean water levels have caused shoreline shifts and the severity of erosion of coastal lowlands [27, 28]. A study of littoral processes of the Atlantic coast of the United States found that storm surges, along with rising Atlantic water levels, caused shoreline shifts and increased severity vulnerabilities in coastal areas [37]. Changes in coastlines around the main ports in the north of the country during the period (2005-2012) were studied by the Ports and Maritime Organization (2008), [29], using Landsat satellite images and it was found that the shoreline displacement is a function of fluctuations in the Caspian Sea water level and processes of deposition. Due to the fact that so far, no comprehensive research has been conducted on the quantitative changes of the coastline of Gorgan Bay and Miankaleh coast during the phase of decreasing water level of the Caspian Sea. Therefore, the main purpose of this study is to calculate and statistically analyze the quantitative intensity of coastline movement in different regions of Gorgan Bay and Miankaleh coast. The intensity of changes in the coastline of Gorgan Bay, using statistical analysis, was assessed by processing multi-time satellite images in the software of digital shoreline analysis (DSAS) in the GIS environment.

2. Materials and methods

2.1. Study area

The Caspian Sea, as the largest lake on Earth, is located in the very important geopolitical region of Eurasia, and the five countries of Azerbaijan, Iran, Kazakhstan, Russia and Turkmenistan are the coastal countries around it (Figure 1). The Caspian Sea stretches along the Earth's meridian and is located between latitudes (07°, 47' and 33°, 36') north and longitudes (43°, 43' and 53°, 54') east. The sea is 1200 km long and its average width is 310 km. Its maximum and minimum widths are 435 and 196 km. The water level of the Caspian Sea is currently -28 meters lower than the water level of the Baltic Sea. Under this altitude level, the Caspian Sea surrounds about 7500 km and an area of more than 390,000 square kilometers. The change in the size of the Caspian Sea is a function of fluctuations in the water level of the Caspian Sea. The volume of water in the Caspian Sea is 78,000 cubic kilometers. Its average depth is 208 meters and its maximum depth is 1025 meters in the southern depression [14]. This large lake has no known tides and its average salinity is about one third of the ocean water salinity, (13 grams per liter), [22]. The salinity of the Caspian Sea water increases

along the north-south from the mouth of the Volga River with the combination of fresh water to the southern part of the Caspian Sea with the combination of brackish water. The Caspian Sea bed is divided along the north-south into three shallow northern areas, the middle Apsheron depression and the southern depression of Darband (Figure 1). The southern part of the Caspian Sea covers about 65% of the Caspian Sea water resources [22]. The deepest part of the Caspian Sea is its southern gorge, which overlooks the northern coast of Iran. Apsheron ridge with a depth of 160 to 180 meters separates the central part from the southern depression of the Caspian Sea. The morphological appearance of the coasts of the southern part of the Caspian Sea is mostly affected by the trend of the northern heights of Alborz. The average height of the Alborz mountains is about 2000 meters and from these heights about 62 main rivers flow to the Caspian Sea. The southern part of the Caspian Sea overlooks the northern coast of the country in the provinces of Golestan, Mazandaran and Gilan from the city of Gomishan in the southeastern tip to Astara in the extreme southwestern part. Specific climatic conditions of this region of the Caspian Sea with different distribution of temperature and precipitation have a direct impact on the formation and structural changes of coastal morphological features such as: coastal plains, sandy areas, mudflats, deltas, alluvial fans, fluvial plains and rivers along the coastline of the Caspian Sea and the geographical location of desert, coastal, forest, river and plain environments in different areas of the southern shores of the Caspian Sea depends on the long-term dominance of climatic factors [22]. Therefore, the climate of the southern coasts of the Caspian Sea is one of the most important criteria for shaping the structure of coastal morphology. Geological structure of northern Alborz mountains from Gorgan to Rasht and from Rezvanshahr to Astara with various stratigraphic characteristics and geodynamic performance of active faults such as: Mazandaran large fault, Lahijan fault and Astara fault play a very important role in creating morphological zones on the coasts South of the Caspian Sea and the hydrodynamic forces of the Caspian Sea (fluctuations in water level, waves and coastal currents) and hydraulic forces of rivers have caused coastal morphological effects. The southern coasts of the Caspian Sea extend from the southwestern tip (Astara port) to the southeastern tip (Gomishan coast) with a length of 890 km [29], (Figure 2). The length of the coastline in Mazandaran, Golestan and Gilan provinces is 487, 131 and 272 km, respectively [29]. The southern coasts of the Caspian Sea are divided into five morphological units based on the geometric structure of coastal areas and the type of coastal landforms [15]. coasts with steep slopes in the dry part in the western part of Mazandaran and northwest of Gilan with coarse-grained and gravel sandy sediments and very

low slopes with silty to clay silty sediments in the southeastern extremity along the southern part of Gorgan Bay is located in the eastern part of the coast of Turkmen port and Gomishan. Low sandy beaches can also be seen in the area overlooking the coast of Astara. The southern coasts of the Caspian Sea, in terms of sediment morphodynamics are classified into types (reflective, dissipative and intermediate) [16] and are divided into categories (erosive, intermediate or equilibrium and active sedimentary) in terms of severity of erosive vulnerability [15]. Gorgan Bay is located in the easternmost part of the southern coasts of the Caspian Sea (Figure 1), [30]. This intercontinental depression is separated from the Caspian Sea by the Miankaleh sand spit and is connected to the Caspian Sea at the northeastern end by the Chapoqli and Ashooradeh communication channels (Figure 1). Gorgan Bay catchment area has an area of about 15,000 square kilometers and includes mountainous areas, foothills and coastal plains [24]. Numerous permanent and seasonal rivers from the southern and eastern part overlooking the northern slopes of Alborz lead to Gorgan Bay, of which Qarasu and Gorgan rivers, with a total average annual discharge of half a billion cubic meters and a volume of sediment of 3.5 million Tons per year are the most important of them [1]. The results of the hydrogeochemical study of Gorgan Bay have shown that the amount of water entering the Caspian Sea to Gorgan Bay has a very important role in the chemical properties of water and sediment in Gorgan Bay and the impact of rivers is very small [6]. The environment of Gorgan Bay is affected by the Caspian Sea, the rivers leading to it and the Miankaleh Peninsula. Gorgan Bay was registered in 1975 along with Miankaleh and Lapoo Zaghmarz wetlands as a biosphere reserve in the first international wetland complex of the world in the list of wetlands of Ramsar Convention. In the classification of wetlands in the Ramsar Convention (1975), [7]. Miankaleh wetland and Gorgan Bay are considered as type A or permanent shallow sea waters. This area includes a collection of valuable ecosystems and sensitive and vulnerable habitats, as well as beautiful landscapes and natural tourist attractions. Therefore, Gorgan Bay has a very high environmental value.

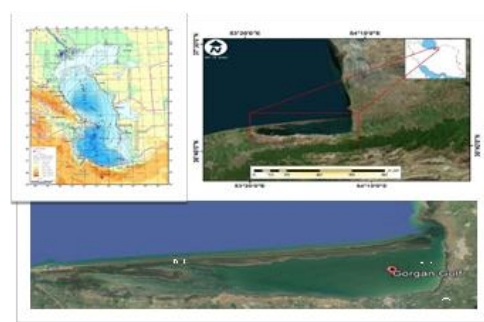


Figure 1. Geographical position of the Caspian Sea, Gorgan Bay, Miankaleh coast and measuring axes (West Miankaleh: MG, Miankaleh West: WM, Miankaleh Central: CM,

Miankaleh: EM, Gorgan Bay Northwest: NWG, Gorgan Northeast: NEG, Turkmen Port: TP, Gaz port: GP, South Central Region of Gorgan Bay: SCG, Southwest Region of Gorgan Bay: SWG).

2.2. Research method

This research has been done by the method of documentary studies and software analysis. At first, the necessary acquaintance with the characteristics of natural geography and morphology of the study area was done by reviewing scientific documents, including: specialized reports, research articles, thematic maps. Then, by initial processing of existing satellite images through Google Earth software (Google Earth Pro, 2020), the morphological appearance of the coast was examined and 10 measuring axes were selected based on the criteria of diversity of coastlines and landforms located in them (Figure 1). The rate of change of Caspian coastlines along transects with a distance of 100 meters in the software of digital shoreline analysis system (DSAS) and Landsat multi-time satellite images (TM and LOI sensors) with a spatial resolution of 30 meters in GIS environment with the help of software (Arc-Map) version 10.6.1 belonging to ESRI company in the years 1995-2019 along the 10-axis shoreline in Gorgan Bay was analyzed (Figure 2). The shoreline displacement was calculated in the GIS software environment, and multi-time images of Landsat satellite sensors from 1995 and 2019 were processed based on the data in band (5) which is close to the infrared spectrum (NIR), and the boundary between the dry coast and the shallow part of the sea was separated and the coastline was drawn (Figure 2). Then, the amount of shoreline movement in the above-mentioned time period (NSM) and its annual average (EPR) compared to the baseline in the software environment of digital shoreline analysis system (DSAS) and with the help of transect module at distances of 100 meters, was drawn and calculated. All numerical data were processed in the form of data tables in Microsoft Excel software environment and curves and graphs related to the shoreline displacement were generated (Figure 2) and finally by summarizing the results, the research objectives were achieved.

3. Results

3.1. Changing the coastline in the northwestern part of Miankaleh

The average rate of positive displacement of the shoreline or retreat of the Caspian Sea water in the northwestern part of Miankaleh coast during the period of 24 years between 1995-2019 is equal to 127 meters (Table 1), which averages 5 meters per year, sand embankment width in this area has increased (Table 2). The maximum shoreline movement is 166 meters and the minimum is 74 meters (Table 1). shoreline changes in this part of the study area are uniform and the change threshold is between 3 to 7 meters per year (Table 2).

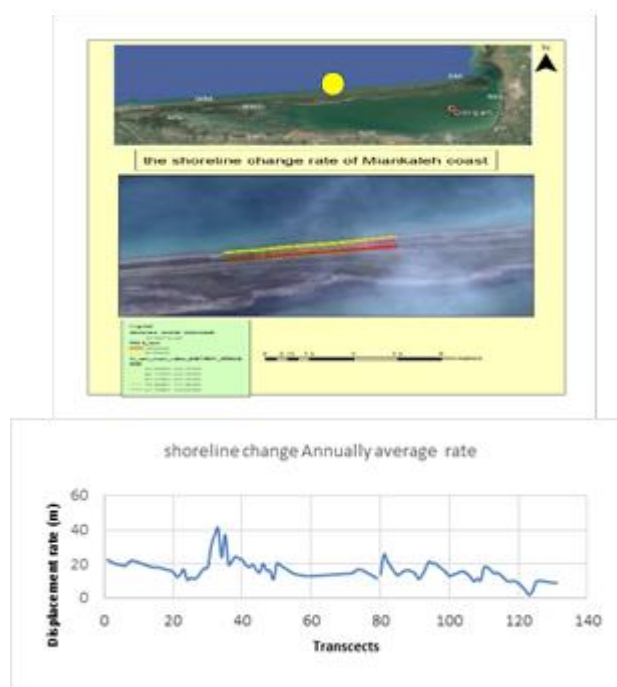


Figure 2. Drawing and comparing the coastline of the study area in the software of the GIS and with the help of ancillary software Digital Analysis of Coastlines (DSAS)

3.2. Changing the coastline in the north-central area of Miankaleh

The average positive displacement of the Caspian Sea shoreline or water retreat in the northwestern part of the Miankaleh coast during the 24-year period between 1995-2019 is 476 meters (Table 1), which averages 20 meters per year, the width of the sand embankment in this area has increased (Table 2). The maximum shoreline movement is 550 meters and the minimum is 434 meters (Table 1). Coastline changes in this part of the study area are uniform and the change threshold is between 18 to 23 meters per year (Table 2).

3.3. Changing the coastline in the northeastern part of Miankaleh

The average positive displacement of the Caspian Sea shoreline or water retreat in the northwestern part of the Miankaleh coast during the 24-year period between 1995-2019 is equal to 1626 meters (Table 1), which averages 68 meters per year, the width of the sand embankment in this area has increased (Table 2). The maximum shoreline movement is 2777 meters and the minimum is 1137 meters (Table 1). The shoreline changes in this part of the study area are very large and the change threshold is between 47 to 116 meters per year (Table 2).

3.4. Changing the coastline in the northeastern part of Gorgan Bay

The average positive displacement of the Caspian Sea shoreline or water retreat in the northwestern part of the

Miankaleh coast during the 24-year period between 1995-2019 is equal to 242 meters (Table 1), which averages 10 meters per year, the width of the sand embankment in this area has increased (Table 2). The maximum shoreline movement is 519 meters and the minimum is 57 meters (Table 1). Coastline changes in this part of the study area are moderate and the change threshold is between 2 to 22 meters per year (Table 2).

3.5. Changing the coastline in the northwestern part of Gorgan Bay

The average positive displacement of the Caspian Sea shoreline or water retreat in the northwestern part of the Miankaleh coast during the 24-year period between 1995-2019 is equal to 381 meters (Table 1), which averages 16 meters per year, the width of the sand embankment in this area has increased (Table 2). The maximum shoreline movement is 982 meters and the minimum is 41 meters (Table 1). The shoreline changes in this part of the study area are large and the change threshold is between 2 to 41 meters per year (Table 2).

3.6. Changing the coastline in the Turkmen port area

The average positive displacement of the Caspian Sea shoreline or water retreat in the northwestern part of the Miankaleh coast during the 24-year period between 1995-2019 is equal to 1058 meters (Table 1), which averages 44 meters per year, the width of the sand embankment in this area has increased (Table 2). The maximum shoreline movement is 1262 meters and the minimum is 729 meters (Table 1). Coastline changes in this part of the study area are very large and the change threshold is between 30 to 52 meters per year (Table 2).

3.7. Changing the coastline in the area of Gaz port

The average rate of positive displacement of the shoreline or retreat of the Caspian Sea water in the northwestern part of Miankaleh coast during the period of 24 years between 1995-2019 is equal to 654 meters (Table 1), which averages 27 meters per year, sand embankment width in this area has increased (Table 2). The maximum shoreline movement is 1288 meters and the minimum is zero meters (Table 1). Coastline changes in this part of the study area are large and the change threshold is between zero and 54 meters per year (Table 2).

3.8. Changing the coastline in the south-central area of Gorgan Bay

The average positive displacement of the shoreline or retreat of the Caspian Sea water in the northwestern part of Miankaleh coast during the period of 24 years between 1995-2019 is equal to 526 meters (Table 1), which averages 22 meters per year, the width of the sand embankment in this area has increased (Table 2). The maximum shoreline movement is 1028 meters and the minimum is 186 meters (Table 1). Coastline changes in this part of the study area are low to

moderate and the change threshold is between 8 to 43 meters per year (Table 2).

3.9. Changing the coastline in the southwestern part of Gorgan Bay

The average positive displacement of the Caspian Sea shoreline or water retreat in the northwestern part of the Miankaleh coast during the 24-year period between 1995-2019 is equal to 1507 meters (Table 1), which averages 63 meters per year, the width of the sand embankment in this area has increased (Table 2). The maximum shoreline movement is 2988 meters and the minimum is 599 meters (Table 1). Coastline changes in this part of the study area are very large and the change threshold is between 25 to 125 meters per year (Table 2).

3.10. Changing the coastline in the Northwesternmost region of Gorgan Bay

The average rate of positive displacement of the shoreline or retreat of the Caspian Sea water in the northwestern part of Miankaleh coast during the period of 24 years between 1995-2019 is equal to 1846 meters (Table 1), which averages 77 meters per year, the width of the sand embankment in this area is enlarged (Table 2). The maximum shoreline movement is 5200 meters and the minimum is 341 meters (Table 1). The shoreline changes in this part of the study area are very large and the change threshold is between 14 to 216 meters per year (Table 2).

Table 1. The shoreline displacement rate of Gorgan Bay and Miankaleh coast during the period 1995-2019

No	Region Code	Average (m)	Maximum (m)	Minimum (m)
1	EM	1626	2777	1137
2	WM	127	166	74
3	CM	476	550	434
4	TP	1058	1263	730
5	GP	654	1288	0
6	NEG	242	519	57
7	NWG	381	982	41
8	SCG	526	1028	186
9	SWG	1507	2988	599
10	MG	1846	5200	341

Table 2. The annually average shoreline displacement rate of Gorgan Bay and Miankaleh coast

No	Region code	Average (m)	Maximum (m)	Minimum (m)
1	EM	68	116	47
2	WM	5	7	3
3	CM	20	23	18
4	TP	44	53	30
5	GP	27	54	0
6	NEG	10	22	2
7	NWG	16	41	2
8	SCG	22	43	8
9	SWG	63	125	25
10	MG	77	216	14

3.11. Comparison of coastline changes in the study area

Comparison of the average rate of shoreline changes over a 24-year period between 1995-2019 shows that the highest shoreline shifts in the westernmost region of Gorgan Bay, northeast coast of Miankaleh and southwest of Gorgan Bay at 1846, 1626, and 1507 meters respectively occurred (Figure 3). The coastline of Turkmen port (1058 m) and Gaz port (654 m) has been determined (Figure 3). The lowest shoreline movement rates are in the west of Miankaleh (127 m), northeast of Gorgan Bay (242 m), northwest of Gorgan Bay (381 m), north-central Miankaleh (476 m) and south-central Gorgan Bay (526 m), respectively (Figure 3).

Comparison of the average annual shoreline movement in the 10 axes measured around Gorgan Bay and Miankaleh coast shows that the highest annual shifts are to the western extremities of Gorgan Bay (77 m), northeast of Miankaleh (68 m), southwest of Gorgan Bay (63 m), Turkmen port (44 m), and Gaz port (27 m) (Figure 4). The lowest annual shoreline movements are in the western regions of Miankaleh (5 m), northeast of Gorgan Bay (10 m), northwest of Gorgan Bay (16 m), north-central region of Miankaleh (20 m) and south-central Gorgan Bay (22 m) (Figure 4).

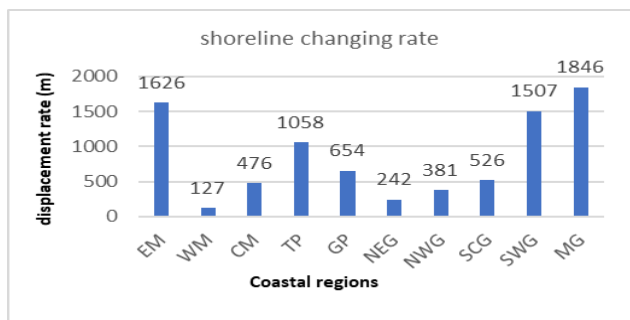


Figure 3. Comparison of the average amount of changes in the shoreline of Gorgan Bay and Miankaleh during the period 1995-2019

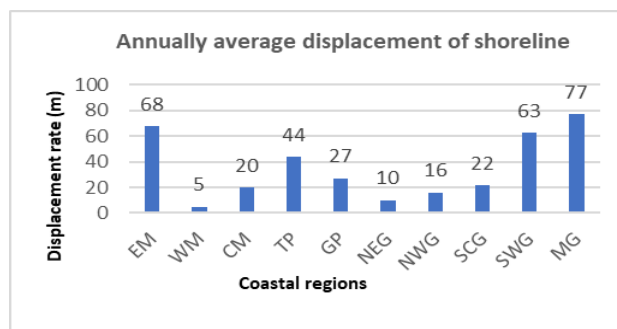


Figure 4. Comparison of the average annual changes of the coastline of Gorgan Bay and Miankaleh during the period 1995-2019

Reduction of the Caspian Sea water level by 150 cm since 1995 has caused a large part of the western extremity of Gorgan Bay and the northeastern part of Miankaleh Wetland to dry up, resulting in the drying of Miankaleh and Gomishan coastal wetlands and decreased more than 30 percent from the area of Gorgan Bay [19]. The results of studies have shown that the rate of variability of Gorgan Bay coastal habitats is subject to changes in the water level of the Caspian Sea and sandy shores of the southeastern Caspian Sea along the northeastern part of Miankaleh wetland and shallow lagoons. The western tip of Gorgan Bay had the most changes during 1995-2019 [19]. Changing the aquatic ecosystem to land and changing the cover of coastal wetlands to saline and brackish marshes are the most important ecological events of Gorgan Bay and Miankaleh wetland during the Caspian Sea water retreat during 1995-2019 [19]. The quantitative variability of coastlines in different coastal areas of Gorgan Bay and Miankaleh wetland is very different and the severity of physical vulnerability of coastlines in the study area depends on the geometric structure of the coast [20]. The rate of drought and coastal shifts in the northeastern regions of Miankaleh and the western end of Gorgan Bay is very high (Figures 3 and 4). The mild topography of the shallow and dry coastal part has caused the behavioral reaction of coastal wetlands to be very severe against the decrease of the Caspian Sea water level, and the drying of coastal wetlands, the growth of sandy islands and the formation of mudflats are signs of natural coastal reaction. Instead, the sensitivity of the coastal areas of the western and central part of the north of Miankaleh wetland, the northeastern and south-central part of Gorgan Bay to the reduction of the Caspian Sea water level is very low (Figures 3 and 4). Rapid shifting of the coastline of the eastern and southeastern parts of Gorgan Bay has reduced the efficiency of water traffic in these areas and an important part of the wooden piers of Turkmen and Gaz ports has been taken out of water [10]. Currently, the possibility of sea traffic between the Caspian Sea and the Gulf of Gorgan has become very difficult and only through the Ashooradeh communication channel, the transportation of small

boats is possible [19, 29, 30] According to the predictions made until 1402, with the decrease of the Caspian Sea water level, Ashuradeh canal will lose its navigation capability and Gorgan Bay will move towards complete drying [32]. The results of this study show that the coastal habitats of the westernmost part of Gorgan Bay and the northeastern part of Miankaleh wetland are changing at an average annual speed of 77 and 68 meters, respectively, and the distance between the shoreline of Turkmen and Gaz ports from the water level of Gorgan Bay is Annually, respectively, increases by 44 and 27 meters (Figure 4). Very high annual shifting speed of the shoreline in the northeastern part of Miankaleh wetland at the rate of 68 meters per year causes a sharp drop in water depth in communication channels and lack of proper exchange of Caspian Sea water with Gorgan Bay. Gorgan bay will be destroyed by the Caspian Sea by 1405 and many environmental problems will occur in the southeastern region of the Caspian Sea. Based on the comparison of the average annual speed of shoreline movement, the study area can be classified into three groups. The first group, which includes coastal areas: northeast of Miankaleh, western and southwestern extremities of Gorgan Bay and Turkmen port, has the highest coastline movement and the threshold of annual shoreline changes in there is between (44-77 meters) per year (Figure 4). The second group includes coastal areas: Gaz port, south-central part of Gorgan Bay, north-central part of Miankaleh, and northwest of Gorgan Bay, and the annual shoreline movement in these areas is moderate and between (16-27 meters) per year (Figure 4). And the third group includes: the northeastern coastal areas of Gorgan Bay overlooking the southern part of Ashooradeh Island and the northwestern part of Miankaleh, where the annual shoreline changes between (5-10 meters) per year (Figure 4). Therefore, the implementation of management programs for the ecological reconstruction of Gorgan Bay and Miankaleh Wetland should be done based on the intensity of shoreline displacement and the western extremities of Gorgan Bay and the northeastern part of Miankaleh Wetland, which have the highest shoreline displacement, are a high priority which they have to organize.

4. Discussion

The conservation value of the coastal habitats of Gorgan Bay and Miankaleh Wetland is very high [31] and Miankaleh International Wetland was registered as a biosphere reserve and sanctuary by the Ramsar Convention in 1975 [7]. The spread of coastal plants along the Caspian Sea coast and on the shores of Gorgan Bay with high species diversity and richness, has led to important habitats including saline marshes, brackish marshes and freshwater along with sandy meadows and pomegranate shrub forests are highly

sensitive to physical changes in the water level of the Caspian Sea and the Gulf of Gorgan [31, 18]. Meanwhile, the importance of the eastern and southeastern ports of Gorgan Bay, such as Turkmen port and Gaz port, is very high in tourism and fishing activities, and the safe connection of Gorgan Bay and the Caspian Sea is an important strategic criterion for protecting economic, social and environmental infrastructure [10, 19]. The fluctuation of the Caspian Sea during the years 1978-1995 with an increase of 250 cm had caused the destruction of a large area of habitats belonging to the land ecosystems of the

5. Conclusion

The study of shoreline displacement is done to determine the severity of physical vulnerability of coasts and their catchments. The different responses of shorelines to sea level fluctuations are a good natural indicator for assessing the variability of habitats and the deformation of physical criteria of coastal areas. The results of this study showed that different coastal areas of Gorgan Bay and Miankaleh wetland show different morphological behavior under the influence of decreasing water level in the Caspian Sea. The western extremities of Gorgan Bay and the northeast of Miankaleh Wetland had the highest shoreline displacement during the period 1995-2019, and as a result, a large part of Miankaleh Wetland and coastal swamps has dried up and aquatic ecosystems have changed their nature to land. The results of this study are used for comprehensive conservation management programs to rehabilitate and rebuild the ecological conditions of Gorgan Bay and create a safe and stable connection for water connection between the Caspian Sea and Gorgan Bay in areas where the shoreline movement rate is low such as: the central to the western part of Miankaleh coast seems to be mandatory. For comprehensive management of coastlines in the study area, focus on areas with high physical vulnerability is necessary and continuous control of quantitative and qualitative changes in coastal habitats affected by fluctuations in the water level of the Caspian Sea can reduce the existing challenges.

References

- [1] Afshin, A. 2004, Iranian rivers report, Ministry of Energy, Jamab Company, Internal Report. Vol. 2, 251 p. (In Persian).
- [2] Alemi Safaval, P, Kheirkhah Zarkesh, M, Neshaei, SA & Ejlali, F 2018, Morphological changes in the southern coasts of the Caspian Sea using remote sensing and GIS. *Caspian Journal of Environmental Sciences*, 16: 271-85.
- [3] Amini, A 2012, Holocene sedimentation rate in Gorgan Bay and adjacent coasts in southeast of the Caspian Sea. *Journal of Basic and Applied Scientific Research*, 2: 289-297.

- [4] Azarmsa, S., A, Razmkhah, F, 2010, Predicting the location and changes of the coastline in the Gulf of Pzm, *Journal of Earth and Space Physics*, Year 36, Number 4, pp. 89-98.
- [5] Ayvazi, W., J, Yamani, M, Khoshraftar, R, 2005, Geomorphological evolution of Sefidrood Delta in Quaternary, *Geographical Research* No. 53, pp. 99-120.
- [6] Bashari, L 2014, Hydro geochemical study on Gorgan Bay. *Journal of Oceanography*, 20: 31-42 (In Persian).
- [7] Convention on wetlands of international importance especially as waterfowl habitat, 1975, Ramsar, Iran. 6 p.
- [8] Davidson, N.C., Fluet-Chouinard, E. & Finlayson, C.M. (2018). Global extent and distribution of wetlands: trends and issues. *Marine and Freshwater Research* doi.org/10.1071/MF17019. Del Río, L., Gracia, F. J., & Benavente, J. (2013). Shoreline change patterns in sandy coasts. A case study in SW Spain. *Geomorphology*, 196, 252–266.
- [9] Franzen, M., Fernandez, E, Siegle, E, 2021, Impacts of coastal structures on hydromorphodynamic patterns and guidelines towards sustainable coastal development: A case studies review, *Regional Studies in Marine Science* Volume 44, 101800.
- [10] Gharibreza, M., Nasrollahi, A., Afshar, A., Amini, A, 2018, Evolutionary trend of the Gorgan Bay (southeastern Caspian Sea) during and post the last Caspian Sea level rise, *CATENA* , Volume 166, July 2018, Pages 339-348.
- [11] Hapke, C. J., Kratzmann, M. G., & Himmelstoss, E. A. (2013). Geomorphic and human influence on large-scale coastal change. *Geomorphology*, 199, 160–170.
- [12] Jabaloy-Sánchez, A., Lobo, F. J., Azor, A., Martín-Rosales, W., Pérez-Peña, J. V., Bárcenas, P., ... Vázquez-Vílchez, M. (2014). Six thousand years of coastline evolution in the Guadalquivir deltaic system (southern Iberian Peninsula). *Geomorphology*, 206, 374–391.
- [13] Kakroodi, A. A., S. B. Kroonenberg, R. M. Hoogendoorn, H. Mohammadi Khani, M. Yamani, M. R. Ghassemi & H. A. K. Lahijani, 2012b, Rapid Holocene Sea level changes along the Iranian Caspian coast. *Quaternary International*, 263: 93-103.
- [14] Kaplin, P.A. & Selivanov, A.O. (1995). Recent coastal evolution of the Caspian Sea as a natural model for coastal response to the possible acceleration of global sea-level rise. *Marine Geology*, 124, 161-175.
- [15] Khoshnavan, H. (2007). Beach sediments, Morphodynamics and risk assessment Caspian Sea coast, Iran, *Quaternary international journal*, 167-168, 35-39.
- [16] Khoshnavan, H 2011, Caspian Sea morphodynamic classification. *Journal of Earth and Space physics*, Institute of Geophysics-University of Tehran, 37: 1-15 (In Persian).
- [17] Khoshnavan, H & Vafai, B 2016, Caspian Sea level fluctuations (past, recent and future). *Proceeding of 18th International Marine Industries Conference*, Kish Island, Persian Gulf, Iran, pp: 71-79 (In Persian).
- [18] Khoshnavan, H. Naqinejad, A. 2018. International conference of Environmental consequence of Caspian rapid sea level changing in Gorgan Bay, UNDERSTANDING THE PROBLEMS OF INLAND WATERS: CASE STUDY FOR THE CASPIAN BASIN (UPCB) 12-14 May 2018 Baku, Azerbaijan, pp: 314- 317.
- [19] Khoshnavan, H., Naqinezhad, A., Alinejad-Tabrizi, T., Yanina, T., 2019, Gorgan Bay environmental consequences due to the Caspian Sea rapid water level change, *Caspian J. Environ. Sci.* Vol. 17 No. 3 pp. 213~226. Doi: 10.22124/CJES.2019.3664.
- [20] Khoshnavan, H., Naqinezhad, A., Alinejad-Tabrizi, T., Yanina, T., 2020, Effects of the Caspian Sea water level change on Boujagh National Park, southwest the Caspian Sea, *Caspian J. Environ. Sci.*, Article in press, Doi: 10.22124/CJES.2020.4313.
- [21] Konlechner, T, Kennedy, D., M'Grady, J, 2020, Mapping spatial variability in shoreline change hotspots from satellite data; a case study in southeast Australia, *Estuarine, Coastal and Shelf Science*, Volume 246, 107018.
- [22] Kosarev, AN & Kostianoy, AG, 2005, *The Caspian Sea environment*. Springer Hand book, Vol. 5, Part:1–3, DOI 10.1007/698_5_001, Springer-Verlag Berlin Heidelberg.
- [23] Kroonenberg, SB, Badyukova, EN, Storms, JEA, Ignatov, EI & Kasimov, NS 2000, A full sea level cycle in 65 years: barrier dynamics along Caspian shores. *Sedimentary Geology*, 134: 257-274.
- [24] Lahijani, H, Haeri Ardakani, O, Sharifi, A & Naderi Beni, A 2010, Sedimentological and geochemical characteristics of Gorgan Bay sediments, *Journal of Oceanography*, 1: 45- 55 (In Persian).
- [25] Luijendijk, A., Hagenaars, G., Ranasinghe, R., Baart, F., Donchyts, G., Aarninkhof, S., 2018, *The State of the World's Beaches*, SCIENTIFIC REPOrTS | (2018) 8:6641 | DOI:10.1038/s41598-018-24630-6.
- [26] Malliouri, D., I, Memos, C., D, Takvor H.Soukissian, T., H, Tsoukala, V., K, 2021, Assessing failure probability of coastal structures based on probabilistic representation of sea conditions at the structures' location, *Applied Mathematical Modelling* Volume 89, Part 1, Pages 710-730.

- [27] Misra, A., Balaji, R, 2015, A Study on the Shoreline Changes and LAND-use/ Land-cover along the South Gujarat Coastline, *Procedia Engineering*, Volume 116, 2015, Pages 381-389.
- [28] Mukhopadhyay, A., Mukherjee, S, Hazra, S., and Mitra, D., SEA LEVEL RISE AND SHORELINE CHANGES: A GEOINFORMATIC APPRAISAL OF CHANDIPUR COAST, ORISSA, *International Journal of Geology, Earth and Environmental Sciences* ISSN: 2277-2081 (Online), An Online nternational Journal Available at <http://www.cibtech.org/jgee.htm> 2011 Vol. 1 (1) September-December, pp.9-17/ Mukhopadhyay et al. Research Article 9.
- [29] Port & Maritime Organization 2008, Intergrated coastal zone management of Iran Seas (national ICZM), 354 pp. (in persian).
- [30] Port & Maritime Organization 2014, Hydrodynamic study on Gorgan Bay, 240 pp. (In Persian).
- [31] Saeidi, Sh, Naghinejad, AR & Kazemi-Gorji, Z 2014, Investigation of vegetation changes and diversity of habitats of coastal of Miankaleh biosphere using ecological transects. *Journal of Natural Environment (Iranian Journal of Natural Resources)*, 68: 67-82.
- [32] Sharbati, S & Ghanghermeh, A 2015, The forecasting of impacts of the Caspian Sea level decreasing on Gorgan Bay, *The Journal of Science and Technology of Environment*, 4: 33-45 (In Persian).
- [33] Saunders, M., Leon, J., Phinn, S. R., Callaghan, D., O'Brien, K. R., Roelfsema, C. M., Lovelock, C. E., Lyons, M. and Mumby, P. J. (2013). Coastal retreat and improved water quality mitigate losses of seagrass from sea level rise, *Global Change Biology*, 19, 2569–2583.
- [34] Shayan, S, Yamani, M, Kakroudi, A, Amunia, H, 1399, Estimation of shoreline changes in the Caspian delta basin using digital coastline analysis system (deltas: Haraz, Babolrood and Talar), *Quantitative Geomorphological Research*, Year 8, No. 4, pp. 34-46.
- [35] Yamani, M, Moghimi, I, Motamed, A, Jafar Begloo, M, Lorestani, G, 2013, Investigation of rapid changes in the coastline of the Sefidrood delta base by the method of equidistant profile analysis, *Natural Geography Research*, Forty-five years, No. 2, pages: 1-20.
- [36] Young, A. P., Flick, R. E., O'Reilly, W. C., Chadwick, D. B., Crampton, W. C., & Helly, J. J. (2014). Estimating cliff retreat in southern California considering sea level rise using a sand balance approach. *Marine Geology*, 348, 15–26.
- [37] Zhang, K., Douglas, B. C., and Leatherman, S. P., 1997. East coast storm surges provide unique climate record. *Eos*, 78(37): 389.

Pile Length Optimization in Fixed Template Offshore Platform Using Risk Reduction Approach

Zahra Omrani^{1*}, Rouhollah Amirabadi², Mahdi Sharifi³

^{1*} Ph.D. Student, University of Qom, Qom, Iran, z.omrani@stu.qom.ac.ir

² Assistant professor, University of Qom, Qom, Iran, r.amirabadi@qom.ac.ir

³ Assistant Professor, University of Qom, Qom, Iran, m.sharifi@qom.ac.ir

ARTICLE INFO

Article History:

Received: 10 Oct. 2021

Accepted: 28 Nov. 2021

Keywords:

Jacket-Type Offshore Platform
Pile Drivability Analysis
Risk Reduction Approach
Pile Length
Bearing Capacity

ABSTRACT

The purpose of risk management is managing the uncertainties by considering activities for identifying, assessing, monitoring, and reducing the impact of risks. Three strategies may be used to deal with the kind of risks that exist in projects: risk acceptance, risk transfer, and risk reduction. Events that can affect the economical goals of a project must be identified and evaluated so that they can be appropriately managed. Fixed jacket-type offshore platform (JTOP) as an expensive and necessary structure in energy facilities. In this research, the effect of knowledge increasing on the risk reduction and cost optimization for JTOP is studying. This paper focuses on optimizing the pile length of the fixed jacket-type offshore platforms and reducing the conservative design by using the risk reduction approach. Fixed offshore platform in South Pars Gas Fields of Iran as a case study. Increasing the Geotechnical knowledge and reducing the pile lengths is performed as considering similar geotechnical study at this regions and pile dynamic driving test (PDA), updating the pile bearing capacity base on increased knowledge for geotechnical data, and finally assessing the result based on in-place analyzing Pile driving result shows increasing the long-term soil bearing capacity. So first of all the required strength and parameters extracted from the existing data with analyzing and comparing where to adjust and matches with the lower limit of the theoretical equations. Finally, this new assumption is used for optimizing the pile length design. This research shows that the numerical analysis and assumptions that have been used in the design procedure are conservative and a proper risk management program with the knowledge increasing could have resulted in risk reduction. The analysis process that has been used in the present research leads to the pile cost reduction by 11% that is considerable for stakeholders in such an expensive structure. The most important innovation in this paper is the use of the results of pile driving operation for optimal pile design because, in pile driving operation, piles with design diameter are used.

1. Introduction

Jacket-type offshore platforms are fixed-base offshore structures that are used to produce oil and gas in relatively shallow water. Driven, open-ended, steel pipe piles are typically used to support this type of structure as a foundation. A significant finding from the performance of jacket platforms in major hurricanes, including Andrew (1992), Roxanne (1995), Lili (2002), Ivan (2004), Katrina (2005), and Rita (2005), is that the pile foundations have performance better than expected (e.g., Aggarwal et al. 1996, Bea et al. 1999 and Energo 2006 and 2007) [1]. Assessment of jacket platforms subjected to greater environmental loads than their

design loading has indicated that the pile foundation often governs the capacity of the structural system and the majority of damages and main failures have been observed in the structural elements above the mud-line level. While the lack of observing foundation failures may be acceptable, but the concern is potential of conservatism from economical point of view. The conservative design of foundation can lead to costly construction of new jacket platforms or unnecessary limitations on the manning and production levels of existing jacket platforms. In this research, the long-term bearing capacity of piles at the site of the South Pars Gas Field (Phase 22 jacket-type offshore platform) will be assessed and reviewed according to the

technical documentation and the results have been compared with similar jacket platforms in the South Pars Gas Field of Iran. The geotechnical and pile drivability reports and dynamic pile driving analyzer (PDA) test results used as a technical reference for the JTOP of phase 22. According to this information, the pile length of the mentioned platform is 97 and 105 meters.

There are three strategies that can be used to deal with the types of risks that projects face: risk acceptance, risk transfer, and risk reduction. Risk reduction typically focuses on the management of vulnerabilities and the rational and appropriate use of operational and technical information. The challenge is that there is a great deal of uncertainty in estimating pile capacity under both axial and lateral loadings. To accounting this uncertainty, there are numerous assumptions used in design practice that tend to be conservative, so that uncertainty does not lead to an unexpected failure. These assumptions are clear in design practice and act in addition to the design factor of safety that is applied to the design capacity.

The following summary of potential sources of conservatism has been extracted from the studies by Tang and Gilbert (1992) [2], Murff et al. (1993) [3,4], Pelletier et al. (1993) [5], Aggarwal et al. (1996) [6], and Bea et al. (1999) [7]. In addition, Andrew (1992) and Roxanne (1995) hurricanes have provided the motivation for presenting this data.

1. Sampling and testing methods used for site investigations.
2. Time Effects: Long-term setup or aging for piles installed in clays and sands may increase the foundation capacity with time.
3. Rate-of-loading effects.
4. Strain-softening and cyclic degradation.
- 5- The greater safety margin for foundation versus Structure in Design standards: the properties of the most critically loaded pile are considered for other piles designs, and all supporting piles of jacket platforms often have the same diameter and thickness; in some cases, there may be up to two different pile designs for a structure. On the contrary, structural members are usually designed and sized separately based on the applied expected forces in each member considering the entire structural system. Therefore, structural members are generally more optimized than piles, and the potential conservatism due to the design practice for piles is higher than that for the structure.

In summary, there are different sources of uncertainty involved in estimating the capacity of offshore piles, and this uncertainty has understandably led to a conservative design method. Factors that could reduce the capacity are generally included in the design, while elements that could increase the capacity are usually neglected in design. Therefore, failure is not necessarily expected if a pile foundation is loaded to its design capacity, particularly for piles loaded axially in

sand layers and laterally in clay layers. However, normal practice desing procedure cause the axial or lateral capacity of a pile foundation were much more than twice the design value and that is noticable [1]. Therefore, the main goal of this study is optimizing the design by using a post analysis of available information in order to reduce risk and increase the benefits of stakeholders.

with regard to this goal, comprehensive studies have been carried out based on the 10 geotechnical and pile driving reports of the South Pars Gas Field of Iran that are included phases 13, 17, 18, 22, 23, and 24. Additionally, in all implemented projects, the results of pile driving operation are never used, while pile driving are much closer to reality, because it is done with piles with design diameter and the soil properties. So, the optimal design in this study is based on the results of pile driving operations.

2. Jacket-Type Offshore Platform Properties

In this study, SPD22 as JTOP where are located in the South Pars Gas Field of Persian Gulf-Phase-22 was investigated. The API RP 2A-WSD (2017) standard wich is most practical design guide is used[8], has been used. The height of the working point from the mud-line is 65.5 meters and the height of the upper level of the topside is 92.325 meters from the mud-line. The SPD22 jacket properties are as follows: Four-legged jacket with four main piles to support wellhead production facilities. Row 2 is a single batter at 1:7, and Row 1 is a double batter at 1:8 and 1:7. Legs Spacing is 13.716 m × 20 m at the working point and 29.237 m × 34.83 m at the mud-line level. Water depth is 65.60 m below LAT, and the upper deck is 26.65 m above the mean water level. The leg diameter is 1.655 m × 0.056 m, and through the leg, the pipe pile dimension is 1.524 m × 0.076 m. Pile penetration is 97 and 105 m. The weight of the topside is 3200 tons. The schematic view of the jacket platform and soil layers is depicted in Figure 1.

Inputs of the model have included the structural properties of all members, connections, piles, the soil surrounding the piles (i.e., t-z, p-y, and Q-z curves), and the environmental loading including the magnitude and directions of waves, wind, and currents, that are considered in the modeling. The three-dimensional finite element model of the structure and its foundation, was modeled by SACS software [9]. The structural model for jacket Platform SPD-22 that was developed in SACSTM is shown in Figure 2.

According to the information presented in reports of the South Pars phases, the overall geotechnical stratum layer consists of soft clay sediments in depth throughout the area. As the depth increases, it rises from stiff clay deposits to very stiff ones and sandy layers with low to moderate cementation that has been reported in Table 1.

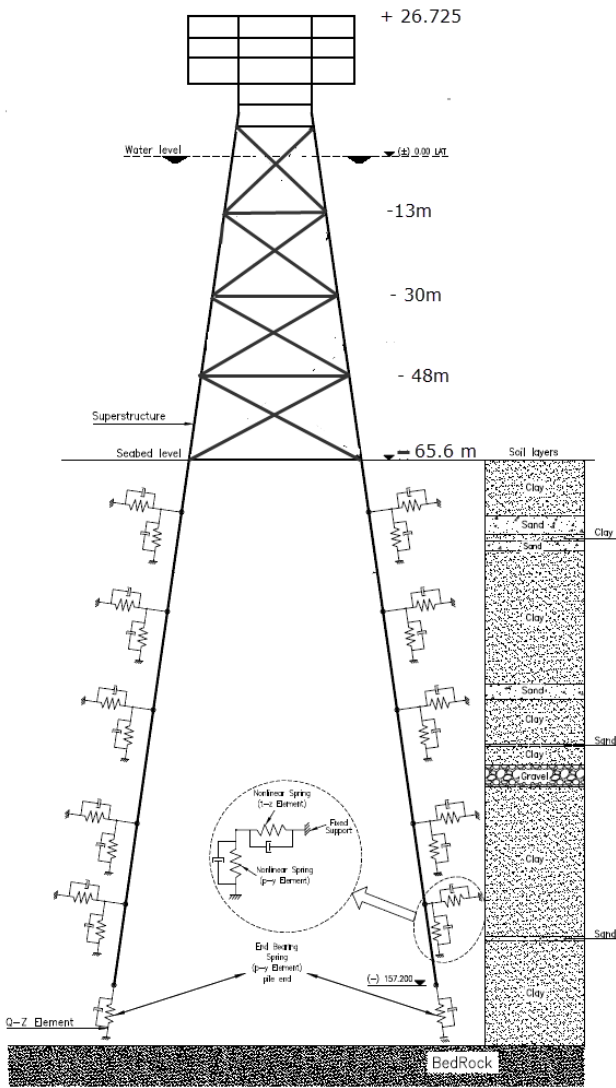


Figure 1. Schematic view of JTOP (SPD 22) and soil layers

Table 1. Soil layer properties

Soil type (Figure 1)	Soil layer depth (m)
Clay	0-10.6
Sand	10.6-14.1
Clay	14.1-15.2
Sand	15.2-17.2
Clay	17.2-42.2
Sand	42.2-45.1
Clay	45.1-53.5
Sand	53.5-54
Clay	54-57.5
Gravel	57.5-61.6
Clay	61.6-89.8
Sand	89.8-90.65
Clay	90.65-110.4

3. Method of Risk Reduction Approach

One way to meet risk reduction is to increase the knowledge of the problems. In this study, we are going to reduce the risk by increasing soil condition data in this area. The chosen area is south pars gas field and includes several jacket platforms. The jacket information of the table 2 has been used in this research. To confidence maintain, the names of geotechnical companies are not mentioned. A satellite image of the South Pars Gas Fields location is shown in Figure 3.

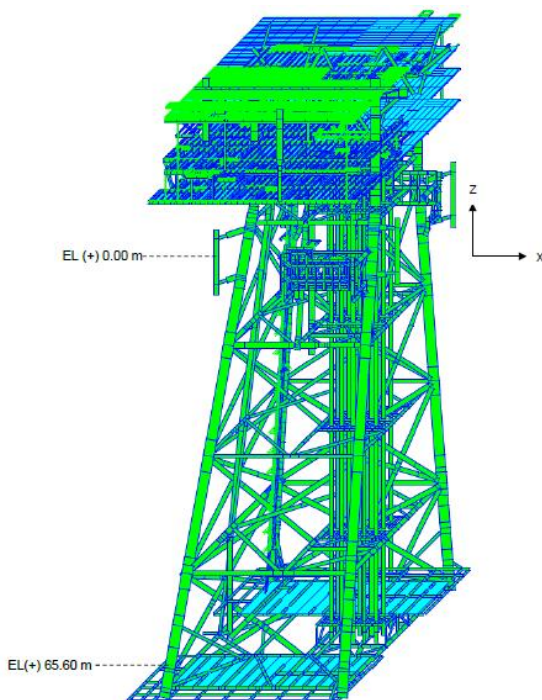


Figure 2. SPD 22 wellhead platform sacs model

Table 2. The name of jacket platforms

Jacket Platform Name	Geotechnical Company
SPD-13A	A
SPD-13B	A
SPD-13C	A
SPD-13D	A
SPD-22	A
SPD-23	A
SPD-24A	A
SPD-24B	A
SPD-17 (25)	B
SPD-18 (26)	B

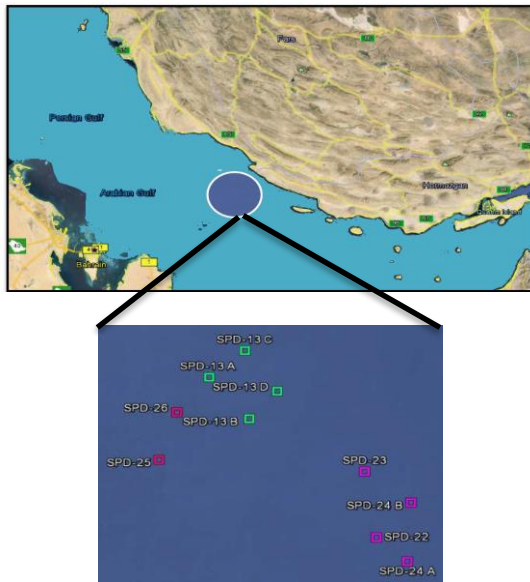


Figure 3. The location of the South Pars Gas Field in the satellite image

The risk reduction procedure that has been used has been shown in the following flowchart (Figure 4). The structure of jacket platform was modeled, risk reduction alternatives were checked and proved, system and related component was evaluated, at the end, the performance goals in light of risks of jacket platform system was clarified and revised.

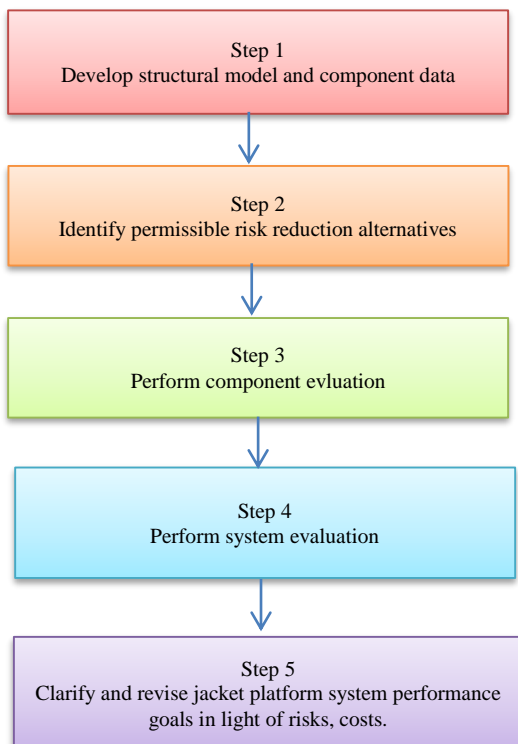


Figure 4. Risk evaluation procedure [10]

In this research, the process of study has been considered as follows in three steps:

- 1) Statistical Analysis: the results of field experiments, laboratory tests, and comparing the soil strength profile of the SPD22 site with the general trend of the observed changes in the other South Pars Gas Fields that a modified strength profile has been proposed based on.
- 2) Back Analysis of Pile Drivability: back analysis of Pile driving has been carried out by GRLWEAP software and the new soil strength profile has been extracted for achieving the long-term properties of the soil parameters.
- 3) Inplace Analysis: the long-term static bearing capacity, according to the proposed soil strength profile (steps 1 and 2) has been calculated.

4. Results and Discussion

In this section, the three previously mentioned steps were reviewed in order and the results were presented and discussed.

4.1. Statistical Analysis

A comparison of the trend of changes in soil properties of field and laboratory experiments provides a good view of the quality of the soil parameters used in engineering analysis. After gathering the geotechnical data, the investigations were carried out on the available evidence. The statistical analyses of all undrained shear strength data for Phases 13, 17, 18, and 22 to 24 of South Pars are presented in Figures 5 to 7.

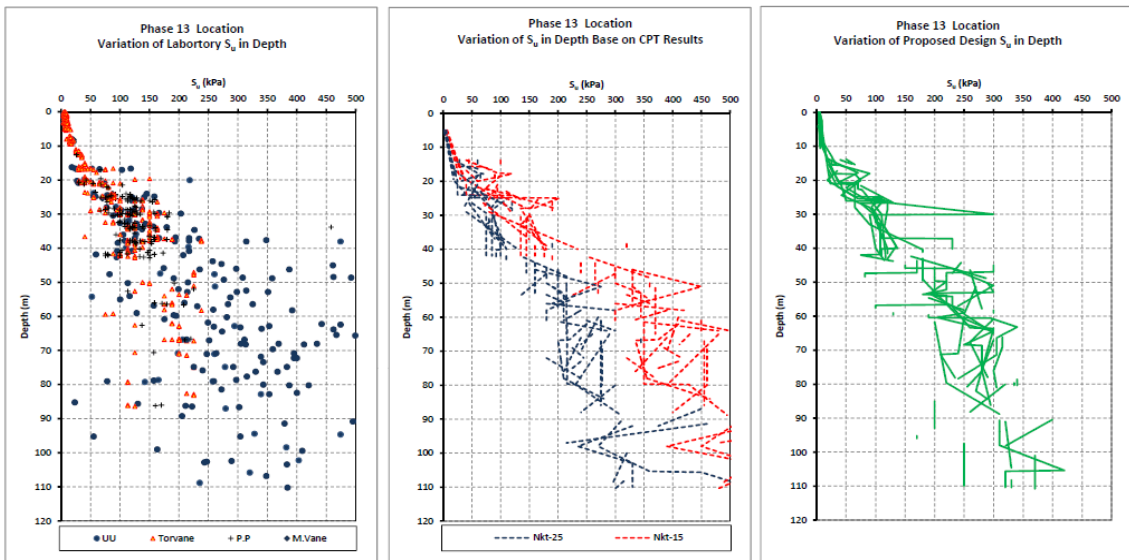


Figure 5. Undrained shear strength in phase 13 boreholes

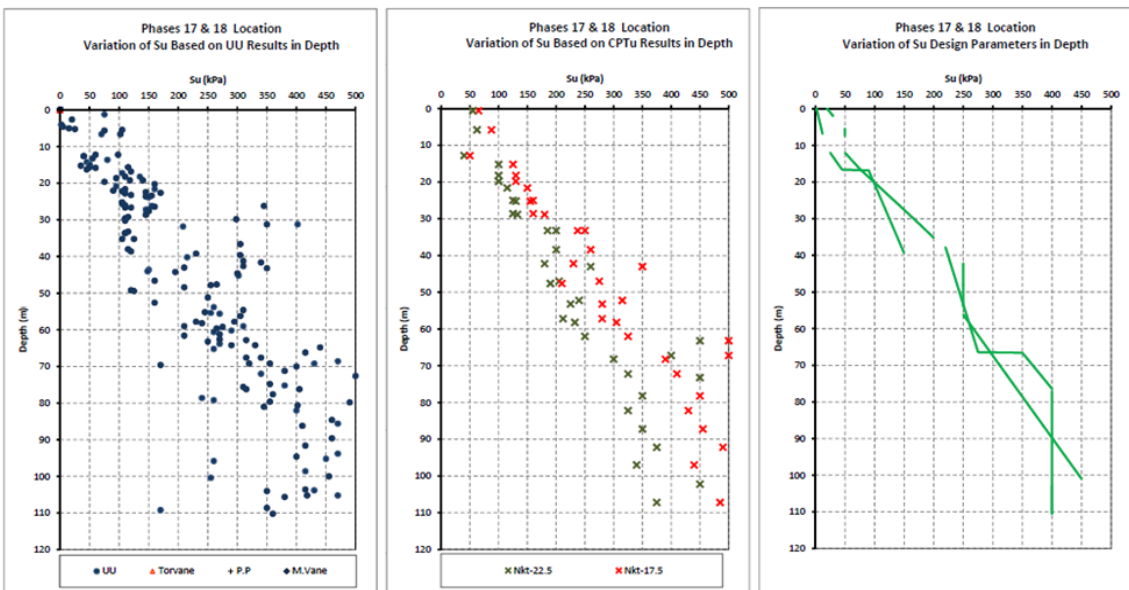


Figure 6. Undrained shear strength in phases 17 & 18 boreholes

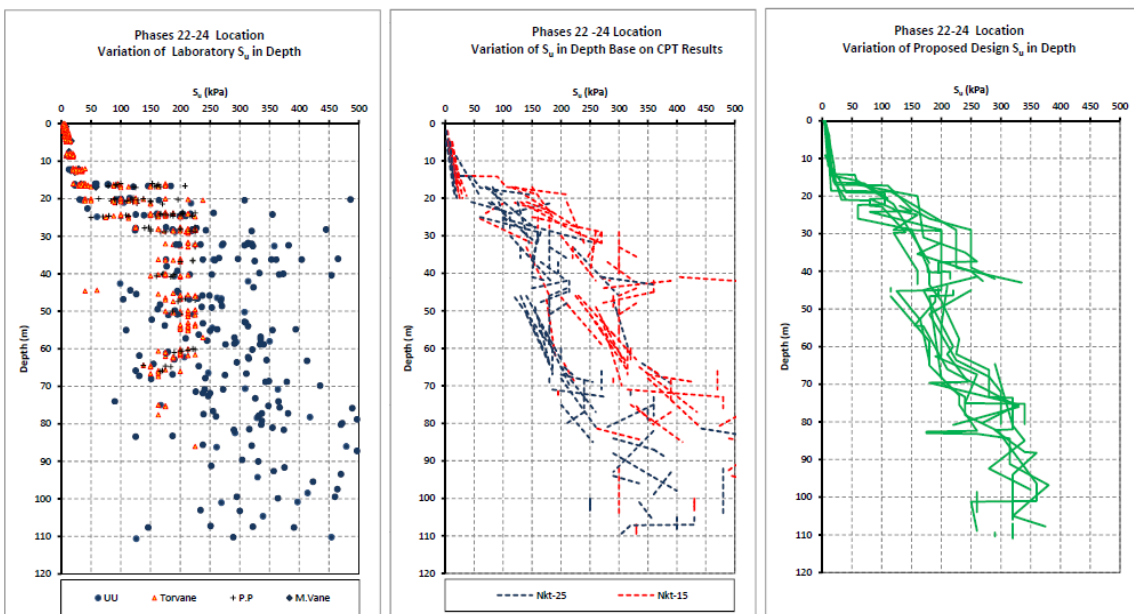


Figure 7. Undrained shear strength in phases 22-24 boreholes

There is three category data in the each figure. The first graphs was obtained by performing statistical analyses of all available experiments and field tests such as Miniature vane cutting, Unconsolidated-Undrained (UU) Triaxial Compression, torvane test, and Pocket Penetrometer results. UU triaxial tests were presented due to the high quality of the results as a suitable measure for comparing the undrained shear strength values (S_u) of clay layers. The second graphs were obtained by the CPT (cone penetration test) results. The undrained shear strength can be extracted from the results of the CPT by applying the experimental N_{kt} coefficient (a dimensionless cone factor) in the pure resistance of pile tip (q_{net}) from the following equation:

$$S_u = q_{net}/N_{kt} \quad (1)$$

The N_{kt} coefficient is dependent on the site sedimentation conditions and applies to increase the confidence of both upper and lower limits in calculations. By examining the reports, it is clear that the two companies have used different N_{kt} coefficient to determine the adhesion factor. According to Table 3, the limits by company A are more conservative.

Table 3. Proposed N_{kt} coefficient values by companies

Company	The upper limit of N_{kt}	Lower limit of N_{kt}
A	25	15
B	17.5	17.5

The third graphs are the proposed measures that were gained by the mean, median, and standard deviation of the data.

The UU and CPT parameters in Figure 8, represent the degree of matching design parameters with the results of the triaxial tests of UU and CPT and the N_{kt} accuracy. The following points can be deduced:

1. The matching of selected parameters by company A with the results of both UU and CPT decreases with the depth increasing. Even at depths of more than 80 meters, matching decreased to less than 30 percent accuracy which indicates the conservative choice of parameters by company A, and can have a significant effect on the pile bearing capacity reduction because of the high sensitivity to adhesion variations.
2. Correlation between the CPT result and the values obtained from the triaxial UU test in the range of depths of 20 to 68 meters shows a significant decrease. However, the review of existing reports suggests that the choice of proposed adhesion values in these layers was based on the results of the CPT and did not pay attention to the difference between the values obtained with the triaxial UU test results.

Finally, it can be concluded that by the statistical analysis, comparisons, reviewing the design parameters, considering all technical aspects in interpreting the results of laboratory and field experiments, the bearing capacity of the pile can be increased.

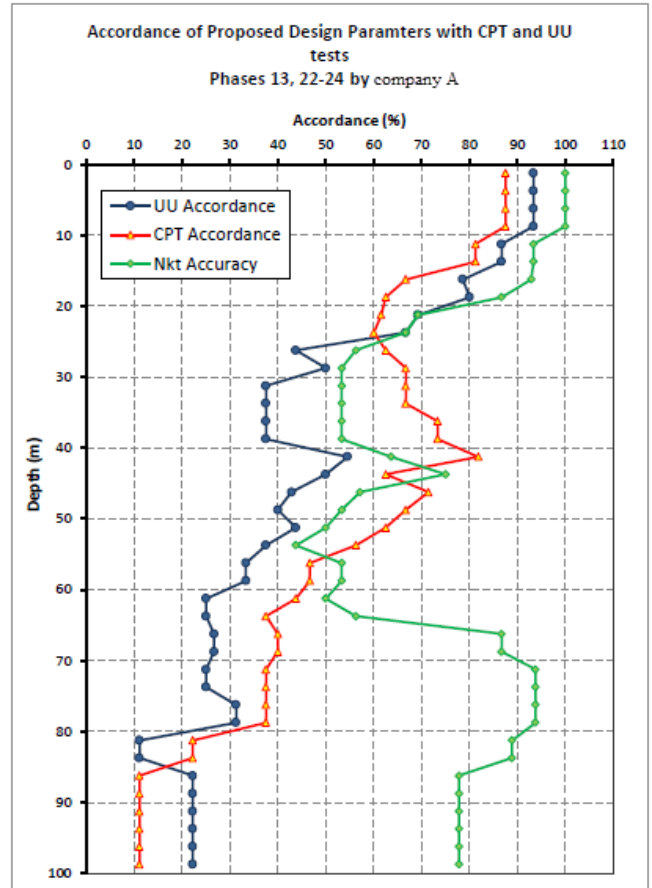


Figure 8. The adaptation variations trend of design parameters and results of laboratory and field experiments in phases 13 and 22- 24 based on the company A reports

The static bearing capacity of the phase 22 piles has been calculated based on the reports provided by Company A, and the length of piles was obtained 97 and 105 meters. Figure 9 provides a comparison between Company A's results and the proposed values derived from the present study. Figure 10 compares the graph of the static bearing capacity, which has shown a significant increase in the bearing capacity of the piles at the end depth of the boreholes.

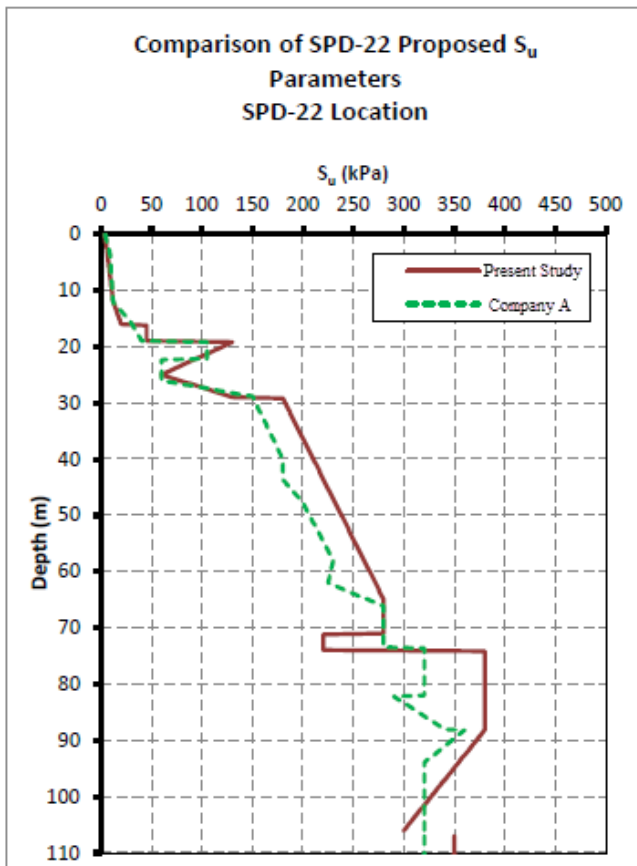


Figure 9. Comparison of S_u - company A and proposed values

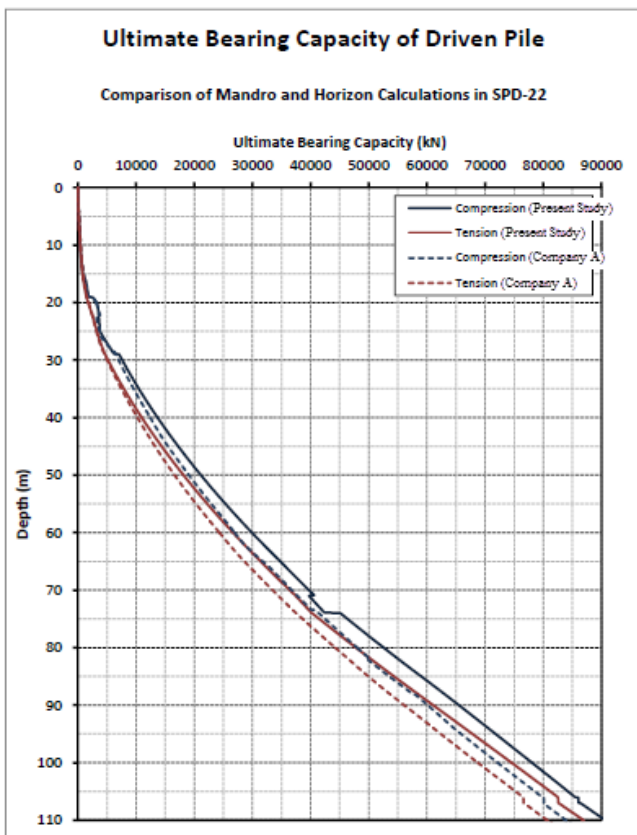


Figure 10. Comparison of the static capacity of the pile - Company A and proposed values

4.2. Back Analysis of Pile Drivability

The analysis on the available pile drivability data was performed in two steps as follows: Step 1 is extracting the soil layers properties using the pile driving simulating by GRLWEAP software [11] as back analysis and the Second step is to compare the results of the back analysis with the values obtained from theoretical relations. In this step, we have reduced the length of the piles by 12 meters and compare the results with the previous step. Each step is given as follows: Step1: To more accurately estimate the soil layers' long-term strength, after the completion of the installation, it was an attempt to simulate the recorded driving data in the GRLWEAP software. Also, The PDA test, and the CAPWAP analysis [12] were used to extract the required software information to determine the dynamic parameters of the soil. The soil strength parameters that were obtained are the result of multiplying the fatigue factor and the undrained shear strength of soil layers. Figure 11 compares the simulated pile driving energy and the back analysis results.

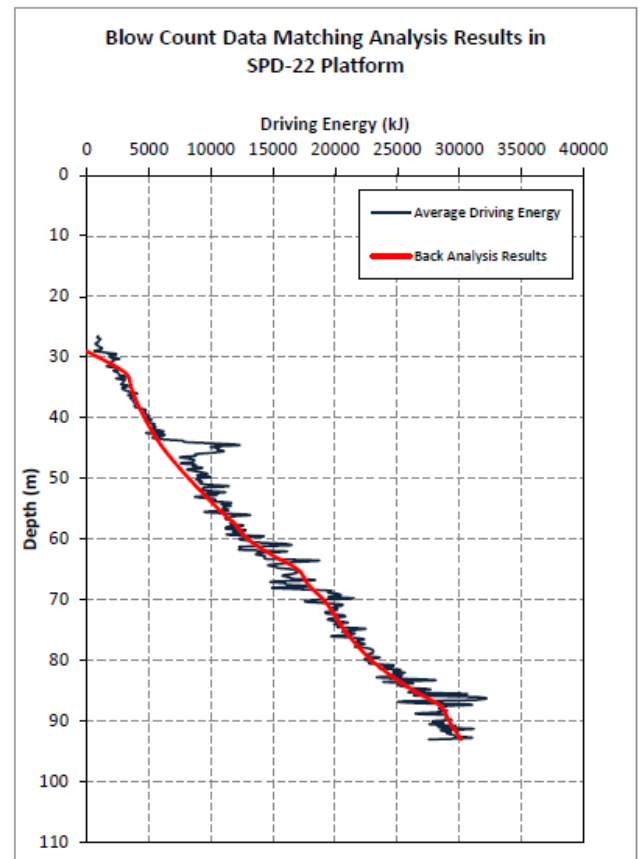


Figure 11. Comparative analysis of pile drivability information on the site of installation

The parameters extracted from the analysis represent the strength of the soil layers during the operation of the pile driving. The clay layers are faced with a considerable reduction in the stresses due to the significant increase of water pressure in the soil texture. Consequently, the adhesion to the pile shaft was

significantly reduced, which this phenomenon is referred to as the fatigue factor. The differences between the short-term strength parameters during pile driving and the proposed values by company A and extracted quantities in this study are shown in Figure 12.

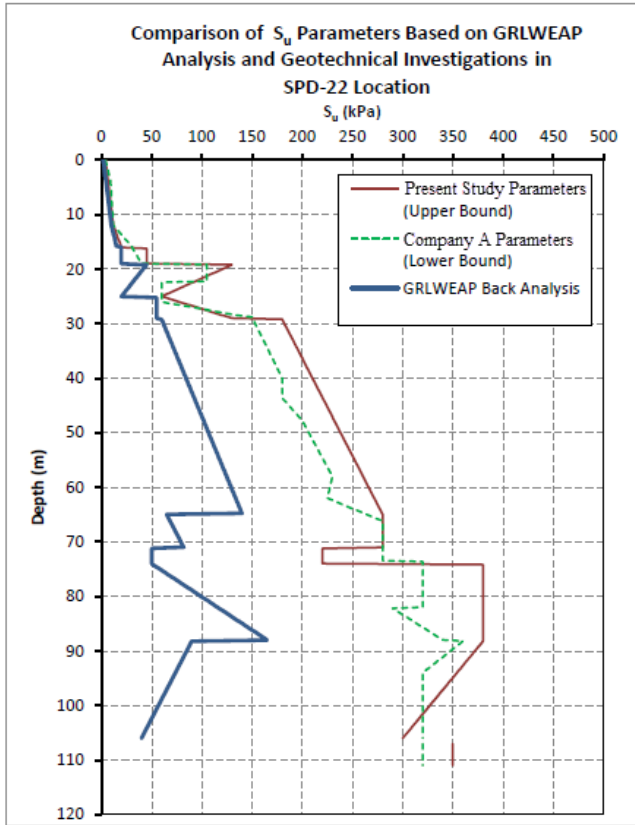


Figure 12. Comparison of short-term parameters during pile driving and suggested values by present study and company A

In this diagram, the proposed strength profile of company A is the lower limit, and the intended profile of the present study is obtained as the upper limit. knowing that the short-term properties have resulted from fatigue factor measure and soil adhesion in each layer, the expected upper and lower limit of the fatigue factor can be estimated by equation 2:

$$setup = \frac{1}{soil\ fatigue} \quad (2)$$

In the technical references (Randolph, Gourvenec, 2011) [13], the expected range of setup factor in clays is between 2 and 8, Also, according to the proposed relationship by Stevens et al., 1982 [14] and Colliat et al., 1993 [15], strength reduction is a function of the over-consolidation conditions (OCR) of soil layers. Company A has used a few corrections based on the pile drivability experiences in the Persian Gulf according to below equations.

$$F_p = 0.5 OCR^{0.3} \quad \text{Stevens et al. (1982)} \quad (3)$$

$$F_p = \lambda OCR^{0.2} \quad \text{Modified Colliat} \quad (4)$$

Company A (5)

	λ Value	
	Lower Bound	Upper Bound
Upper Section of Pile (Seabed to 10 m above toe)	0.1	0.2
Lower Section of Pile (10 m above toe to final depth)	0.25	0.4

In Figure 13, the setup factor comparison was provided. The significant difference between the results of various theoretical relationships indicates that the accurate fatigue factor prediction of the clay layer is very complicated. The values were obtained from the numerical analysis show a good matching with theoretical values based on the general trend of changes. The average value of the setup factor is equal to 2.83 based on modified data. In other words, With passing a little time from the pile driving operation, the ultimate strength of the pile becomes about 2.8 times. The complete elimination of the excess water pressure in the clay layers and achieving the effective stresses of the static state can be the main reasons. In the following, the simulation of the PDA test was carried out and the results of this analysis are presented in two depths of 85 m and 93 m in figure 14 while applying the coefficient of setup equal 2.5, as shown in table 4.

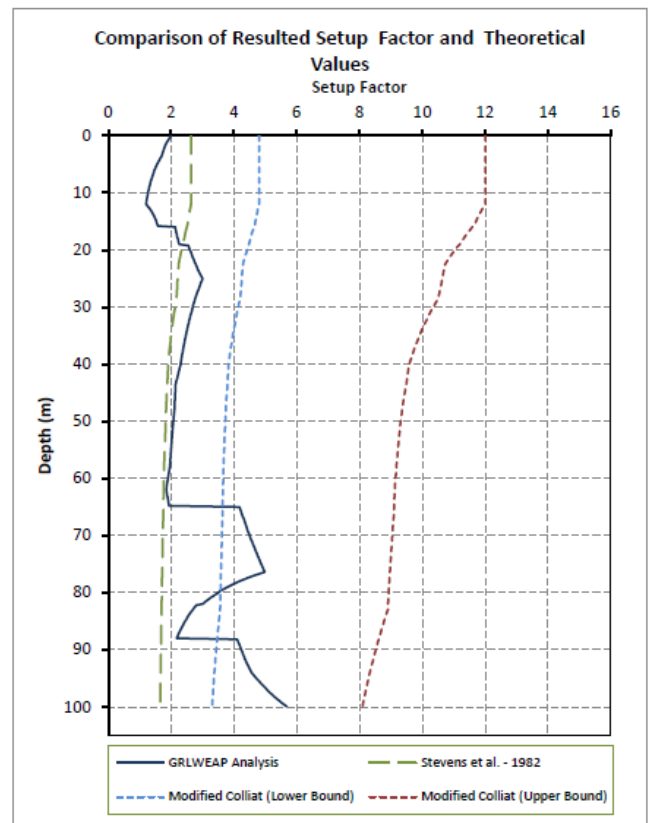


Figure 13. Comparison of set up values based on the results of back analysis and theoretical relations

Step 2: In this section, we will try to estimate the long-term bearing capacity after the completion of the operation, using various theoretical equations. In the absence of loading experiments, theoretical relationships can provide an estimate of the process of variation in the final bearing capacity of the piles over time from the end of the operation. Among the various researches, the relationships provided by both Skov and Denver, 1988 [16, 17] and Svinkin, 1996 [18] are more practical. The equations used to determine long-term bearing capacity are as follows:

Skov and Denver (1988)

$$Q_t = Q_0 [A \log(t/t_0) + 1] \tag{6}$$

Q_t = pile capacity as time t

Q_0 = Pile Capacity at $t=t_0$

For Clays, $A=0.6$ and $t_0=1.0$

Svinkin and Skov (2000) (7)

$$Q_t/Q_{EOD} - 1 = B[\log(t) + 1], \quad B \text{ is the same as } A, \text{ in Skov and Denver}$$

Svinkin (1996)

Upper Bound: $Q_t = 1.4 Q_{EOD} t^{0.1}$ (8)

Lower Bound: $Q_t = 1.025 Q_{EOD} t^{0.1}$

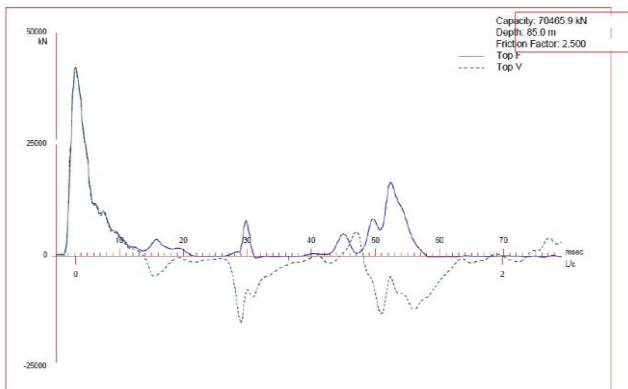
Table 4 presents a comparison between the results of long-term bearing capacity determination using GRLWEAP software and theoretical equations.

Table 4. Comparison of long-term bearing capacity using software and theoretical equations

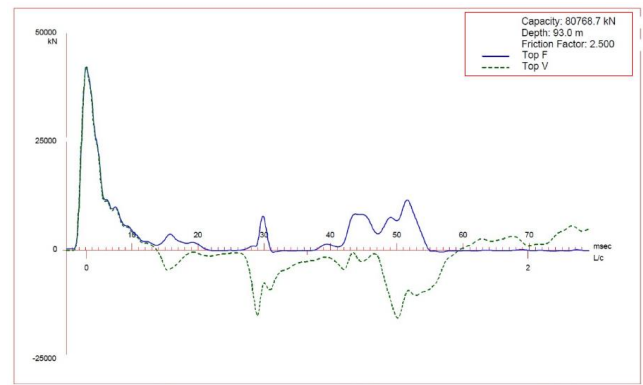
Pile ID	Tip Penetration (m)	Anticipated Long Term Bearing Capacity (kN)				
		GRLWEAP results	Skov & Denver ¹	Svinkin ¹ (LB)	Svinkin ¹ (UB)	Svinkin & Skov ¹
A1	85	70,466	97,496	71,212	97,265	118,388
A2	93	80,769	114,044	83,299	113,774	138,482

¹ Anticipation are presented for approximately 1000 days after EOID

Also, the pile bearing capacity increase in time has shown based on theoretical relationships in Figure 15 both different pile lengths.



(a)

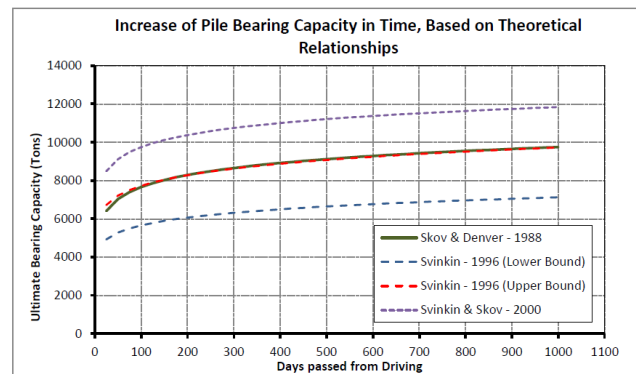


(b)

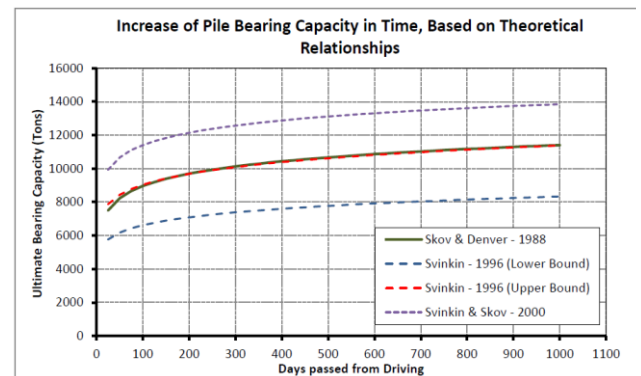
Figure 14. The result of long term loading capacity of piles at depths (a) 85 m & (b) 93 m by applying the setup factor of 2.5

Table 5. Expected long-term bearing capacity after the pile driving operation

Tip Penetration (m)	Applied Setup Factor	Anticipated Ultimate Long-term Bearing Capacity (kN)
85	2.5	70466
93	2.5	80769



a) Pile A1



b) Pile A2

Figure 15. Increase in pile bearing capacity in time based on theoretical relationships

It can be concluded that the process of numerical analysis is very conservative and even less than the minimum value obtained from the equation

4.3. Inplace analysis

In the third step, inplace Analysis of the SPD22 jacket platform was performed with the new pile length of 85 and 93 meters. Using the geotechnical report of company A, the length of piles is 97 & 105 m, but with the modified soil properties of the present study, 85 & 93 m is obtained with a safety factor of 2.5 for both analyses in SACS software (table 6).

Table 6. Maximum factor of safety for all piles

Pile	Minimum Factor of Safety
A1	3.08
A2	2.87
B1	3.24
B2	3.00

5. Conclusion

The results obtained can be summarized as follows:

- By data gathering and statistic analysis, the bearing capacity of piles has been increased by 10 percent, which can be concluded that the exact research on field and laboratory tests results can reduce the over-conservatism and leads to risk reduction.
- By performing the pile drivability analysis of the selected platform in the South Pars Gas Field and comparing the results with the other fields' data, it was found that the sensitivity of the clay layers was increased in depth when pile driving operation. In other words, soil resistance decreases.
- From the pile drivability analysis, back analysis, and comparing these results, the estimated soil strength is about 2.8 times more than the pile driving operation time. However, if this value is considered to be 2.5, the pile length can be reduced by 12 m which reduces the use of the material by 11%.
- The practical conclusion that can be drawn is that the Svonkin equation (lower bound) can be used for the estimation of the long-term bearing capacity to reduce the over-conservative.
- Since pile driving operation is done with a pile with a design diameter, then the resulting soil properties are much closer to reality, so the results of pile driving in a field can be used for optimal pile design.

6. References

- Chen, J.Y., Matarak, B.A., carpenter, J.F., and Gilbert, R.B., (2009), Analysis of Potential Conservatism in Foundation Design for Offshore Platform Assessment, Final Project Report Prepared for the Minerals Management Service.
- Tang, W.H., and Gilbert, R.B., (1992), Offshore Pile System Reliability, Final Report to American Petroleum Institute (Project PRAC 89-29).
- Murff, J. D., and Hamilton, J. M., (1993), P-Ultimate for Undrained Analysis for Laterally Loaded Piles, Journal of Geotechnical Engineering, ASCE, Vol. 119, No. 1, pp. 91-107.
- Murff, J.D., Lacasse, S., and Young, A.G., (1993), Discussion and summary on foundation elements, system and analysis, Proceedings of an International Workshop Assessment and Requalification of Offshore Production Structures, New Orleans, Louisiana, pp. 151-165.
- Pelletier, J. H., Murff, J. D., and Young, A. C., (1993), Historical Development and Assessment of the Current API Design Methods for Axially Loaded Piles, Offshore Technology Conference, Houston, Texas, OTC 7157.
- Aggarwal, R.K., Litton, R.W., Cornell, C.A., Tang, W.H., Chen, J.H. and Murff, J.D., (1996), Development of pile foundation bias factors using observed behavior of platforms during Hurricane Andrew, Offshore Technology Conference, Houston, Texas, OTC 8078, pp. 445-455.
- Bea, R.G., Jin, Z., Valle, C. and Ramos, R., (1999), Evaluation of reliability of platform pile foundations, Journal of Geotechnical and Geoenvironmental Engineering, ASCE, Vol. 125, No. 8, pp. 695-704.
- American Petroleum Institute, (2000) Recommended practice for planning, designing and constructing fixed offshore platforms, 21st ed., Washington, D.C.
- SACS Suite program, (2011), version 5.3.
- Werner, S. D., Dickenson, S. E., and Taylor, C. E., (1997), Seismic Risk Reduction at Ports: Case Study and Acceptable Risk Evaluation, Journal of Waterway, Port, and Coastal Engineering, American Society of Civil Engineers, Vol. 123, November-December, pp. 337-346.
- PDI, (2010), GRLWEAP Manual for Windows, 30725 Aurora Road, Cleveland, OH 44139 USA: PDI.
- CAPWAP Signal Matching, Art of Foundation Engineering Practice (GSP 198), p. 534-553.
- Randolph, M.F., and Gourvenec, S., (2011), Offshore Geotechnical engineering, Spon Press, London.
- Stevens, R., Wiltsie, E. & Turton, and T., (1982), Evaluating Drivability for Hard Clay, Very Dense Sand, and Rock, Offshore Technology Conference.
- Colliat, J., Vergobbi, P. and Puech, A., (1993), Friction Degradation And Set-Up Effects In Hard Clays Offshore Congo And Angola, Offshore Technology Conference.
- Skov, R., Denver, H., (1988), Time-dependence of bearing capacity of piles, The 3rd International Conference on Application of Stress-wave Theory to Piles, Ottawa, Canada, pp. 879-888.
- Svinkin, M.R., and Skov, R., (2000), Set-up effect of cohesive soils in pile capacity, The 6th International Conference on Application of

Stress-wave Theory to Piles, Sao Paulo, Brazil,
pp. 107–111.

- [18] Svinkin, M.R., (1996), Setup and relaxation in glacial sand-discussion, Journal of Geotechnical and Geo-environmental Engineering – ASCE, 122 (4), pp. 319-321.

Wavelet based detection of vortex shedding around a cylinder oscillating in still water

Seyede Masoome Sadaghi^{1*}, Seyed Taghi Omid Naeeni², Hasan Yousefi Ghalejoogh³

^{1*} Assistant Professor, Road, Housing & Urban Development Research Center; S.sadaghi@bhrc.ac.ir

² Associate professor, School of Civil Engineering, University of Tehran, Tehran, Iran

³ Assistant Professor, School of Civil Engineering, University of Tehran, Tehran, Iran

ARTICLE INFO

Article History:

Received: 31 Jul. 2021

Accepted: 25 Nov. 2021

Keywords:

Wavelet Analysis
Oscillatory Cylinder
Vortex Shedding

ABSTRACT

The present paper aims to study the lift forces acting on a cylinder oscillating in still water from spectral point of view. In the previous researches, vortex shedding frequency has been related to the fundamental lift frequency. Here, the wavelet analysis is used as a relatively new concept in spectral analyses. The simultaneous time-frequency representations of the lift forces are investigated to localize the flow induced transitory characteristics. The peaks in the wavelet coefficients attributed to vortex shedding are studied. The abrupt changes in the lift forces have also been studied by discrete wavelet decomposition. Small spikes have been observed in the results due to vortex shedding. Wavelet analysis is considered as an efficient alternative method to predict vortex shedding for larger Keulegan-Carpenter numbers (KC). Two different gap-to-diameter ratios, 0.1 and 1.0, are considered to account for the effect of bed proximity. Regular vortex shedding is suppressed for lower gap ratios; this fact is confirmed by wavelet analysis as well. The KC numbers in the present study are in the range of 15 to 40. The flow is in the subcritical regime with Reynolds number in the range of 9500-26000. The cylinder and the plane bed are both smooth.

1. Introduction

Submarine pipelines are very important in economical and safe transportation of oil, gas, petroleum products, fresh water and even communication cables. Generation of coherent structures in the pipe wake flow, which is generally referred to as vortex shedding, is responsible for inducing the basic excitational forces on the pipeline free spans. These forces are of great importance as they can result in the large amplitude vibrational span responses. The mechanism of vortex shedding and its influence on the flow induced forces are among the classic and important topics in fluid mechanics and have drawn attention of the researchers over the years. The growth and shedding of vortices from a submerged body (specially a pipeline) affect the velocity field and the consequent pressure on the pipeline surface. The time-varying pressure field imposes time-varying forces on the pipe surface. The velocity field around the pipe has a fluctuating pattern due to alternate vortex shedding. The frequencies of the fluctuations are highly related to the vortex shedding process. Hudgins and Kaspersen have presented and compared various conventional and wavelet-based algorithms for detecting coherent structures in wake flows.[1]

Wavelet Transform (WT) is capable of providing the simultaneous time-frequency representation of signals. Most wavelet based coherent structure detection algorithms are presented for uniform flow condition and are based on velocity variations in wake flows. In this study, WT has been used for detecting vortex shedding in oscillatory flows. It has directly been applied on the lift forces to reveal the variation of frequency content in time for an average oscillation cycle.

Vortex shedding in oscillatory flows is more complicated because the near cylinder flow field has to rebuild itself twice per complete cycle as the velocity reverses direction. The cyclic acceleration of the fluid motion results in the formation of strong and usually asymmetric vortices. The flow becomes asymmetric as the vortices are swept back past the cylinder in the return half of the flow cycle. This complicated flow field affects the forces on the cylinder. WT has the advantage of revealing the peaks in the lift force traces attributed to the dominant frequency. These peaks may be attributed either to a vortex detaching from the shear layer or to a vortex washed over the cylinder in the reversal phase. Due to the simultaneous time-frequency representation of the

wavelet analysis, different sources of the peaks can be identified.

Over the years, vortex shedding process and its relation to the subsequent in-line and lift forces have been extensively investigated by force measurement and flow visualization techniques. A brief description of the achievements in this regard is presented in the following section.

2. Vortex Shedding in Oscillatory Flows

Williamson (1985) has classified vortex shedding regimes around oscillatory cylinder for different KC numbers [2]. According to the results of his studies, the number of vortex pairs being shed and convecting away from the cylinder increases with the increase in KC number. In his experiments, the force time series are obtained simultaneously with the flow visualizations. He has established a direct relation between the lift variation and the motion of vortices by using the fundamental lift frequency of his experimental data. He has concluded that the peaks in the lift force time series are attributed either to vortex shedding or to the return of the vortices towards the cylinder just after the flow reversal. The fact that a positive lift force is produced when there is a vortex moving over the cylinder was also shown by the theoretical work of Maull and Milliner (1978) [3]. Table 1 summarizes the classification of vortex shedding patterns for different KC numbers based on Williamson [2]. N_L is the normalized fundamental lift frequency by flow cycle and N is the number of vortices per half cycle.

Sumer and Fredso [4] have also investigated the vortex shedding regimes and their relation to the lift

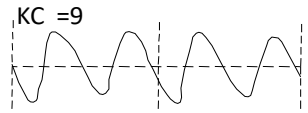
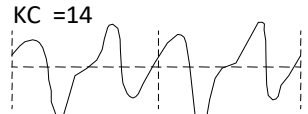

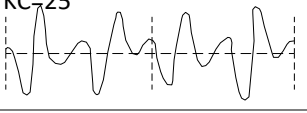
variations based on previous works by Williamson. A similar conclusion about the different vortex shedding regimes has been presented in their book.

Different modes of vortex shedding and pairing have also been introduced in the report by J. P. Kenny and partners Ltd. (1993) [5]. According to this report, at smaller KC numbers, the distances moved by fluid particles past the cylinder between the flow reversal phases are relatively small; hence fewer vortices have time to form and be shed in each half cycle. In the idealized plane oscillatory flows used in laboratory experiments such as Sarpkaya's, it has been found that for KC values in the approximate range of 5 to 15, the vortex generation, shedding and pairing patterns lock-in to the primary flow oscillation cycle. During these locked-in phases, a single vortex is shed from the cylinder in each half cycle. The consequent transverse lift force fluctuates at a frequency, f_v , equal to twice the flow oscillation frequency, f_w .

For KC numbers in the approximate range of 15 to 25, a second mode of locked-in vortex shedding and pairing has been introduced in the aforementioned report. Two vortices are shed from the cylinder in each half cycle which pair and are swept back past alternating sides of the cylinder in sequential half cycles. This generates a fluctuating transverse lift force with a dominant frequency of three times the primary flow frequency. The detailed mechanics of these two locked-in modes of vortex shedding are addressed to the studies of Grass et al. [6].

For KC numbers greater than approximately 25, it has been concluded that there is an increasing randomization and decoupling of the interaction between the shed wake vortices and the newly forming ones in the return half flow cycle. As the KC number increases, the number of vortices completely

Table 1. Vortex shedding regimes around smooth circular cylinder in oscillatory flow. Fundamental lift frequencies observed in the experiments of Williamson [2].

KC regime	KC range	Re	$N_L=f_L/f_w$	N	Lift force trace (2 cycles)
Single pair	$7 < Kc < 15$	$1.8-3.8 \times 10^3$	2	1	
Double pair	$15 < Kc < 24$	$3.8-6.1 \times 10^3$	3	2	
Three pair	$24 < Kc < 32$	$6.1-8.2 \times 10^3$	4	3	
Four pair	$32 < Kc < 40$	$8.2-10 \times 10^3$	5	4	

formed and shed in each half cycle of the flow increases until the wake resembles a steady flow. According to the report by J. P. Kenny and partners Ltd., as KC number increases, the vortex shedding frequency and hence the number of complete vortices shed in each half cycle also become progressively decoupled from the primary flow oscillation frequency [5]. The number of vortices completely formed and shed in each half flow cycle, N , is directly related to the frequency of the fluctuating transverse lift force, f_v . Isaacson and Maull have suggested that f_v is given by the simple relationship $f_v=(N+1) f_w$ [7]. This formula is clearly valid for the two dominant vortex shedding modes discussed above for which $N=1$ and 2 and the lift force dominant frequencies are $2f_w$ and $3f_w$ respectively. However at larger KC values, this simple relationship can only be expected to yield approximate estimate of the overall average lift force frequency. On the other hand, the flow visualization techniques are not easily applicable for investigation of vortex shedding regimes in large KC numbers.

As stated earlier, all the peaks in the lift force time series are not induced by vortex shedding. Some peaks are associated with the return of the shed vortices towards the cylinder just after flow reversal. It is hence desirable to investigate the simultaneous time-frequency representation of the lift force traces. One drawback of using the power spectrum or frequency content of the lift force via ordinary spectral methods is that the time information of the signal is lost. It means that the ordinary spectral methods do not show when each frequency component exists in the signal. In this study, the measured forces acting on a circular cylinder oscillating in still water are used to further investigate the vortex shedding and its relation to lift force fluctuations. Wavelet analysis, which can provide the time and frequency information simultaneously, has been used to reveal the variation of frequency content in time for an average oscillation cycle.

3. Experimental Details

3.1. Experimental Apparatus

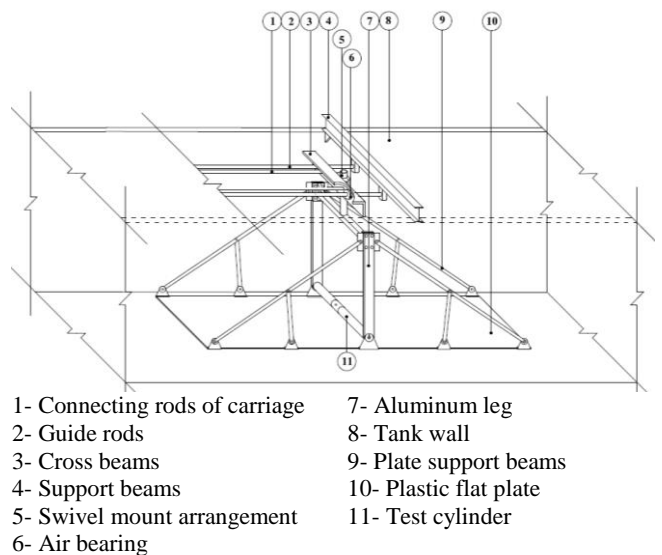
The experimental details have been fully described in the former paper by Naeni et al [8,9]; hence only a brief description is presented here.

The experiments were carried out in the Department of Civil and Structural Engineering, University of Manchester, United Kingdom. The experimental apparatus consisted of an oscillating cylinder of 50 mm diameter kept at different gaps above a plane bed in still water. The use of air bearings in the oscillation system ensured elimination of vibrations and friction from the system interfaces thus the cylinder was free from this kind of mechanical vibrations. The motion of the oscillatory cylinder in the experiments was purely sinusoidal. The velocity of oscillation is

determined according to Eq.(1). A schematic diagram of the apparatus is shown in Figure 1.

$$u(t) = U_m \cos(\omega t) \tag{1}$$

The force transducer used in the experiments was a cantilever beam with a full arrangement of four strain gauges. The test cylinder housed the force transducer. The pressure distribution around the cylinder has also been obtained. For the pressure measurement, two pressure transducers were fixed from the inside to the wall of the cylinder in a diametrically opposite orientation. The cylinder could be rotated to locate the transducers at 36 angular positions of 10° intervals. Even though only two pressure transducers were used at a time, extreme care was taken to match the phase of the oscillations and the pressure patterns. The forces exerted on the cylinder were determined from pressure patterns as well as from direct force transducer outputs. For the same conditions of flow, forces determined from the pressure measurements are found to be in good agreement with those measured by the force transducers thus validating the measurements.



- 1- Connecting rods of carriage
- 2- Guide rods
- 3- Cross beams
- 4- Support beams
- 5- Swivel mount arrangement
- 6- Air bearing
- 7- Aluminum leg
- 8- Tank wall
- 9- Plate support beams
- 10- Plastic flat plate
- 11- Test cylinder

Figure 1. Experimental apparatus

3.2. Experimental Conditions

The range of test conditions for the present study is given in Table 2.

Table 2. summary of the test conditions for pressure measurements

KC	G/D	Re	$\beta = \frac{Re}{KC}$	U_m (m/s)	Temp (°C)	T (s)
15	0.1,1.0	9.5×10^3	630	0.19	between 17 and 23	4
20	0.1,1.0	1.3×10^4	640	0.25		
25	0.1,1.0	1.6×10^4	640	0.31		
30	0.1,1.0	1.9×10^4	640	0.38		
35	0.1,1.0	2.3×10^4	650	0.44		
40	0.1,1.0	2.6×10^4	650	0.50		

The experimental parameters in the table include the Keulegan-Carpenter number (KC), the gap ratio (G/D) which is the ratio of the gap between the cylinder and

plane bed (G) to the diameter of cylinder (D), the Reynolds number (Re), maximum velocity of the cylinder (U_m), the temperature at which the experiments were performed (Temp) and the period of oscillation (T). Each experimental run consisted of 40 cycles of oscillation of the cylinder and 256 samples were collected in each cycle.

4. Wavelet Analysis

Traditionally, turbulent statistical measures are often calculated in Fourier space. However, important temporal information is lost owing to the non-local nature of the Fourier modes and transient nature of data. Fourier Transform (FT) gives the frequency information of the signal, which means that it tells us how much of each frequency exists in the signal. However, it does not show the time when these frequency components exist. For stationary signals in which signal properties do not change over time, this drawback is not important. For non-stationary signals, transitory characteristics are often the most important part of the data series and it is important to show when these particular events took place hence FT is not suited to detect them in time domain.

Wavelet Transform (WT) can provide the time and frequency information simultaneously, hence giving a time-frequency representation of the signal. Another useful property of WT is its ability to identify abrupt discontinuities ('edges') in signals. Edges are considered as distinct variations in the smoothness or continuity. Over the past decades, the wavelet transform has emerged as a particularly powerful tool for the elucidation of fluid signals [10]. Due to their high resolution in the wavelet domain, continuous wavelets are normally employed for feature detection in flows with recognizable coherent structures. The abrupt changes in the signals or the hidden discontinuities can also be detected using wavelet decomposition.

4.1. Continuous Wavelet Transform

The continuous wavelet transform (CWT) is capable of detecting smoother signal features as well as abrupt transitions in signals in the time-frequency domain. The peaks or discontinuities in time series can be detected using this transform. The CWT uses shifted and compressed\stretched versions of a localized

small wave like function to watch and measure their similarity to the data in different spatial locations. These moving functions have localized supports in both spatial and frequency domains; thereby they are known as "wavelets" or "small waves". Stretching or compressing the wavelet corresponds to the physical notion of scale. The comparison of the signal and the wavelet at different scales and positions gives the CWT coefficients. For a scale parameter (s) and position (u), the CWT coefficient is defined as Eq.(2), (Mallet, 2009)[11]:

$$C(a,u) = \int_{-\infty}^{\infty} f(t) \frac{1}{\sqrt{a}} \psi^* \left(\frac{t-u}{a} \right) dt \quad (2)$$

In which $f(t)$ is the signal, ψ is the mother wavelet function and * denotes the complex conjugate. This equation measures the similarity between function $f(t)$ and the window $\psi((t-u)/a)$ centered at u with scale a . The mother wavelet function is the basic form of the wavelet from which dilated and translated versions are derived and used in the wavelet transform. Multiplying each coefficient by the corresponding scaled and shifted wavelet yields the constituent wavelets of the original signal. The CWT coefficient for each position and scale represents how closely correlated the wavelet is with that section of the signal. The larger the coefficient C is in absolute value, the more the similarity. In this way the wavelet transform quantifies the local matching of the wavelet with the signal and can reveal the peaks in the lift force trace for the present study.

There are a large number of wavelets with different features which can be used for data analyses. The best one for a particular application depends on both the nature of the signal and what we desire to interrogate from the analysis. The Morlet wavelet which is believed to offer a good trade-off between detecting oscillations and peaks or discontinuities has been chosen for the present investigation. The Mother Morlet wavelet function is defined in Eq.(3) and shown in Figure 2. The C constant is used for normalization in view of reconstruction.

$$\psi(t) = C e^{-t^2/2} \cos(5t) \quad (3)$$

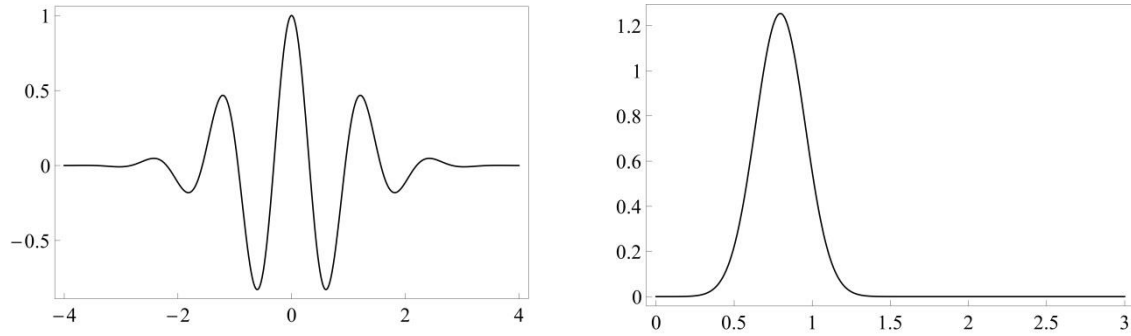


Figure 2.The mother Morlet wavelet function in time and frequency domains, (a): Time Domain, (b): Frequency Domain

In wavelet analysis, higher scales correspond to coarser signal features with lower frequencies and vice versa. While there is a general relationship between scale and frequency, no precise formula exists. As it is desired to map between a wavelet at a given scale with a specified sampling period to a frequency in Hertz, a pseudo-frequency corresponding to each scale is defined in a general sense according to Eq.(4).

$$F_a = \frac{F_c}{a \cdot \Delta} \quad (4)$$

In which ‘a’ is a scale, ‘ Δ ’ is the sampling period, ‘ F_c ’ is the center frequency maximizing the Fourier transform of the wavelet modulus in Hz and ‘ F_a ’ is the pseudo-frequency corresponding to the scale a, in Hertz.

4.2. CWT of Lift Force Variations

4.2.1. Real Wavelet Transform

The present oscillatory flow has four different phases. At the beginning of the flow cycle, the cylinder has its maximum velocity. The cylinder velocity reduces until reaching zero after a quarter of the oscillation period. Then the velocity direction reverses and the cylinder reaches its maximum velocity at the middle of the oscillation cycle. The next half of the oscillation is the same but in the reverse direction. The CWT coefficient diagram of the lift forces for KC number of 15 and two gap ratios, 1.0 and 0.1, are shown in Figure 3 as examples. The four distinct flow phases

are clearly detectable in the wavelet representation of the lift force variations. The peaks in the wavelet coefficients around the dominant frequency of the lift forces, represent the vortex shedding as described earlier. The first peak occurring after the flow reversal is associated with the return of the most recently shed vortex in the previous half cycle toward the cylinder. In a half cycle between two zero velocity points ($0.25 < t/T_w < 0.75$), the number of vortices being shed can be found by counting the number of peaks minus one in the vicinity of the dominant frequency. As it could be seen in Figure 3, for KC number of 15 in both gap ratios, two peaks are noticeable in the wavelet scalogram. The first one which is observed just after flow reversal should be due to the return of the most recently shed vortex toward the cylinder and the second one is attributed to a new vortex being shed. Hence it indicates that for this KC number, one vortex is being shed in a half cycle for both gap ratios. This result is in accordance with previous studies for example by Williamson[2]. It is clear that the peaks could not be easily identified from the data tracing in time domain.

The CWT of lift forces on an isolated cylinder ($G/D=1.0$) with different KC numbers are presented in Figure 4 (a-f). The peaks in CWT coefficients around the dominant frequency of the lift forces in a half cycle are specified and the numbers of vortices being shed in each half cycle are counted accordingly.

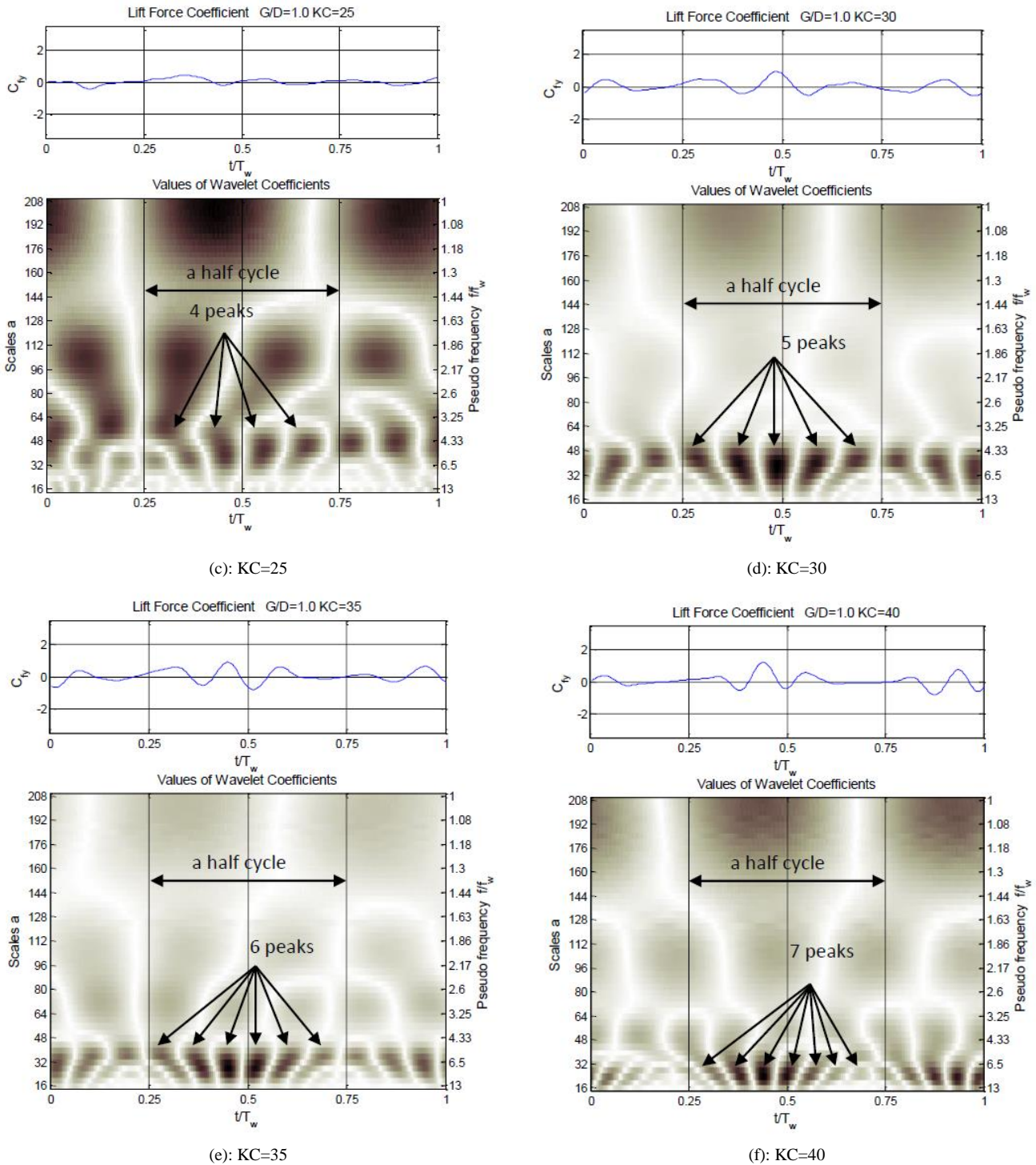


Figure 4. The CWT coefficients of lift force for different KC numbers and $G/D=1.0$, extremum values in black and zero values in white

As can be seen in Figure 4, the maximum CWT coefficients for KC number of 15, are detected at the relative frequency around two ($f/f_w \approx 2$). It shows that for this KC number, the dominant frequency of the lift force measurements is twice the frequency of the main oscillation. This result is due to the existence of two similar half cycles hence the velocity field contributes to the second harmonic of the lift variations. The second harmonic in the lift forces is observed for almost all studied KC numbers but it is clearly seen that the contribution of higher harmonics in the lift force variations increases for larger KC numbers.

Every time a vortex is detached from the cylinder, a sudden change in form of a peak is expected in the lift force trend and consequently in the CWT coefficients. It is important to consider the peaks in CWT coefficients around the dominant frequency.

4.2.2. Complex Wavelet Transform

For further accuracy, we have also investigated the complex Morlet wavelet by which the amplitude and phase components of the signal could be separated. The amplitude component of the complex wavelet clearly shows the dominant frequency and its region. The real part which is often used to detect sharp signal

transitions is then used to count the number of peaks associated with the dominant frequency. The number of vortices being shed in each half cycle is estimated accordingly. The imaginary part of the transform detects the local extremums in the first derivatives which measures the speed of variations in data; here it can be used to detect the speed of lift force variations due to vortex shedding.

A complex Morlet wavelet is defined by Eq.(5) [10].

$$\psi(t) = \pi^{-1/4} (e^{i2\pi f_0 t} - e^{-(2\pi f_0)^2/2}) e^{-t^2/2} \quad (5)$$

Where f_0 is the central frequency of the mother wavelet. The second term in the brackets is known as the correction term, as it corrects for the non-zero mean of the complex sinusoid of the first term. In practice it becomes negligible for values of $f_0 \gg 0$ and can be ignored, in which case, the Morlet wavelet can be written in a simpler form of Eq.(6), [10].

$$\psi(t) = \frac{1}{\pi^{1/4}} e^{i2\pi f_0 t} e^{-t^2/2} \quad (6)$$

This wavelet is a complex wave within a Gaussian envelope. The complex sinusoidal waveform is contained in the term $e^{i2\pi f_0 t} (= \cos(2\pi f_0 t) + i \sin(2\pi f_0 t))$.

The Gaussian envelope $e^{-t^2/2}$ has unit standard deviation and confines the complex sinusoidal waveform. The central frequency has been considered equal to unity for the present study. The real and imaginary sinusoids of the Morlet wavelet differ in phase by a quarter period (Figure 5). The $\pi^{1/4}$ term is a normalization factor which ensures that the wavelet has unit energy[10]. As it can be seen in Figure 5, the real part of ψ is symmetric which detects local extremums in data and the imaginary part is anti-symmetric which captures extremums in first derivative of the data.

The complex Morlet wavelet coefficient is composed of the real and imaginary parts hence we can write it in terms of its phase angle and modulus as defined in Eq.(7) and Eq.(8) respectively.

$$\varphi(s,u) = \tan^{-1} [\text{Im}(C(s,u))/\text{Re}(C(s,u))] \quad (7)$$

$$|C(s,u)| = \sqrt{[\text{Im}(C(s,u))]^2 + [\text{Re}(C(s,u))]^2} \quad (8)$$

The imaginary part is phase-shifted by one quarter of a cycle from the real part. As we use the complex conjugate in the transform, the imaginary part is inverted and lags behinds by one quarter of a cycle from the real part. The phase angle varies cyclically between $-\pi$ and π over the duration of the component waveforms. Zero phase corresponds to the real part of the Morlet wavelet centered at the maximum amplitude of the sinusoidal waveforms. A phase of π (and $-\pi$) corresponds to the minima of the real transform plot.

As examples, the results of the complex Morlet wavelet transform for KC number of 15 and 20 are shown in Figure 6 and Figure 7 respectively. For KC=15, the modulus of coefficients shows the dominant frequency of 2 hence in the graph of real parts of coefficients, the peaks around the mentioned frequency should be chosen. As it could be seen in Figure 6, in the graph for the real parts of wavelet coefficients around the dominant frequency, two peaks (one positive and one negative) are detectable. The second one is related to the vortex shedding. The graph for the imaginary parts detects the peak values of the first derivatives which are indicative of local minimum lift forces in absolute values. For KC number of 20, the dominant frequency is around 3 and there are 3 peaks in the real part of coefficients in a half cycle for the mentioned frequency (Figure 7).

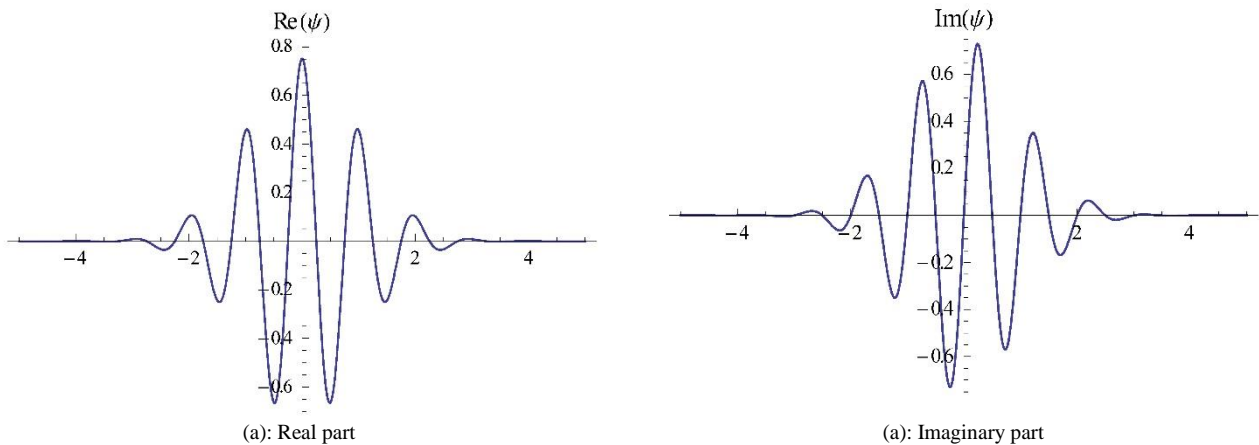


Figure 5. The real and imaginary parts of complex Morlet wavelet ($f_0=1$)

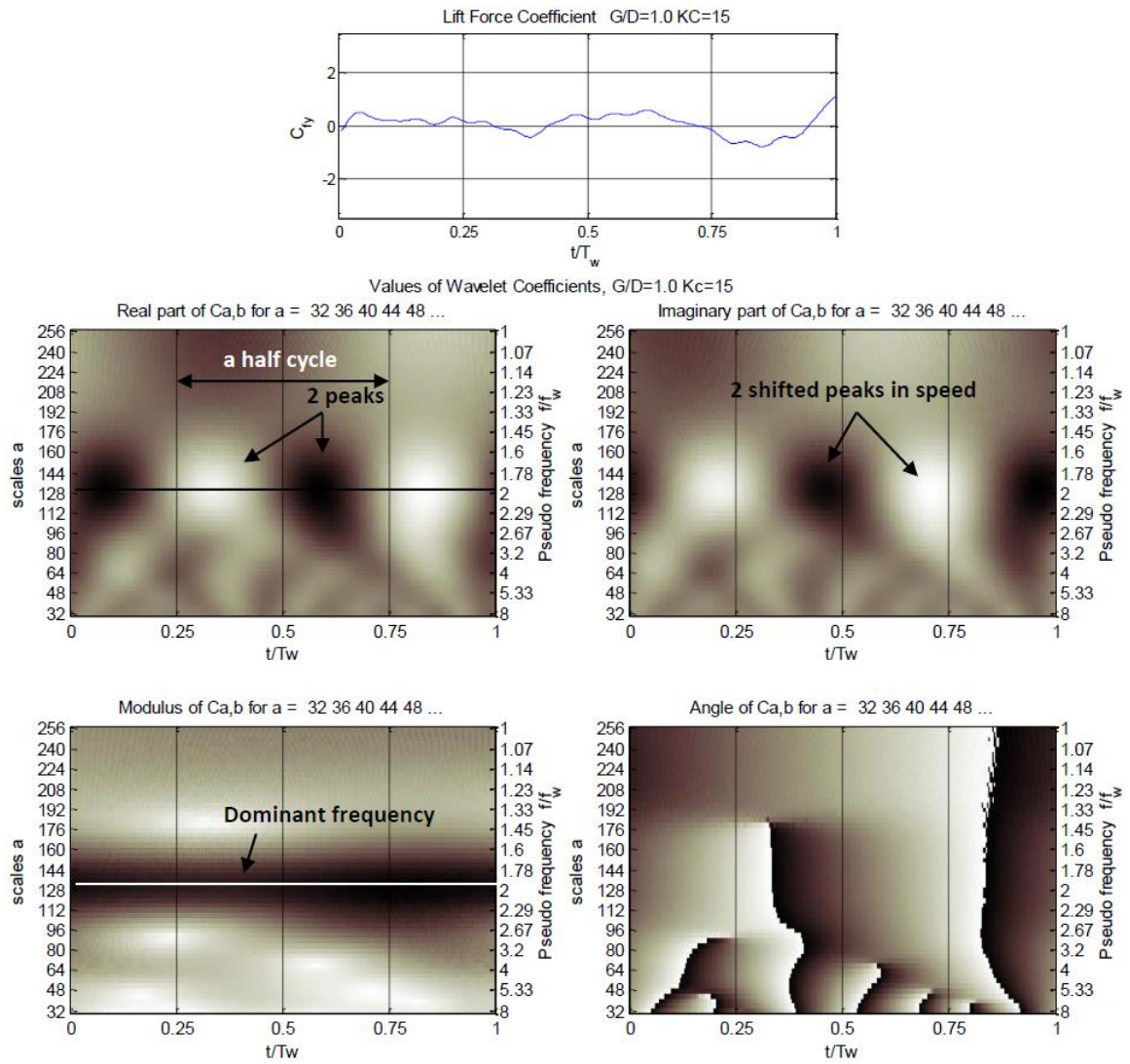


Figure 6 The complex Morlet coefficients for lift force, $G/D=1.0$, $KC=15$ (raw signal at the top followed by the different parts of the wavelet transform as specified in subplots)

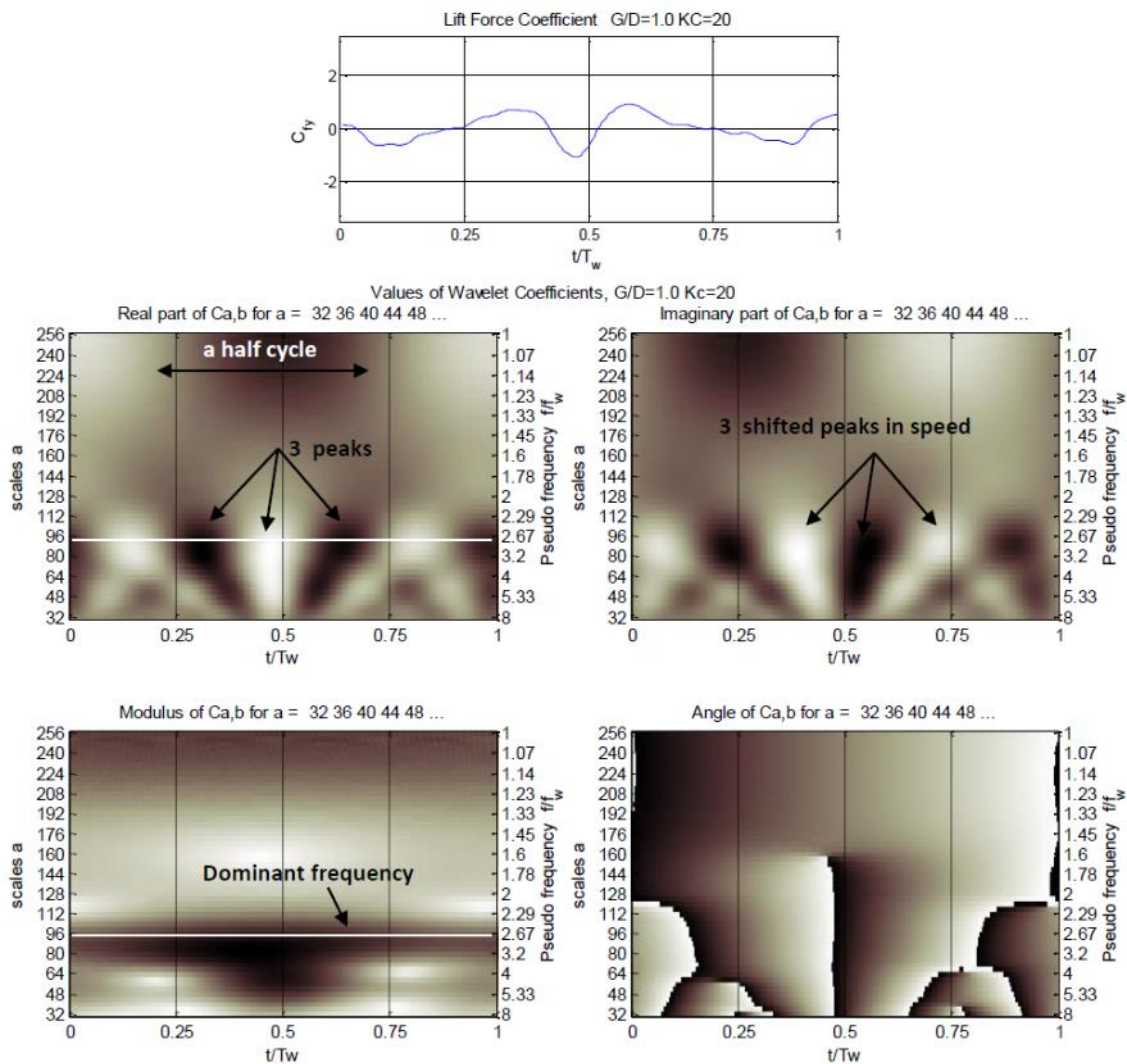


Figure 7 The complex Morlet coefficients for lift force, $G/D=1.0$, $KC=20$; (raw signal at the top followed by the different parts of the wavelet transform as specified in subplots)

The approximated numbers of vortex shedding in different KC numbers are compared with those estimated by previous works (see section 2) in Table 3. The results show that the former studies estimated less vortex shedding in a half cycle for larger KC numbers. As reported in former studies[5], for larger values of KC number, there is an increasing randomization in the formation and shedding of the vortices and flow visualization techniques are hardly applicable to trace the vortices. In fact visual tracing in higher flow velocities and consequently larger KC numbers, can lead to faulty and unreliable results. The wavelet analysis which is capable of representing the signal in simultaneous time/frequency domains could be considered as an alternative method to predict the vortex shedding in different flow conditions especially for larger KC numbers.

Table 3 Vortex shedding regimes around smooth circular cylinder in oscillatory flow.

KC range in former studies	N₁= Vortices per half cycle concluded from former studies	KC number in present study	N₂= Vortices per half cycle concluded from present study
7<KC<15	1	15	1
15<KC<24	2	20	2
24<KC<32	3	25	3
		30	4
32<KC<40	4	35	5
		40	6

N₁=Vortices per half cycle concluded from former studies, N₂=Vortices per half cycle according to the present study.

4.3. Discrete Wavelet Decomposition

As stated earlier, wavelet analysis can identify abrupt changes in the signal. Signals with very rapid evolutions such as transient signals in dynamic systems may undergo abrupt changes such as a jump or a sharp change in the first or second derivatives.

These features can be detected by wavelet decomposition. In this method, the signal is written in the form of an orthogonal sum of a rough approximation and an infinite number of finer details as shown in Eq.(9), [11].

$$f(x) = \sum_{l=0}^{2^{j_{\min}}} c_{J_{\min},l} \cdot \varphi_{J_{\min},l}(x) + \sum_{j=J_{\min}}^{J_{\max}-1} \sum_{n=0}^{2^j} d_{j,n} \cdot \psi_{j,n}(x) \quad (9)$$

here $\varphi(x)$ and $\psi(x)$ are the scaling and wavelet functions and $\varphi_{j,k}(x)$ and $\psi_{j,k}(x)$ are the dilated and shifted versions of $\varphi(x)$ and $\psi(x)$, respectively. In cases of non-interpolating wavelets, they are:

$$\varphi_{j,k}(x) = \sqrt{2^j} \varphi(2^j x - k), \quad \psi_{j,k}(x) = \sqrt{2^j} \psi(2^j x - k). \quad c_{j,k}$$

and $d_{j,k}$ are approximation and detail coefficients

which can be obtained by the projection method using the orthogonal or bi-orthogonal feature of the wavelet family.

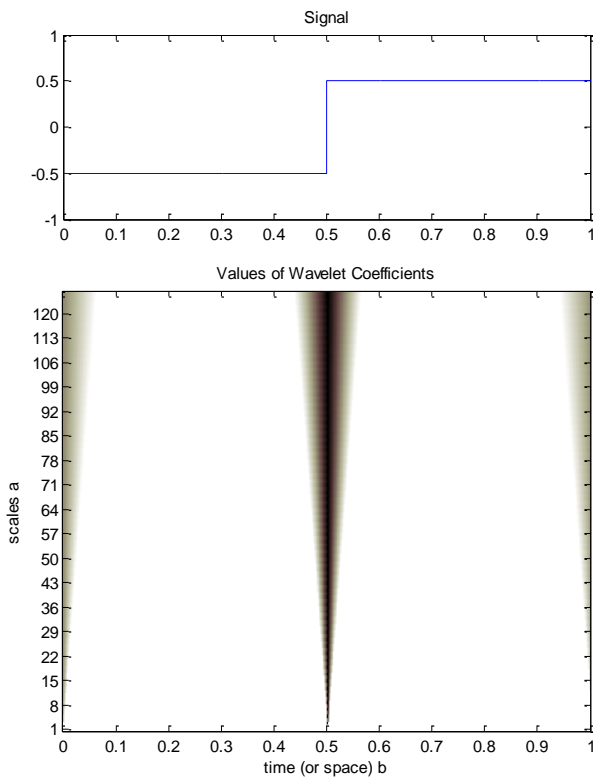
4.4. Discontinuity Detection

Considering wavelet transform, there are two methods to detect discontinuity in a signal namely the continuous wavelet transform (CWT) and the discrete wavelet transform (DWT). In the following examples, the application of these two methods in the detection of discontinuities in signals will be presented. The simplest form of a rupture in a signal is a step function which is investigated by CWT and DWT methods. The results are presented in Figure 8 (a-b) which show the ability of both methods to detect the rupture at time $t=0.5$.

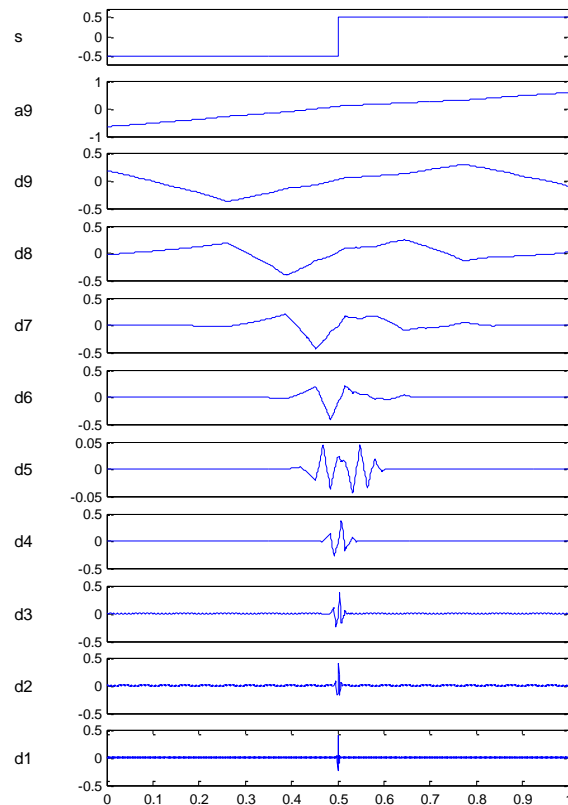
The following example illustrates how the wavelet decomposition with DWT detects hidden singularities, for example, a jump in the second derivative of a signal[12]. Figure 9 shows the smooth-looking function $f(t)$ defined by Eq.(10) and its continuous wavelet transform. As it can be seen, the CWT analysis of the signal does not show the localized singularity.

$$f(t) = \begin{cases} \frac{t^3}{6}, & 0 \leq t < 0.5 \\ \frac{t^3}{6} - \frac{t^2}{2} + \frac{t}{2} - \frac{1}{8}, & 0.5 \leq t < 1. \end{cases} \quad (10)$$

The Daubechies-3 wavelet decomposition for this function is presented in Figure 10 in which a_9 is the coarsest level approximation of the signal (s) and d_1 to d_9 are finest to coarsest details. The coarsest approximation shows an average or “trend” of the signal where d_1 with its higher frequencies in the wavelet series would show abrupt changes and discontinuities. As it can be seen in Figure 10, the discontinuity in the second derivative of the function $f(t)$ is detected with a very good resolution as sharp spikes at $t = 0.5$.



(a): CWT



(b): DWT

Figure 8 The continuous and discrete wavelet transform of a step function

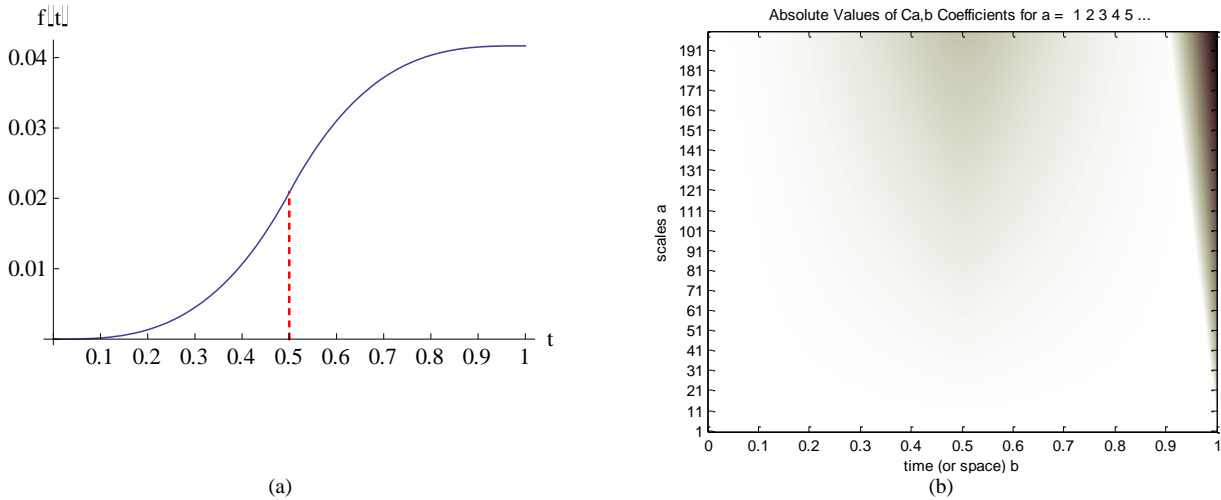


Figure 9 The smooth-looking function $f(t)$ defined by Equation (10) (a) and the corresponding CWT (b)

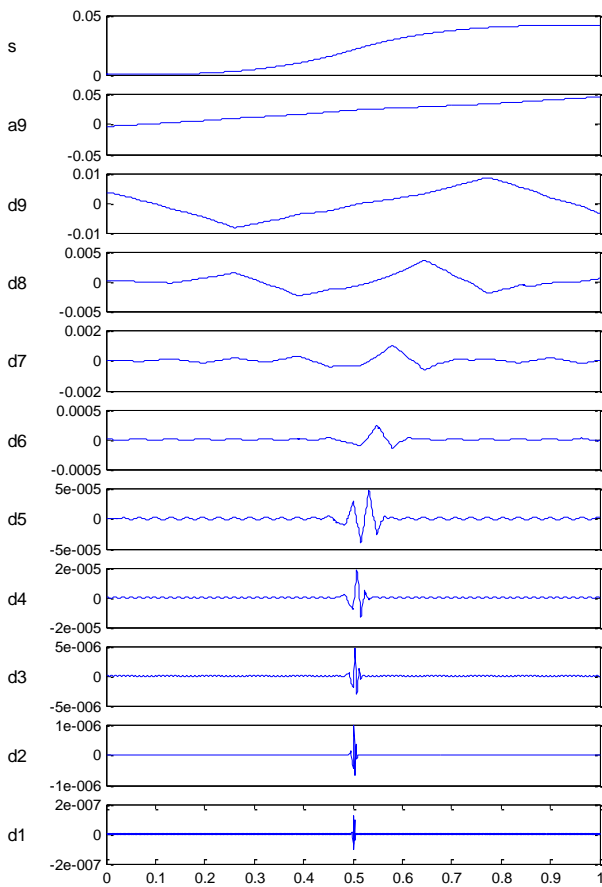


Figure 10. The Daubechies-3 wavelet decomposition for the function in Eq.(10)

The sudden changes in the lift forces attributed to vortex shedding can be detected by both CWT & DWT wavelet transforms. The inherent discontinuity can be captured by DWT; hence, DWT can be used as a robust tool to capture both sudden and inherent changes in data. For this purpose, the lift force traces for three cycles of oscillations are decomposed with Daubechies-2 wavelet. The results pertaining to KC

numbers of 20 and 40 are typically presented in Figure 11.

The discontinuities between three cycles are clearly recognizable in the finest detail level (D_1) by large amplitude spikes in frequency space. Moreover, small noise like spikes can be seen in each cycle which are the consequence of changes in the lift force due to vortex shedding; however it is clear that there are no inherent sudden changes in data. The comparison of results for different KC numbers shows that these spikes are more bolded for larger KC values. The reason is that in larger KC numbers, the distances moved by the fluid particles past the cylinder between the flow reversal phases are relatively long and the vortices have more time to completely form, grow and be shed in each half cycle. For the case of $KC=40$, six successive spike groups can be clearly detected in each half cycle as shown in the close-up illustration of first level detail (D_1) in **Error! Reference source not found.** This result is in accordance with the estimations from the CWT analysis. For smaller KC numbers, estimation of the vortex shedding number is not so straightforward but the discontinuities are still noticeable. Hence, this method is more suitable for flow conditions with larger KC values for which conventional methods based on flow visualization or Fourier based spectral analyses could not accurately estimate the vortex shedding frequency.

4.5. Effect of Bed Proximity on Vortex Shedding

Various studies have shown that regular vortex shedding is suppressed for lower gap ratios namely for $G/D < 0.3$ (Naeeni and Narayanan, 2003)[13]. The wavelet analyses clearly confirm these results. The CWT coefficients of lift forces for a near bed cylinder with gap ratio of 0.1 and different KC numbers are presented in Figure 13(a-f).

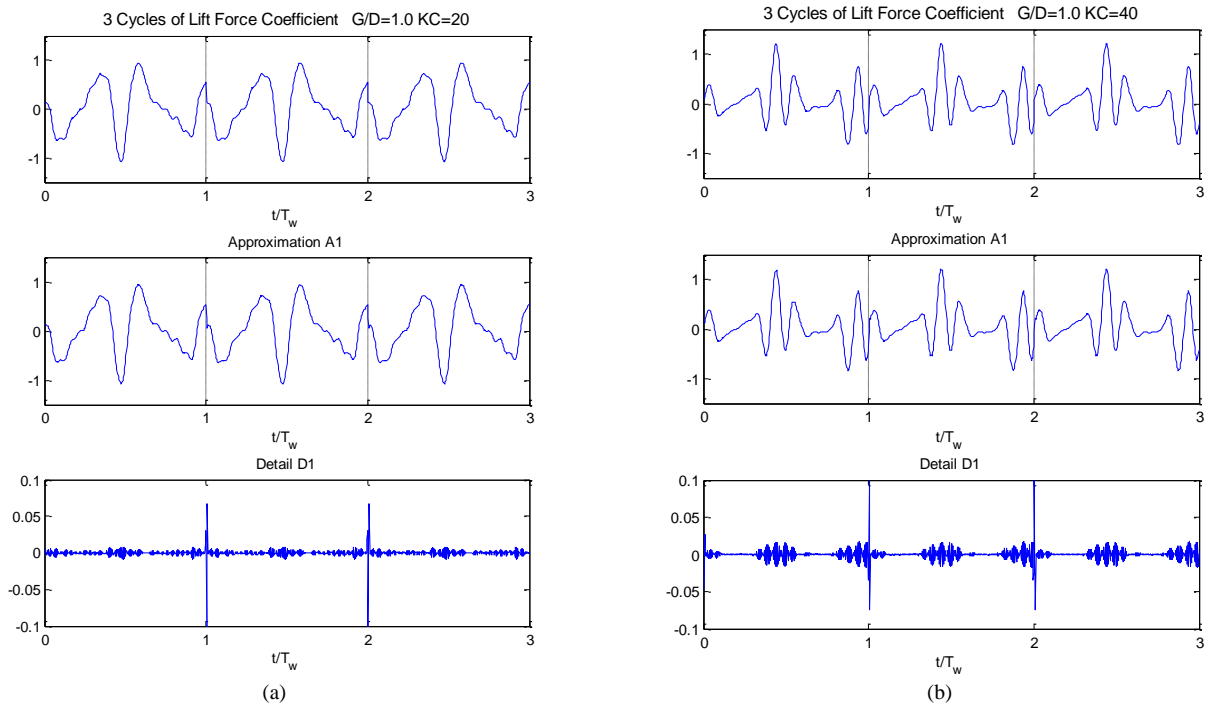


Figure 11. The Daubechies-2 wavelet decomposition of lift forces, $G/D=1.0$, (a) $KC=20$, (b) $KC=40$

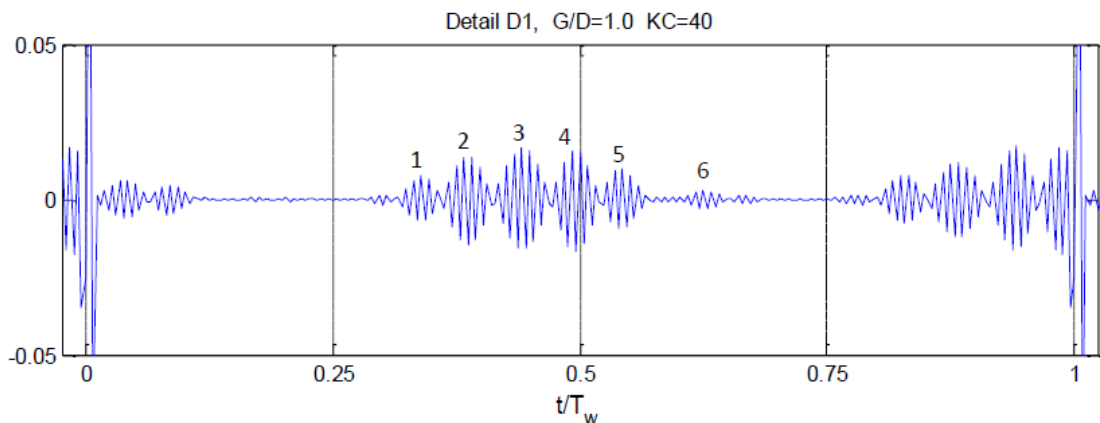


Figure 12. Close-up illustration of first level detail (D_1) of lift forces in a single oscillation cycle($G/D=1.0$, $KC=40$), six spike groups in a half cycle indicate the number of vortex shedding

The results show that the dominant frequency of the lift force measurements for a near bed cylinder remains twice the frequency of oscillation of the cylinder for all studied KC numbers which is due to the existence of two similar half cycles in the flow regime. The flow field is divided to four distinct phases as explained in section 4-2. The higher frequency contents in lift forces which are believed to be the consequence of vortex shedding and are observed for the case of isolated cylinders are not present for the case of near bed cylinders. For a closer look, the lift force traces and their corresponding

CWT coefficient scalograms for KC number of 40 and gap ratios of 1.0 and 0.1 are compared in Figure 14. The effect of vortex shedding on the creation of higher harmonics are clearly seen for the case of an isolated cylinder ($G/D=1.0$). These effects do not exist in the scalogram related to the near bed cylinder confirming the suppression of regular vortex shedding.

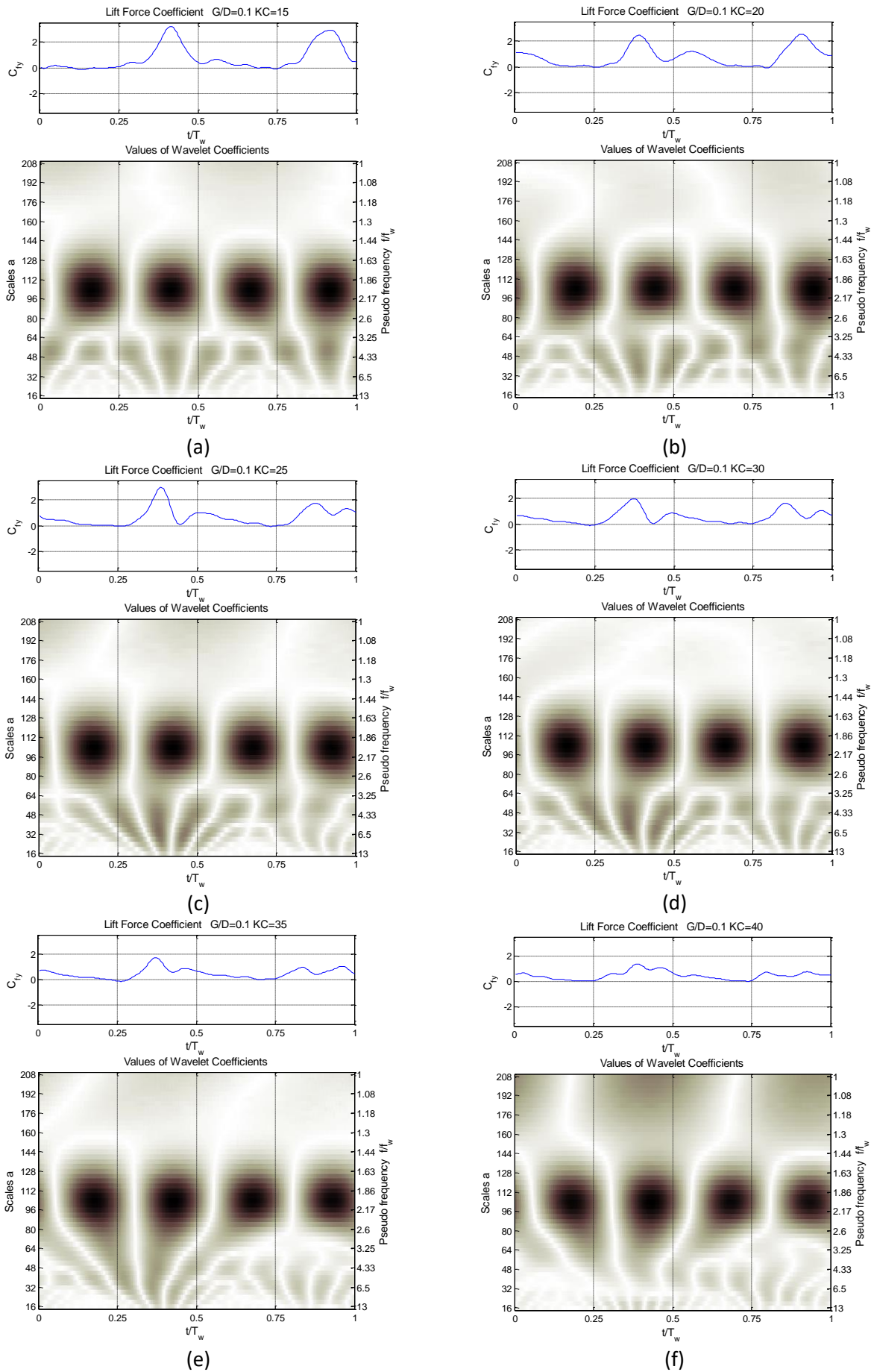


Figure 13. The CWT coefficients of lift force for different KC numbers and $G/D=0.1$, extremum values in black and zero values in white

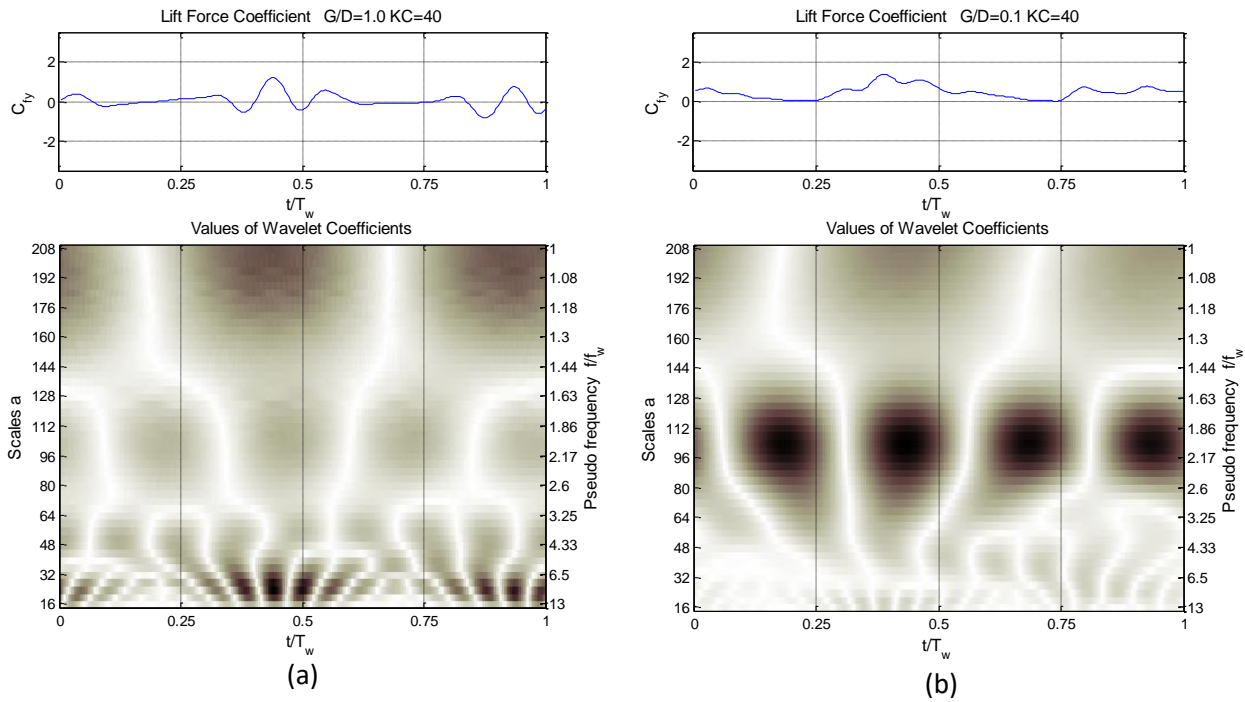


Figure 14. The CWT coefficients of lift force for KC number of 40 and two gap ratios of $G/D=1.0$ (a) and $G/D=0.1$ (b), extremum values in black and zero values in white

5. Conclusion

Wavelet analysis is an efficient method for feature detection in flows with recognizable coherent structures due to its high resolution nature. So far, most wavelet based coherent structure detection algorithms are presented for uniform flow condition and are based on velocity variations in wake flows. In the present study, wavelet analysis has been used to reveal the variation of lift force frequency content in time for an average oscillation cycle of an oscillatory flow. The four distinct oscillatory flow phases are clearly detectable in the wavelet representation of the lift force variations. Every time a vortex is detached from the cylinder, a sudden change in form of a peak is expected in the lift force trend. The symmetrical Morlet wavelet can reveal these peaks in a simultaneous time-frequency domain. The first peak in the CWT coefficient is related to the return of the most recently shed vortex in the previous half cycle. The rest of the peaks are attributed to the vortex shedding. The number of vortices shed in each half cycle is counted accordingly. This is conceivable due to the simultaneous time-frequency representation of lift force variations by wavelet analysis. Since for larger values of KC number, the randomization in the formation and shedding of the vortices increase and flow visualization techniques are hardly applicable to accurately estimate the vortex shedding frequency, the wavelet analysis is proved to be an efficient alternative method to predict the vortex shedding in different flow conditions. The wavelet analyses show more vortex shedding in a half cycle for larger KC numbers in comparison with the estimations of former studies. The discrete wavelet decomposition of the lift

force time series also reveals the abrupt changes attributed to vortex shedding in the finest detail level. The discontinuities are more distinguishable for larger KC numbers. It is concluded that the method is more suitable for flow conditions with larger KC values for which conventional methods based on flow visualization or Fourier based spectral analyses could not accurately estimate the vortex shedding frequency. The fact that the regular vortex shedding is suppressed for lower gap ratios is also investigated by wavelet analysis. The results for the gap ratio of 0.1 show that the higher frequencies which are believed to be the consequence of vortex shedding and are observed for the case of isolated cylinders are not present for near bed cylinders. The dominant frequency of the lift force for a near bed cylinder remains twice the frequency of oscillation of the cylinder for all studied KC numbers which is due to the existence of two similar half cycles in the flow regime.

Acknowledgement

The authors would like to thank Dr. Rangaswami Narayanan, a former reader at the department of civil and structural engineering, University of Manchester for his assistance in experiments and also his invaluable technical supports that greatly improved the manuscript.

References

- [1]Hudgins, L., Kaspersen, J.H., (2004). Wavelets and detection of coherent structures in fluid turbulence, Wavelets in Physics, Edited by J.C. Van Den Berg, Cambridge University Press, UK, 201-226.

- [2] Williamson, C. H. K., (1985). Sinusoidal Flow Relative to Circular Cylinders. *J. Fluid Mech.*, 155, 141-174.
- [3] Maull, D. J., Milliner, M. G., (1978). Sinusoidal Flow Past a Circular Cylinder, *Coast. Eng.*, 2, 149-168.
- [4] Sumer, B.M. and Fredsoe, J., (2006). Hydrodynamics around Cylindrical Structures, Advanced Series on Ocean Engineering - Volume 26, World Scientific Publishing Co., Singapore.
- [5] Kenny, J. P. and partners Ltd., (1993). Evaluation of Vortex Shedding Frequency and Dynamic Span Response, Development of Guidelines for Assessment of Submarine Pipeline Spans, Background Document One, OTI93614, Published by Health and Safety Executive.
- [6] Grass, A. J., Kemp, P.H., Stuart, R. J., (1981). Vortex Induced Velocity Magnification and Loading Effects for Cylinders in Oscillatory Flow. SERC London Centre for Marine Technology. Report Number FL 28 January.
- [7] Isaacson, M., Maull, D. J., (1976). Transverse forces in vertical cylinders in waves, *J. Waterw. Port Coast. Ocean Eng.*, Div. ASCE WWI.
- [8] Naeeni, S.T.O., Sadaghi, S.M., Narayanan, R., (2013). Effect of bed proximity on the in-line forces acting on a cylinder oscillating in still water, *Ocean Eng.*
- [9] Naeeni, S.T.O., Sadaghi, S.M., Narayanan, R., (2015). Spectral Features of the Pressure Distribution Around a Cylinder Oscillating in Still Water, *Coastal Engineering Journal*, Vol. 57, No. 3
- [10] Addison, P. S., (2002), *The Illustrated Wavelet Transform Handbook, Introductory Theory and Applications in Science, Engineering, Medicine and Finance.* Institute of Physics Publishing, Bristol and Philadelphia.
- [11] Mallat, S., (2009). *A Wavelet Tour of Signal Processing*, Elsevier Inc., United States.
- [12] Jerri, A.J., (2011). *Introduction to Wavelets*, Sampling Publishing, Potsdam, New York.
- [13] Naeeni, S.T.O., (2003). Force on Yawed Circular Cylinder Oscillating over a Plane Bed in Current, PhD thesis, UMIST, Manchester, UK.